Holography, hydrodynamics and the transseries expansion

Ben Meiring

Balliol College

University of Oxford

A thesis submitted for the degree of

Doctor of Philosophy

Trinity 2020

Abstract

The transseries is an ansatz for generating solutions to classical problems which are both perturbative and non-perturbative in some limit of parameter space. In this thesis we apply this technique to three systems described by classical gravity with relevance to holographic plasmas of strongly coupled gauge theories.

To begin we compute the gradient expansion to arbitrarily high orders for an $\mathcal{N} = 4$ Super Yang-Mills (SYM) plasma at infinite 't Hooft coupling undergoing Bjorken evolution, later finding the full transseries by including non-perturbative (in gradient) terms. Mathematical relations exist between these transseries sectors, which we verify by calculating the leading terms of the first non-hydrodynamic series solution entirely through the coefficients of the gradient expansion. Relaxing the limit of infinite 't Hooft coupling we compute the leading transseries solution for a family of finitely coupled gauge theories, and estimate the typical path of Bjorken evolution a far-from-equilibrium system might take while evolving to the hydrodynamic regime.

Next we consider a holographic Bjorken expanding system in arbitrary spacetime dimensions D, now instead using the number of dimensions as our large parameter. Due to a greater degree of analytic control we can compute combinations of transport coefficients relevant for Bjorken flow up to 6-th order in gradients to $\mathcal{O}(D^{-3})$, finding that our perturbative solution recovers the same dynamics controlled by the hydrodynamic gradient expansion. Computing the non-perturbative (in $1/D$) contributions of this set up we demonstrate an identification between these terms and the non-hydrodynamic solutions of the small gradient transseries.

Lastly we apply the transseries to study the near equilibrium dynamics of blackbranes. Due to the simplicity of this system we can analytically find the time-evolving divergence of the entropy current ($\partial_\mu s^\mu$) to second order in the transseries, determined entirely the blackbrane's quasinormal modes frequencies and equilibrium temperature. This pedogogical example demonstrates the power of the expansion which can be easily applied to wider contexts.

Acknowledgements

I give my sincere gratitude to my supervisor Jorge Casalderrey-Solana for his significant support and invaluable guidance throughout my D.Phil. A special thanks also goes to Christopher P. Herzog who met with me regularly and offered me helpful advice and direction. I'd also like to thank both Joseph Conlon and Andrei Starinets for a number of thoughtful discussions on both work and administative matters.

In addition to Jorge and Chris I am grateful to my collaborators Aron Jansen, Nikola I. Gushterov, Inês Aniceto, Jakub Jankowski and Michal Spaliński who were all crucial in completing the projects mentioned in this thesis, as well as offering helpful advice in the early drafts of this thesis. I'd also like to acknowledge R. Rodgers, A. Kurkela, W. van der Schee, M. Heller, D. Mateos, R. Janik, P. Romatschke, T. Andrade, R. Emparan, R. Suzuki, P. Witaszczyk, J. Magan, A. Ficnar, S. Grozdanov, P. Kovtun, D. Licht, U. Gürsoy and G. Nijs for insights I have gained from discussions through the course of my degree. I am especially grateful to Hannah Pullen who offered a great deal of support throughout the completion of this thesis.

Finally, I am thankful to Balliol College, the Commonwealth Scholarship Commission, the Skye Foundation, and the Harry Oppenheimer Trust who have supported me financially through the completion of this doctoral thesis.

Statement of Originality

This thesis, entitled *Holography, hydrodynamics and the transseries expansion*, is based on my own research and contains no material that has already been accepted or is being concurrently submitted for any university qualification unless otherwise stated. To the best of my knowledge this thesis contains no material previously published or written by another person without due reference made in the text. This thesis is based on the works [1–4] for which I am an author on each paper.

Contents

Chapter 1

Introduction

Problems in mathematical physics can rarely be solved exactly. To make progress in most physically interesting cases one typically perturbs a system about solved limits of parameter space. In this thesis we apply a transseries expansion, a series ansatz including both perturbative and non-perturbative contributions in the asymptotic parameter, as a means to generate solutions to generic problems in classical mechanics [5]. In particular we will be interesting in applying this method to the framework of classical gravity with relevance to holographic plasmas of strongly coupled gauge theories [6, 7].

The gauge/gravity duality is an invaluable framework derived from string theory which allows one to reorganize difficult systems in strongly coupled quantum field theories as accessible problems in classical supergravity. A common example of this duality is the AdS/CFT correspondence, a conjectured equivalence between the conformal $\mathcal{N} = 4$ Super Yang-Mills theory (SYM) in $3 + 1$ dimensions with gauge group $SU(N_c)$ and General Relativity in asymptotically AdS spaces with one higher dimension [8–10].

In this thesis we will apply the transseries expansion within the holographic context of AdS/CFT, as well as to the related study of black holes. Of particular interest to us will be the strongly coupled Quark Gluon Plasma (QGP) which has been routinely studied through the use of this formalism. This state of matter, created through ultra-relativistic heavy ion collisions at the Relativistic Heavy Ion Collider

(RHIC) [11–13] and Large Hadron Collider (LHC) [14–16], can be well described by hydrodynamics soon after its creation. As such while studying this system it will be natural to organize our transseries through the gradient expansion.

In preparation for the topics to follow, in the remaining sections of Chapter 1 we briefly review the theory of hydrodynamics, as well as outline the AdS/CFT conjecture and its applications. Each chapter in this thesis is largely self contained and can be read independently, although the results of the later chapters do comment on the findings of the earlier sections.

In Chapter 2 we mimic the early time dynamics of a QGP by constructing a transseries solution (in gradients) at infinite coupling for $\mathcal{N} = 4$ SYM matter expanding under boost invariant evolution. We find that our transseries solution is resurgent and demostrate that we can construct distinct non-perturbative solutions from our perturbative sector. Finally we extend our analysis to include finite coupling corrections and use our solution to estimate the typical path of evolution a similar QGP might follow during a heavy ion collision.

We study this same system in Chapter 3 by exchanging the parameter of small gradients for instead an expansion in large numbers of spacetime dimensions D. This approximation method, now well known in General Relativity, affords us a strong degree of analytic control and allows us to extract combinations of the transport coefficients relevant for Bjorken flow up to 6-th order in gradients to $\mathcal{O}(D^{-3})$. analysing the non-perturbative (in D) contributions of the system we find the familiar transseries structure to naturally emerge and can identify a one-to-one correspondence between the solutions of the small gradient transseries and that of the large-D transseries.

In Chapter 4 we shift our focus to the relaxation of black holes themselves, applying the transseries expansion to analytically track the non-linear evolution of a blackbrane horizon during equilibration. We find a closed form and remarkably general expression for the divergence of the blackbrane's associated entropy current ($\partial_\mu s^\mu$) which depends on only near equilibrium information, such as the quasinormal mode frequencies of the blackbrane and it's equilibrium temperature. Finally in 5

we summarize the findings presented in this thesis and their implications for future calculations.

1.1 Hydrodynamics and beyond

Hydrodynamics is an effective long wavelength description of many body systems at finite temperature, used to describe the low energy excitations of globally conserved quantities such as the energy and charge. The framework relies on the conservation of the energy-momentum tensor, symmetry arguments, and the second law of thermodynamics and as such it uses a universal structure to describe broad classes of phenomena. Specific details that differentiate theories within this description are characterized by a set of temperature dependent parameters called *transport coefficients* as well as an equation of state, both of which can be must be computed from an underlying microscopic theory.

1.1.1 Hydrodynamics and the gradient expansion

We begin by identifying the conversed current associated with spacetime translation symmetry, the energy-momentum tensor $T^{\mu\nu}$ in n spacetime dimensions. The corresponding conservation law is given by the conservation equation,

$$\nabla_\mu T^{\mu\nu} = 0\,, \tag{1.1}$$

where we can defined $T^{\mu\nu} = T^{\nu\mu}$ to be symmetrized without loss of generality. One is able to in general include further conservation laws associated with additional charges, but these will not be needed in our analysis. First we consider a particular choice of $T^{\mu\nu}$ known as the ideal energy-momentum tensor $T_0^{\mu\nu}$ obeying the form,

$$T_0^{\mu\nu} = \epsilon U^\mu U^\nu + p_{eq}\Delta^{\mu\nu}\,, \tag{1.2}$$

with local energy density $\epsilon(x)$, local equilibrium pressure given by the equation of state which we have pre-emptively named $p_{eq}(\epsilon)$, $U^\mu(x)$ the local fluid 4-velocity with respect to the lab frame obeying $U^2 = -1$, and $\Delta^{\mu\nu} = U^\mu U^\nu + \eta^{\mu\nu}$ is an operator

which projects onto the directions transverse to the fluid velocity, where all fields are taken to be slowly varying.[1] Applying the conservation equation to the ideal energy-momentum tensor we find

$$U_\nu \left(\partial_\mu T_0^{\mu\nu}\right) = 0 \quad \Rightarrow \quad \partial_\mu \left((\epsilon + p_{eq})U^\mu\right) = U^\mu \partial_\mu p_{eq} \,. \tag{1.3}$$

If the system were in local thermal equilibrium we could apply the thermodynamic relation $\epsilon(T) = -p_{eq}(T) + T s_{eq}(T)$ with $s_{eq} = \frac{\partial p_{eq}}{\partial T}$ where $T(x)$ is a locally defined auxillary parameter which we call the local effective temperature.[2] Assuming the thermodynamic relation holds we can rewrite Eq. (1.3) to find that for *ideal* evolution

$$\partial_\mu \left(s_{eq} U^\mu\right) = 0 \,, \tag{1.4}$$

where $s_{eq}U^\mu$ can be identified as the equilibrium entropy current. This statement justifies the interpretation of $T_0^{\mu\nu}$ to be associated with isentropic flow retroactively justifying our assumption that the system was in local equilibrium. One can still define notions of an out of equilibrium temperature and entropy current satisfying $\partial_\mu \left(s^\mu\right) \geq 0$, however the definitions of s^μ and T can depend on the choice of fluid frame and are not unique [17, 18].

We can note that Eq. (1.2) was the most general isotropic tensor that we could write down containing no derivative terms. The assumption of hydrodynamics is that we can describe $T^{\mu\nu}$ for a generic theory in terms of an expansion in gradients about this equilibrium stress tensor,

$$T^{\mu\nu} = \epsilon U^\mu U^\nu + p_{eq}\Delta^{\mu\nu} + \Pi^{\mu\nu} \,, \tag{1.5}$$

where $\Pi^{\mu\nu}$ is an infinite power series given by all possible combinations of ∂_μ, U^μ and $\Delta^{\mu\nu}$ encoding the deviations from local thermal equilibrium. Because these deviations

[1] The identification of the scalar functions ϵ and p_{eq} with the local energy density and the pressure can be made by noticing that in the fluid rest frame where $U^\mu = (1, 0, 0, 0, ...)$ an arbitrary energy momentum tensor should take the form $T^\mu_\nu = \mathrm{diag}\left(-\epsilon, p, p, p, ...\right)$.

[2] The notion of a local thermal equilibrium can be made precise by dividing the medium into infinitesmal spacetime cells, such that each cell individually satisfies the assumptions of thermodynamics and is itself in equilibrium.

are assumed to be small one expects that higher derivative terms can be ordered in progressively smaller contributions, with the number of derivatives acting as a counting parameter. Ideal hydrodynamics, given by the evolution of $T_0^{\mu\nu}$, is the limit where we set all derivative terms to zero. Lastly, as in the ideal case, we define the fluid velocity U^μ to be the 4-velocity of the local energy density in the lab frame by choosing the Landau frame via the condition $T^\mu_\nu U^\nu = -\epsilon U^\mu$, implying the condition that $\Pi^{\mu\nu} U_\nu = 0$.

We can interpret the gradient terms from $\Pi^{\mu\nu}$ as the source of entropy production for a generic fluid which is saturated in the ideal case by Eq. (1.4). Symmetry constraints of $T^{\mu\nu}$ as well as the positivity of $\partial_\mu (s^\mu) \geq 0$ can be used to determine the form of $\Pi^{\mu\nu}$ at each order in gradients. The first order expression can be written as,

$$\Pi^{\mu\nu} = -\eta\sigma^{\mu\nu} - \zeta\Delta^{\mu\nu}\partial_\lambda U^\lambda + \dots , \tag{1.6}$$

where η and ζ are the first order transport coefficients, known as the shear and bulk viscosities, $\sigma^{\mu\nu} = \Delta^{\mu\alpha}\Delta^{\mu\beta}\left(\partial_\alpha U_\beta + \partial_\beta U_\alpha - \frac{2}{n-1}\eta_{\alpha\beta}\partial_\lambda U^\lambda\right)$ is the shear tensor, and the ellipses indicate higher order terms in gradient. These transport coefficients are not fixed by hydrodynamics and must be determined by an underlying microscopic theory. For weakly coupled systems these coefficients can be fixed through Boltzmann's kinetic theory as a consequence of microscopic collision processes. [19–21]. At strong coupling the quasi-particle picture breaks down but nevertheless the robust framework of hydrodynamics still holds even without a clear understanding of the underlying microscopic dynamics. For holographic theories one can extract transport coefficients from the Green's functions of the theory via the Kubo formula [22, 23]. We will be interested in particular in *conformal* theories, which will set $\zeta = 0$, fix the equation of state to be $p_{eq} = \frac{\epsilon}{n-1}$ and will set the T dependence of our hydrodynamic quantities by dimensional analysis.

1.1.2 Bjorken Flow

Bjorken flow is the solution of relativistic hydrodynamics under the assumption that the fluid motion is invariant under boosts along the longitudinal direction $x_\parallel$. First described by Bjorken as a model for particle production in high energy hadronic collisions [24], the assumption of boost invariance is motivated by the observation that particle multiplicities in this type of collision exhibit relatively flat momentum-rapidity distributions. The model reasonably describes the initial evolution of deconfined nuclear matter following the ultra-relativistic collisions of heavy ions, and is routinely used when studying their phenomenology (see [25] for review).

This flow is conveniently expressed in Milne-type coordinates

$$ds^2 = -d\tau^2 + \tau^2 dy^2 + dx_\perp^2 \,, \tag{1.7}$$

where $\tau = \sqrt{t^2 - x_\parallel^2}$ the proper time, $y = \operatorname{arctanh}\left(\frac{x_\parallel}{t}\right)$ the rapidity, and $x_\perp$ are the coordinates for $(n-2)$ transverse spatial dimensions. We will leave the number of transverse dimension general to anticipate the analysis of Chapter 3. In the absence of transverse dynamics, boost invariance imposes that the velocity field of the fluid U^μ is given by $U^\tau = 1$. In addition $T^{\mu\nu}$ is fixed to be a diagonal function of only τ, as invariance under spatial reflections will set the off-diagonal terms to zero.

A remarkable aspect of this effectively 1-dimensional flow is that once the functional form of the energy density is determined, stress tensor conservation ($T^{\mu\nu}{}_{;\nu} = 0$) and conformal symmetry ($T^\mu_\mu = 0$) completely fix the stress tensor of the theory [26]. To show this explicitly we start with the simple result of these conditions,

$$\tau T'_{\tau\tau} + T_{\tau\tau} + \tau^{-2} T_{yy} = 0 \,, \quad -T_{\tau\tau} + \tau^{-2} T_{yy} + (n-2) T_{x_\perp x_\perp} = 0 \,. \tag{1.8}$$

Putting these terms into more intuitive notation we define the longitudinal pressure $p_L = T^y_y$, and transverse pressure $p_T = T^{x_\perp}_{x_\perp}$ as the diagonal components of the stress tensor in the fluid rest frame so that

$$T_{\mu\nu} = \operatorname{diag}\left(\epsilon, \tau^2 p_L, p_T, p_T, ...\right) \,, \tag{1.9}$$

where as before we have identified the energy density with $\epsilon = -T^{\tau}_{\tau}$. Using the constraints given to us by Eq. (1.8) we can express the energy momentum tensor purely in terms of a single function, the energy density $\epsilon(\tau)$, through the relations

$$p_L = -\epsilon(\tau) - \tau\epsilon'(\tau)\,, \tag{1.10}$$

$$p_T = \frac{2\epsilon + \tau\epsilon'(\tau)}{-2+n}\,. \tag{1.11}$$

Note that these expressions are valid independent of whether the system is far from local thermal equilibrium, and that in thermal equilibrium both pressures must be the same. This feature will be useful in Chapter 2 where we use them to track the evolution of a system outside the hydrodynamic regime.

While the conservation equation (1.10) must be satisfied in any interacting theory (without external sources), in the hydrodynamic limit we can express p_L in a gradient expansion around the equilibrium pressure $p_{\rm eq}$. For a conformal theory we can use the conformal equation of state to write the longitudinal pressure as

$$p_L = \frac{1}{n-1}\epsilon(\tau) + \Delta p_L\,, \tag{1.12}$$

where Δp_L encodes all deviations from the equilibrium pressure, ultimately coming from gradient terms embedded in the viscous tensor $\Delta p_L = \Pi^y_y$ which, for 1+1 dimensional expansion and to second order in gradients is [27]

$$\Pi^{\mu\nu} = -\eta\sigma^{\mu\nu} + \eta\tau_\Pi\left(D_u\sigma^{\mu\nu} + \frac{\nabla\cdot u}{n-1}\sigma^{\mu\nu}\right) + \lambda_1\sigma^{\langle\mu}{}_{\lambda}\sigma^{\nu\rangle\lambda}\,, \tag{1.13}$$

where η is the shear viscosity, and τ_Π and λ_1 are second order transport coefficients[3]. If we consider the ideal case with $\Delta p_L = 0$, we can easily find $\epsilon_{eq}(\tau)$. As we are considering a conformal theory, T_{eq} will be the only dimensionful parameter and $\epsilon_{eq}(T)$ will be fixed by dimensional anaylsis,

$$\epsilon_{eq}(\tau) = g_* T_{eq}(\tau)^n = g_*\Lambda^n\left(\Lambda\tau\right)^{\frac{n}{1-n}}\,. \tag{1.14}$$

[3]To define some standard notation in Eq. (1.13), D_u is the covariant derivative along the fluid velocity u^μ defined as $D_u X \equiv u^\mu X_{;\mu}$, ∇ is the projection of the covariant derivative to the fluid rest frame $\nabla^\mu X \equiv \Delta^{\mu\nu}X_{;\nu}$, and the brackets denote symmetrization and tracelessness in the rest fluid rest frame, $2A^{<\mu\nu>} = \Delta^{\mu\alpha}\Delta^{\nu\beta}\left(A^{\alpha\beta} + A^{\beta\alpha} - \frac{2}{n-1}g^{\alpha\beta}A^{\rho}_{\rho}\right)$, with $\Delta^{\mu\nu} \equiv (g^{\mu\nu} + u^\mu u^\nu)$.

where g_* is a constant set by the equation of state and Λ is a dimensionful scale of mass parameter one. At late times, all information about the initial conditions of this highly symmetric expansion is condensed in the value of this constant Λ, which may be defined as

$$\Lambda = \lim_{\tau\to\infty} \tau^{\frac{1}{n-2}} \left(\frac{\epsilon(\tau)}{g_*}\right)^{\frac{n-1}{n(n-2)}} . \tag{1.15}$$

Away from local equilibrium each gradient correction can only depend on the dimensionless combination $u^{-1} \equiv (\Lambda\tau)^{-\nu} \sim \frac{1}{\tau T_{eq}}$, where $\nu = \frac{n-2}{n-1}$ and we call u the inverse gradient correction, not to be confused with the fluid velocity U^μ. The energy density for Bjorken flow must take the simple form

$$\epsilon(\tau) = \epsilon_{eq}(\tau)\left(1 + \epsilon_1^{(0)} u^{-1} + \epsilon_2^{(0)} u^{-2} + ...\right) = g_*\,\Lambda^n u^{-\left(\frac{n}{n-2}\right)} \sum_{i=0}^{\infty} \epsilon_i^{(0)}\, u^{-i}\,, \tag{1.16}$$

where $\epsilon_i^{(0)}$ are dimensionless coefficients given by combinations of the transport coefficients (with their temperature dependence factored out).[4] These coefficients are solely determined from the microscopic theory. A surprising outcome is that in many phenomenologically relevant theories in which one can find numerical expressions for these coefficients $\epsilon_i^{(0)}$, the contribution of higher order coefficients appears to grow factorially instead of falling off [1, 2, 28–32]. This indicates that even in these realistic theories where we might expect ideal hydrodynamics to hold in some region of applicability, the hydrodynamic gradient expansion does not converge. As we will see in the following chapters, not only can we make sense of such an occurance, this behaviour is in fact expected.

Lastly we note that it is convenient to define a dimensionally correct effective temperature far from equilibrium through

$$\epsilon(\tau) = g_*\, T(\tau)^n \tag{1.17}$$

so that the relation reduces to Eq. (1.14) in local equilibrium when the flow is ideal. Such a definition will be used later in Chapters 2 & 3.

[4] In our conventions we will set $\epsilon_0 = 1$, taking the normalization of the series to be given completely by Λ. Also note that we have explicitly factored out g_* in the definition of our coefficients.

1.1.3 Beyond hydrodynamics

In the previous section we learned that in many phenomenologically relevant theories the hydrodynamic expansion can be found to diverge. A similar and ultimately related conflict is the issue of acausality. For any practical computation one must truncate the series given by Eq. (1.13) at some finite order but the resulting equations of motion due to this truncation will not be well-posed, resulting in superluminal modes [18, 32, 33]. While it is clear that these fast moving modes are outside the hydro regime and should be ignored, practically they can hinder the implementation of numerical computations. To resolve this Müller-Israel-Stewart (MIS) theory abandons the notion of $\Pi^{\mu\nu}$ as a definition of the gradient expansion about the equilibrium flow, and instead promotes $\Pi^{\mu\nu}$ to a dynamical variable obeying,

$$\left(\tau_\Pi U^\alpha \partial_\alpha + 1\right)\Pi^{\mu\nu} = -\eta\sigma^{\mu\nu} + \eta\tau_\Pi\left(D_u\sigma^{\mu\nu} + \frac{\nabla\cdot u}{n-1}\sigma^{\mu\nu}\right) + \lambda_1\sigma^{\langle\mu}{}_\lambda\sigma^{\nu\rangle\lambda} + \dots\,, \quad (1.18)$$

where the additional terms shown on the right hand side of this equation are given by the gradient expansion to second order for 1+1 dimensional expansion in n dimensions [27]. The parameter τ_Π is known as the relaxation time, and the linearization of the resulting theory is causal provided $T\tau_\Pi \geq \eta/s$. For our purposes we will truncate the additional terms at higher orders, and adopt the symmetries of Bjorken flow in $n = 4$ spacetime dimensions while setting the transport coefficient $\lambda_1 = 0$. This simplification amounts to selecting a specific family of microscopic theories, but does not change our argument beyond making our expressions more concise.

Together with the conservation of the stress tensor given by Eq. (1.5) we can find the equations of motion to be

$$\Delta p_L(\tau) + \tau\epsilon'(\tau) + \frac{4\epsilon(\tau)}{3} = 0\,, \quad (1.19)$$

$$3\tau\tau_\Pi\Delta p_L'(\tau) + \Delta p_L(\tau)(3\tau + 4\tau_\Pi) + 4\eta = 0\,, \quad (1.20)$$

Where for the conformal theory we can express $\epsilon = g_*\,T^4$ defining T out of equilibrium through ϵ as a local effective temperature where for convenience we will choose $g_* = 1$

in this section. The transport coefficients have a simple T dependence given by,

$$\tau_{\Pi} = \frac{C_{\tau_{\Pi}}}{T}\,, \quad \eta = C_{\eta} s\,, \tag{1.21}$$

where $C_{\tau_{\Pi}}$ and C_{η} are undetermined and define a family of theories. Expressing Eqs. (1.19) and (1.20) in terms of the energy density as a function of $u = (\Lambda\tau)^{2/3}$ we find a single second order non-linear ODE which governs the dynamics of the system,

$$\frac{2C_{\tau_{\Pi}} u\left(u\epsilon''(u) + 5\epsilon'(u)\right)}{\epsilon(u)} + 8\left(C_{\tau_{\Pi}} - C_{\eta}\right) + \frac{3u^{5/2}\epsilon'(u)}{\epsilon(u)^{3/4}} + 6u^{3/2}\epsilon(u)^{1/4} = 0\,. \tag{1.22}$$

One can check that as before a power series solution of the form of Eq. (1.16) with $n = 4$ will solve Eq. (1.22). However as expected from the number of derivatives contained in Eq. (1.22) a second independent solution can found, this time of the form

$$\delta\epsilon(\tau) \sim u^{\beta_1} e^{-A_1 u} \sum_{k=0} \epsilon_k^{(1)} u^{-k} + \mathcal{O}\left(e^{-2A_1 u}\right)\,, \tag{1.23}$$

where the equations of motion fix,

$$A_1 = \frac{3}{2C_{\tau_{\Pi}}}\,, \quad \text{and} \quad \beta_1 = -3 + \frac{C_{\eta}}{C_{\tau_{\Pi}}}\,, \tag{1.24}$$

as well as an infinite sum of coefficients $\epsilon_k^{(1)}$, distinct from the coefficients $\epsilon_k^{(0)}$ found in the original hydrodynamic series. We can note that the series given by Eq. (1.23) is non-perturbative in the $u \to \infty$ limit and so we refer to these types of solutions as *non-hydrodynamic* modes.[5]

While curing the problem of acausal modes in the gradient expansion we have effectively invented a family of microscopic theories whose data is fixed after setting parameters C_{η} and $C_{\tau_{\Pi}}$, and which automatically includes a non-hydrodynamic sector controlled by $C_{\tau_{\Pi}}$. The non-hydrodynamic contribution followed a particular characteristic form common to transseries solutions, which will be discussed further in Chapter 2. There is however nothing special about having chosen MIS theory to fix the ultra-violet behaviour of the gradient expansion. One could have equally chosen

[5] As indicated by the correction term in Eq. (1.23) the non-linear terms in Eq. (1.22) also lead to an infinite series in powers of $e^{-A_1 u}$ for $\delta\epsilon(\tau)$.

any causal microscopic theory with a hydrodynamic regime, such as Heller-Spalinski-Janik-Witaszczyk theory, kinetic theories with various choices of collision kernels, or even $\mathcal{N} = 4$ SYM theory [31,34]. What we will find in Chapter 2 however is that these perturbative and non-perturbative sectors are not independent and that specifying the coefficients $\epsilon_k^{(0)}$ to higher orders in k will fully determine the non-perturbative sectors of the theory.

1.2 The AdS/CFT correspondence

We would like to study the real time evolution of strongly coupled gauge theories far from equilibrium. While such an analysis for Quantum Chromodynamics does not yet exist, interest in describing strongly coupled systems such as the quark-gluon plasma (QGP) has provided a good motivation to consider related and more tractable theories for this purpose. To gain some insight into qualitative aspects of QCD which remain relevant in experimentally accessible regimes, it will be useful to consider the QCD equation of state given in Figure 1.1 given for $N_f = 3$ with physical quark masses.

On the left panel we see the pressure in units of T^4, with a dramatic rise above a temperature of approximately 200 MeV. This is characteristic of a phase transition and indicates an increase in the degrees of freedom in the medium. On the top right of the left figure we see the non-interacting Stefan-Boltzman limit which deviates from the slow rising plateau of the plot, even at temperatures of 1 GeV. On the right panel we display the trace anomaly $I = (\epsilon - 3P)$ in units of T^4, which indicates a greater degree of conformality as it approaches zero. In the temperature range of above $\sim 300 - 400$ MeV, which can be readily scanned by both RHIC and the LHC, we expect to find an interacting but near conformal medium. This suggests that qualitative features of QCD in this regime could be extracted instead from simpler conformal gauge field theory, a natural candidate being the $\mathcal{N} = 4$ supersymmetric Yang-Mills (SYM) theory.

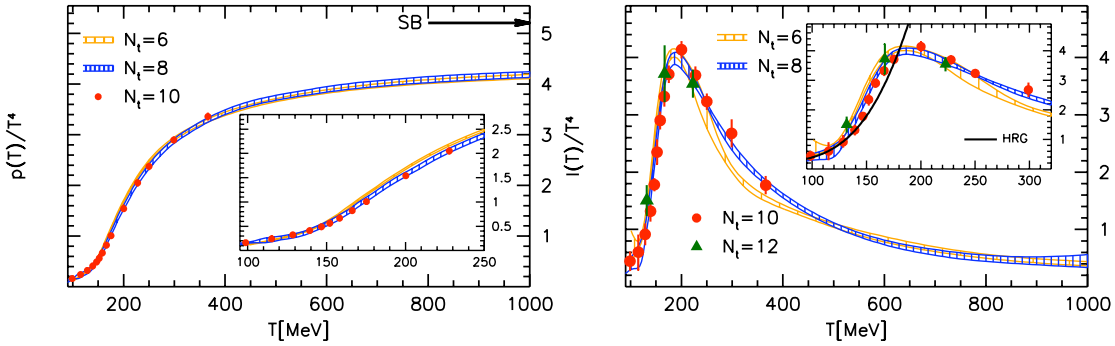

Figure 1.1: Results of lattice QCD computations taken from [35,36] with $N_f = 3$. Displayed are the pressure (left panel) and trace anomaly ($\epsilon - 3P$) (right panel) in units of T^4. The data is taken with a varying number of points in the euclidean time direction given by N_τ, which corresponds in the continium limit to $N_\tau \to \infty$.

An important framework has been developed for studying $\mathcal{N} = 4$ SYM at infinite coupling through the use of classical Supergravity [6, 10, 37] which we will further explain in this section. While $\mathcal{N} = 4$ SYM and QCD maintain fundamental differences the conformal nature of QCD above the critical temperature allows one to derive qualitative insights into the dynamics of the QGP from this related theory.

To begin we outline some basic concepts of string theory and D-branes before motivating the correspondence between IIB string theory in $AdS_5 \times S^5$ and $\mathcal{N} = 4$ SYM with gauge group $SU(N_c)$. The action of a relativistic point particle is specified as the integral of its proper time over a path of evolution through some higher dimensional target space. Analogously the Nambu-Goto action of a classical string is given by an integral over a 2-dimensional worldsheet

$$S_{str} = -T_{str} \int d^2\sigma \sqrt{-\gamma}\,, \tag{1.25}$$

where σ parameterizes the coordinates along the string worldsheet and $\gamma_{\alpha\beta} = \partial_\alpha x^M \partial_\beta x^N g_{MN}$ tracks the trajectory of the string in the D-dimensional target space via x^M, with background metric given by g_{MN}. $T_{str} = \frac{1}{2\pi l_s^2}$ is the string tension, sometimes expressed through the string length l_s.

When quantizing the action given by Eq. (1.25) the condition that there are no negative norm states implies that the number of dimensions in the target space will

be fixed to $D = 26$. The spectrum of states corresponds to different vibrations of the string given by a finite number of massless modes as well as an infinite tower of massive modes set by $m_s \sim l_s^{-1}$. One such massless rank 2 mode, known as the graviton, is identified with a closed string. For our purposes we will be interested in type IIB superstring theory, a model including a fermionic worldsheet in the action (1.25) which when quantized will enforce $D = 10$.

Interactions in such a string theory are mediated by a vertex parameter g_s which controls string scattering amplitudes.[6] At low energies one can simplify the system by integrating out the massive string modes to find a low energy effective action for the remaining massless modes. Because the massless spectrum of a closed string theory always contains a graviton the low energy effective action will be type IIB supergravity [38, 39],

$$S_{\text{SUGRA}} = \frac{1}{16\pi G_{10}} \int d^{10}x \sqrt{-g} \left(R + ...\right) , \tag{1.26}$$

where the ellipses denote massless matter fields. From enforcing that the low energy effective action is given by tree level interactions of the gravitons we will find that

$$16\pi G_{10} = (2\pi)^7 g_s^2 l_s^8 , \tag{1.27}$$

where the dependence on l_s follows from dimensional analysis.

In string theory we also find higher dimensional solitonic objects known as D-branes. A Dp-brane can be intuitively understood as a subspace spanning p dimensions of our target space upon which strings can start and end. Just like domain walls, D-branes are dynamical objects sweeping out a $(p+1)$-dimensional worldvolume in spacetime. For type IIB string theory stable Dp-branes are given when p is odd.

An interesting feature of D-branes is the emergence of non-Abelian gauge theories as an effective low energy description of the strings attached to them. For N_c parallel coinciding D3-branes one can find a low energy effective action consisting of a gauge field A_μ, six scalar fields ϕ^i and four Weyl fermions in the adjoint representation of

[6] Typically g_s can be defined as the vacuum expectation value of a particular scalar field measured at the boundary known as the dilaton, but for our purposes this detail will not be important.

$U(N_c)$ [40]. Since these fields are supported on the D-brane, they depend only on the x^μ coordinates along the $3+1$ worldvolume. This theory turns out to be precisely $\mathcal{N}=4$ SYM with gauge group $SU(N_c)$ whose bosonic part of the Lagrangain is given by,

$$\mathcal{L}_{YM} = -\frac{1}{g_{YM}^2}\mathrm{Tr}\left(\frac{1}{4}F^{\mu\nu}F_{\mu\nu} + \frac{1}{2}D_\mu\phi^i D_\nu\phi^i + \left[\phi^i,\phi^j\right]^2\right), \tag{1.28}$$

with Yang-Mills coupling constant given by,

$$g_{YM}^2 = 4\pi g_s\,, \tag{1.29}$$

where the high degree of super symmetry present in this resulting theory will enforce that the constant coupling is scale independent. In finding the Lagrangian given by (1.28) we have neglected the higher mass modes given by $m_s \sim l_s^{-1}$ as well as ignored the gravitational interactions mediated by the dimensionless coupling parameter $G_{10}E^8$ in 10 dimensions and as such would be suppressed in the low energy limit. Interactions between closed and open strings are also controlled by the same dimensionless parameter due to the universal coupling of gravity to matter. Therefore at low energies from this decoupling we must conclude that the interacting sector is sufficiently described by $\mathcal{N}=4$ SYM in $(3+1)$ dimensions with gauge group $SU(N_c)$.

However, at the same time one can explicitly solve the supergravity equations of motion for a spacetime metric sourced by N_c Dp-branes [41, 42]. For a stack of D3-branes in type IIB theory one finds

$$ds^2 = H^{-1/2}\left(-dt^2 + dx_1^2 + dx_2^2 + dx_3^2\right) + H^{1/2}\left(dr^2 + r^2 d\Omega_5^2\right) \tag{1.30}$$

where coordinates $(t,\vec{x})$ denote the $3+1$ dimensions spanned by the D3-branes while (r,Ω_5) are the coordinates transverse to them. Here $dr^2 + r^2 d\Omega_5^2$ can be recognized as the flat metric written in spherical coordinates and the function $H(r)$ is set to

$$H = 1 + \frac{L^4}{r^4}\,, \quad L^4 = 4\pi g_s N_c l_s^4\,, \tag{1.31}$$

where L is the radius of curvature, a length scale parameterizing the strength of the gravitational interaction. The metric (1.30) depends only on the coordinate r and

can be intuitively divided into two regions. When $r \gg L$ we will have $H \sim 1$ and the metric reduces to flatspace with a small correction of the order L^4/r^4, consistent with a gravitational potential due to a massive object in the six remaining spatial dimensions.[7]

Conversely in the region given by $r \ll L$ the effects of gravity are strong and the metric (1.30) reduces to

$$ds^2 = ds^2_{AdS_5} + L^2 d\Omega_5^2 \,, \tag{1.32}$$

where by defining $r = L^2/z$ we can find

$$ds^2_{AdS_5} = \frac{L^2}{z^2}\left(-dt^2 + dx_1^2 + dx_2^2 + dx_3^2 + dz^2\right) \,, \tag{1.33}$$

which can be recognized as the $AdS_5 \times S^5$ metric. In the low energy limit the gravitons in the asymptotic $r \gg L$ region will decouple as the dimensionless coupling $G_{10}E^8$ vanishes, but gravitons in the "throat" region given by $r \ll L$ will be sufficiently blueshifted to survive. Therefore in this description, the interacting sector at low energies will be controlled by closed strings in $AdS_5 \times S^5$.

Let us re-evaluate the discussion above where we have considered two very different descriptions for the same stack of N_c D3-branes. In the first picture, known as the open string description, the D-branes correspond to a hyperplane in flat spacetime upon which open string excitations at low energies follow an effective description in terms of $\mathcal{N} = 4$ SYM theory. In contrast the second picture, the closed string description, is given by a non-trivial geometry resulting from interacting gravitons. The AdS/CFT correspondence is the conjecture that these two descriptions, $\mathcal{N} = 4$ SYM with gauge group $SU(N_c)$ and type IIB string theory in $AdS_5 \times S^5$, are equivalent.

Astonishingly, even while these two very different pictures appear to describe the same system, they become tractable in different regions of parameter space. For the combination $g_s N_c \ll 1$ we can see from Eq. (1.31) that the supergravity solution of

[7] This is to be expected as the D3-branes full the $3+1$ dimensional volume, leaving a Newtonian potential to be felt in the remaining 6.

Eq. (1.30) will probe length scales where the radius of curvature is much smaller than the string scale $L \ll l_s$ where low energy supergravity fails to be a valid description. On the other hand this very same region is easily calculable in $\mathcal{N} = 4$ SYM with standard perturbative methods. In the opposite regime, $g_s N_c \gg 1$, one avoids the inclusion of massive string states given by $m_s \sim l_s^{-1}$ and supergravity will be applicable, while computing Feynman diagrams for the gauge theory in this region becomes impractical. A further constraint to consider is the suppression of quantum gravity fluctuations controlled by the Planck length $l_p = G_{10}^{1/8}$. These contributions are given by loop diagrams present in the expansion of the closed string interaction amplitude and will be proportional to l_p relative to the radius of curvature. Therefore in order to perform computations with classical supergravity we will require that $l_p^8 \ll L^8$.

Rewriting these conditions in terms of parameters relevant for $\mathcal{N} = 4$ SYM, we can re-express g_s, l_s and G_{10} through Eqs. (1.29), (1.27) and (1.31) to find,

$$\lambda \equiv \left(\frac{L}{l_s}\right)^4 = g_{YM}^2 N_c \,, \quad \left(\frac{l_p}{L}\right)^8 = \frac{G_{10}}{L^8} = \frac{\pi^4}{2N_c^2} \,, \tag{1.34}$$

where the fixed parameter λ is known as the 't Hooft coupling. Therefore the condition that both quantum gravity effects and higher order stringy effects are suppressed translates to the condition that

$$\lambda \gg 1 \,, \quad N_c \gg 1 \,. \tag{1.35}$$

Because this region of parameter space is typically inaccessible for interacting gauge theories with other standard methods, the duality described above offers invaluable insight into gauge theories at strong coupling. Higher order corrections corresponding to the string length l_s/L result in a classical effective action with higher derivative corrections. Therefore we can associate corrections in $1/\lambda$ with higher derivative gravity while corrections in $1/N_c$ correspond to loop corrections when computing the interactions of closed strings.

1.3 The holographic dictionary

Previously we have argued that the $\mathcal{N} = 4$ SYM theory with $SU(N_c)$ gauge group in $3 + 1$ dimensions can be identified with type IIB classical supergravity in the large N_c and large 't Hooft coupling λ limit. Now we will explore how this correspondence can be used to extract useful information from classical gravity to study our CFT at infinite coupling.

Before we explain this process in detail we will first remark on a common simplification which is often used to further reduce the complexity of the $AdS_5 \times S^5$ spacetime in practical computations. For example, a scalar field $\phi(x, \Omega)$ supported on $AdS_5 \times S^5$ can be decomposed into a basis of spherical harmonics

$$\phi(x, \Omega) = \sum_l \phi_l(x) Y_l(\Omega) \,, \tag{1.36}$$

where x and Ω denote the coordinates on the AdS_5 and S^5 subspaces respectively. One may consider solutions which are a consistent trunctation of the full supergravity equations of motion where all but the uniform spherical harmonic are set to zero. The effective action one finds after dimensional reduction is given by

$$S_{\text{reduced}} = \frac{L^5 \Omega_5}{16\pi G_5} \int d^5x \sqrt{-g_5} \left(R_5 + \frac{12}{L^2} \right) \tag{1.37}$$

where the g_5 and R_5 are the determinant and Ricci scalar of the reduced 5-dimensional metric, $\Omega_5 = \pi^3$ is the volume of the unit S^5 and G_5 is the 5 dimensional Newton constant.[8] The specific value of the cosmological constant is fixed when choosing a uniform solution for the anti-symmetric 5-form field strength F_5 which lies in the classical supergravity action of the 10-dimensional theory. Where comparing the action in Eq. (1.37) to the 10-dimensional action in (1.26) and substituting the 10-dimensional Newton's constant found in Eq. (1.34) we can fix

$$G_5 = \frac{G_{10}}{\Omega_5 L^5} \quad \Longrightarrow \quad \frac{G_5}{L^3} = \frac{\pi}{2N_c^2} \,. \tag{1.38}$$

[8] For the general case of S^D, we would find $\Omega_D = \frac{2\pi^{\frac{D+1}{2}}}{\Gamma\left(\frac{D+1}{2}\right)}$.

In the following sections we will suppress the "5" subscript in the metric tensor while replacing the number of dimensions with a general $D = n+1$ with coordinates (x^μ, z) which will be useful in Chapter 3.

Within the AdS/CFT framework boundary values of fields in the AdS bulk can be viewed as sources of gauge-invariant operators in the boundary CFT. More formally, observables in gauge theory can be extracted from the gravity dual by using the GKPW formula [8]

$$\int d\mathcal{O}\, e^{iS_{CFT}[\mathcal{O}]+\int d^n x\, \mathcal{O}(x)\phi_0(x)} \equiv Z_{CFT}\left[\phi_0\right] = Z_{string}\left[\phi(x,z)\big|_{\partial AdS}\right] \approx e^{iS[\phi_0(x)]}\,, \quad (1.39)$$

which relates the generating functionals of the gauge and gravity theories given by Z_{CFT} and Z_{string}. Here Z_{CFT} is the generating functional for an operator $\mathcal{O}(x)$ of the CFT in n spacetime dimensions coupled to source ϕ_0. Z_{string} is the generating functional of a bulk field $\phi(x,z)$ evolving on an AdS spacetime with the condition that $\phi(x,z)$ be related to the dual CFT source $\phi_0(x)$ at the boundary of AdS parameterized by the holographic coordinate z. The precise relation between $\phi_0(x)$ and $\phi(x,z)$ will be made clear below. The final approximation on the RHS of Eq. (1.39) is the result of taking the infinite 't Hooft and large N_c limits, allowing the string generating functional to be described by classical supergravity.

1.3.1 The dual of the scalar field

As an example of this field-operator correspondence we follow [10,43] in considering a minimally coupled scalar of mass m in vacuum AdS, with boundary value determined by $\phi_0(x)$, which through Eq. (1.39) will source a scalar operator $\mathcal{O}(x)$ in the CFT. We will perform our calculation on the static background AdS background in $D = n+1$ dimensions which for the case of $D = 5$ remains a solution of Eq. (1.37),

$$ds^2 = \left(\frac{L}{z}\right)^2 \left(-dt^2 + d\vec{x}^2 + dz^2\right)\,, \quad (1.40)$$

where from the point of view of the boundary field theory $x = (t, \vec{x})$ are the n spacetime dimensions, and z is an auxillary coordinate parameterizing the dual bulk

space. The action for a free scalar field minimally coupled to gravity is given by,

$$S = \frac{1}{2}\int dz d^n x \sqrt{-g}\left[g^{MN}\partial_M\phi\partial_N\phi + m^2\phi^2 + ...\right] , \tag{1.41}$$

where indicies M and N run over all $n+1$ coordinates, the gravity action is hidden in the ellipses, and has an equation of motion given by a simple wave equation $(\Box - m^2)\,\phi(z,x) = 0$. For evolution on a background given by Eq. (1.40), this linear operater has no explicit dependence on x coordinates allowing us to Fourier transform these derivatives into a momentum basis, solve the resulting ODE as a power series in near the $z = 0$ boundary, and transform the solution back to x coordinates. We can find,

$$\phi(z,x) = z^{\Delta_-}A(x)\,(1 + \mathcal{O}(z)) + z^{\Delta_+}B(x)\,(1 + \mathcal{O}(z)) , \tag{1.42}$$

with exponents $\Delta_\pm$ given by

$$\Delta_\pm = \frac{n}{2} \pm \nu\,, \quad \nu = \sqrt{\frac{n^2}{4} + m^2L^2}\,, \quad \Delta_+ + \Delta_- = n\,. \tag{1.43}$$

We can notice immediately for this scalar to be real we require that the mass m satisfies,

$$m^2L^2 \geq -\frac{n^2}{4}\,. \tag{1.44}$$

This inequality is known as the Breitenlohner-Freedman (BF) bound, below which scalar fields in AdS have become unstable [44, 45]. We will restrict our argument to the case where $(mL)^2 \geq 0$ where $\Delta_+ > 0$ and $\Delta_- < 0$, so that the near boundary behaviour of $\phi(x,z)$ will be set by $A(x)$ while the term proportional to $B(x)$ vanishes, which we will call the non-normalizable and normalizable modes respectively.

As motivated in Eq. (1.39) the boundary value of a bulk field ϕ should be identified with the source for the corresponding boundary operator $\mathcal{O}(x)$, which by Eq. (1.42) is controlled by $A(x)$. As such we identify the smooth deformation of the CFT with the non-normalizable mode evaluated at the boundary as,

$$S_{CFT} \to S_{CFT} + \int d^n x\,\phi_0(x)\mathcal{O}(x)\,, \quad \phi_0(x) = A(x)\,, \tag{1.45}$$

where in order to maintain a finite source $\phi_0(x)$ we have factored out the diverging dependence on z,

$$\phi_0(x) = \phi(x,z)\big|_{\partial AdS} = \lim_{z\to 0} z^{\Delta_+ - n}\phi(x,z)\,. \tag{1.46}$$

Taking $A(x) \to 0$ then corresponds to taking the boundary source to zero, as is usual when computing vacuum expectation values for the dual field theory. Performing a scale transformation $x \to \lambda x$, $z \to \lambda z$ we can read off the scaling dimenions of $A(x)$ as $d - \Delta_+$ and $B(x)$ as Δ_+ respectively. Because the deformation Eq. (1.45) is scale invariant this implies that the scaling dimension of $\mathcal{O}(x)$ is Δ_+, the same as $B(x)$, suggesting that $B(x)$ will be proportional to $\langle\mathcal{O}(x)\rangle$.

While we have made some identifications, strictly the action given by Eq. (1.41) will be infinite at the boundary and so any meaningful calculation will need to be renormalized. By introducing a cut off at $z = \epsilon$ one can perform *holographic renormalization* by including local counterterms S_{ct} defined on this cut off surface to cancel all divergences as $\epsilon \to 0$. Following this process we define the finite renormalized action $S^{(ren)}$ as the limit of this sum as the cut off surface approaches the AdS boundary [9, 46–49]. Using this new renormalized action one can fix the constant of proportionality relating $B(x)$ and $\langle\mathcal{O}(x)\rangle$ through the GKPW formula Eq. (1.39),

$$\langle\mathcal{O}(x)\rangle = \frac{\delta S^{(ren)}[\phi]}{\delta\phi_0(x)} \equiv \lim_{z\to 0} z^{n-\Delta_+}\frac{\delta S^{(ren)}[\phi]}{\delta\phi(x,z)} = 2\nu B(x)\,. \tag{1.47}$$

The specifics of this calculation are cumbersome and not particularly enlightening, but can be found in the Appendix of [10]. From this example we learn a general lesson, that the non-normalizable mods of the bulk fields correspond to deformations of boundary field sources while the normalizable modes are given by expectation values of operators in the dual field theory.

1.3.2 The holographic stress tensor

To find the expectation value of the stress tensor one should deform the boundary theory by a candidate source which is a rank two tensor,

$$S_{CFT} \to S_{CFT} + \int d^n x \, \gamma_{\mu\nu}(x) T^{\mu\nu}(x) \,, \tag{1.48}$$

which can be interpreted as a spacetime metric deformation, and from Eq. (1.39) should be associated with the boundary value of a bulk metric $g_{MN}(x,z)$. Therefore we can understand that the evolution of the conserved stress tensor in the translationally-invariant gauge theory should involve the dynamics of gravity in the dual description.

In a similar fashion to Eq. (1.47) a stress tensor can be computed of the form,

$$\langle T^{\mu\nu}(x) \rangle = \lim_{z \to 0} \frac{2}{\sqrt{-g(x,z)}} \frac{\delta S^{(ren)}[g]}{\delta g_{\mu\nu}(x,z)} \,, \tag{1.49}$$

where we have replaced the $g_{MN}(x,z)$ indicies with $g_{\mu\nu}(x,z)$ to exclude the components corresponding to the z coordinate, and the factor of $\frac{1}{\sqrt{-g(x,z)}}$ is needed to ensure that this object is a tensor.

Following the prescription of [49] the renormalized classical gravity action used in Eq. (1.49) is given by,

$$S^{(ren)} = \frac{1}{16\pi G_D} \int_{\mathcal{M}} dz d^n x \sqrt{-g} \left(R + \frac{n(n-1)}{L^2} \right) + \frac{1}{8\pi G_D} \int_{\partial \mathcal{M}} d^n x \sqrt{-\gamma} K - \frac{1}{8\pi G_D} S_{ct}(\gamma_{\mu\nu}) \tag{1.50}$$

where we have included a Gibbons–Hawking boundary term [50] where K is the trace of the extrinsic curvature given by $K_{\mu\nu} = -(\nabla_\mu n_\nu + \nabla_\nu n_\mu)/2$, n_μ is the outward pointing unit normal vector to the boundary, and ∇_μ is the covariant derivative with respect to the induced metric at the boundary $\gamma_{\mu\nu}$. The counter terms S_{ct} can be fixed by requiring that the divergences cancel in Eq. (1.49), which for $n \leq 4$ will give us,

$$S_{ct} = \int_{\partial \mathcal{M}} d^n x \, \sqrt{-\gamma} \left[\frac{n-1}{L} + \frac{L}{2(n-2)} \mathcal{R} \right] \tag{1.51}$$

where $\mathcal{R}$ is the Ricci scalar for the induced metric $\gamma_{\mu\nu}$. For higher dimensions more counter terms will be required, but these will not be relevant in this thesis. Putting these together one finds,

$$\langle T_{\mu\nu}(x)\rangle = \lim_{z\to 0}\frac{1}{8\pi G_D}\frac{L^{n+2}}{z^{n+2}}\left[K_{\mu\nu} - \gamma_{\mu\nu}K - \frac{n-1}{L}\gamma_{\mu\nu} - \frac{L}{n-2}\mathcal{G}_{\mu\nu}\right], \tag{1.52}$$

where $\mathcal{G}_{\mu\nu}$ is the Einstein tensor given by $\gamma_{\mu\nu}$. To lighten notation in the rest of this thesis we will refer to the expectation value of the boundary stress tensor as $T_{\mu\nu} \equiv \langle T_{\mu\nu}(x)\rangle$. In later chapters we will use Eq. (1.52) to extract the energy density associated with specific gravity solutions in non-equilibrium contexts.

1.3.3 The static AdS-blackbrane and thermodynamic properties

In Section 1.2 we related type IIB string theory to $\mathcal{N} = 4$ SYM at zero temperature but this discussion can be generalized to non-zero temperatures by exciting degrees of freedom on the N_c D3-branes [7, 51]. On the gravity side this modification is made manifest through the appearance of a horizon in the $AdS_5 \times S^5$ spacetime. After the standard program of dimensional reduction one will be left with a static AdS-blackbrane metric, written in general dimensions as[9]

$$ds^2 = \left(\frac{L}{z}\right)^2\left(-f(z)dt^2 + d\vec{x}^2 + \frac{dz^2}{f(z)}\right), \tag{1.53}$$

with $f(z) = 1 - \left(\frac{z}{z_h}\right)^n$. We can note that this thermal system explicitly breaks supersymmetry as well as scale invariance by introducing a dimensionful constant z_h.

Applying Eq. (1.52) we find that the stress tensor resulting from this solution can be computed as,

$$T_{\mu\nu} = \frac{1}{16\pi G_D}\frac{L^{n-1}}{z_h^n}\left[\eta_{\mu\nu} + n\,\delta_{\mu 0}\delta_{\nu 0}\right]. \tag{1.54}$$

We learn that the gravity solution of an AdS blackhole corresponds to a state containing matter in the dual field theory. Black objects in General Relativity are known to carry a Hawking temperature T given by defining a Euclidean time coordinate with

[9] The usual AdS/CFT correspondence will correspond to the case of $n = 4$.

fixed period $\beta = 1/T = \pi z_h$ set by solution continuity. One could speculate if this Hawking temperature is related to the temperature of a thermal medium in the dual field theory. This intuition is correct as can be seen from the GKPW formula of Eq. (1.39) the introduction of a periodic Euclidean time coordinate on the gravity side automatically turns the LHS of the equation into a thermal expectation value with temperature T as the time coordinates are required to be the same on both sides of the duality [7].

Similarly the entropy of the field theory can be identified with the Bekenstein-Hawking entropy, which is calculated from the area of the horizon

$$s_{BH} = \frac{S_{BH}}{\int dx_1 ... dx_{n-1}} = \frac{\sqrt{-g}}{4G_D \int dx_1 ... dx_{n-1}} = \frac{1}{4G_D}\left(\frac{L}{z_h}\right)^{n-1} , \tag{1.55}$$

where anticipating that the total entropy of a blackbrane extending over an infinite transverse volume will be infinite, we have defined s_{BH} as the finite entropy density per unit volume. Identifying the result of Eq. (1.55) with the entropy of the dual theory $s = s_{BH}$ we write the thermodynamic quantities for $\mathcal{N} = 4$ SYM in terms of the temperature, in the limit of large N_c and infinite 't Hooft coupling,

$$\epsilon = \frac{3}{8}\pi^2 N_c^2 T^4 , \quad p_{eq} = \frac{1}{8}\pi^2 N_c^2 T^4 , \quad s = \frac{1}{2}\pi^2 N_c^2 T^3 . \tag{1.56}$$

where we have fixed $n = 4$ and used Eq. (1.38) to fix the value of Newton's constant. As a check we can easily verify that the quantities of Eq. (1.56) are consistent with the thermodynamic relation $\epsilon = -p_{eq} + Ts$, as expected for the static system.

Away from equilibrium the stress tensor given by Eq. (1.52) can always be defined, however in this region thermodynamic quantities do not have an unambiguous meaning. One can however define notions of a dimensionally correct out of equilibrium effective temperature through ϵ in a fashion similar to Eq. (1.17). Similarly, horizons are dynamical objects whose areas can in principle always be determined. An issue arises here in that multiple surfaces exist out of equilibrium on which to define an effective entropy. Proposals for a non-equilibrium entropy have been explored holographically for the apparent [52] and event horizon [53], and near local equilibrium through the fluid gravity correspondence [54–57].

Chapter 2

Transseries solutions of holographic theories

One major insight for the study of strongly coupled, many body systems has been the use of hydrodynamics as a perturbative expansion in small gradients about a local equilibrium state. In this chapter we summarize some of the key findings of [1, 2] by explicitly constructing the transseries expansion (in gradients) of an $\mathcal{N} = 4$ SYM plasma undergoing Bjorken flow at infinite 't Hooft coupling and large N_c. This solution completes the hydrodynamic gradient expansion with additional sectors which are non-perturbative in the gradient.

We go on to confirm a curious property of the transseries, that distinct sectors in the theory can be used to recover information about other transseries sectors. Next we apply a basic resurgence analysis to Gauss-Bonnet gravity, a toy model for finitely coupled holographic gauge theories, to estimate the typical path of evolution for a system far from equilibrium towards the hydrodynamic regime. As such we constrain the location of a special *attractor* trajectory to which other solutions rapidly converge.

2.1 Introduction and motivation

The discovery and ongoing study of the quark-gluon plasma (QGP) has lead to a burst of activity attempting to understand this new phase of matter. Strong multi-particle correlations observed in heavy ion collisions both at RHIC [11–13] and the LHC [14–16] and the successful description of this phenomena via hydrodynamical

modelling [58–63] motivate an exploration into relativistic hydrodynamics and its emergence from microscopic theories. One of the most surprising observations of this program is the finding that a hydrodynamic description can accurately describe the bulk properties of the QGP in the presence of extreme pressure gradients [64], challenging our understanding of hydrodynamics as a long distance effective theory with applicability in the regime where gradients are small. In addition the relaxation of the system to relativistic hydrodynamics occurs over a rapid timescale with the mechanism of this fast equilibration being unknown from first principles.

Consistent with these phenomenological findings, numerical experiments constructing the full evolution of the stress tensor given by the strongly coupled limit of $\mathcal{N} = 4$ SYM explicitly show that this evolution can be approximated by hydrodynamics far from local thermal equilibrium [65–69]. Similar results can be found for weakly coupled gauge theories obeying a kinetic theory description [70].

Within the context of Bjorken flow these numerical analyses led Heller and Spaliński to suggest the existence of a hydrodynamic attractor [32] which may be considered as an extension of hydrodynamics beyond local thermal equilibrium [71]. These are special time dependent configurations to which all other boost invariant evolutions of the system converge at different times. Such solutions appear to have been found in Müller-Israel-Stewart (MIS) [32, 72] and Baier-Romatschke-Son-Starinets-Stephanov (BRSSS) [27, 73] hydrodynamics, $\mathcal{N} = 4$ SYM and kinetic theory [71, 74, 75] and anisotropic hydrodynamics [76] as well as in non-conformal theories and theories with less symmetric flows [77–80]. For reasons not well understood, the attractors of these theories were well approximated by first order hydrodynamics even while the system remained highly anisotropic; indicating the presence of large gradient corrections.

In subsection 1.1.3 we briefly studied the behaviour of MIS theory and found an equation describing Bjorken-like dynamics far from equilibrium, which could be solved for a finite number of solutions. It stands to reason that an attractor solution may be identified, or at least approximated, through the full solution of the equations of motion which was given there by the transseries [32, 74]. In addition the observed

rapid decay to hydrodynamics may be a characteristic feature of the exponential form of the non-hydrodynamic modes, completing the hydrodynamic description through a transseries solution.

To further understand the evolution of highly non-equilibrium states towards hydrodynamics in the QGP, in this chapter we will similarly construct the transseries solution for realistic gauge theories at strong coupling undergoing Bjorken expansion. Here we will use the AdS/CFT correspondence to study the infinite 't Hooft coupling limit of $\mathcal{N}=4$ SYM through the classical Einstein's equations [6,10]. While this theory is very different from QCD, they are qualitatively similar at finite temperature and the correspondence can be used to give a useful picture of QGP dynamics. In addition we will relax the limit of infinite coupling by performing computations in Gauss-Bonnet gravity, a toy model known to qualitatively replicate features of $\mathcal{N}=4$ SYM at intermediate coupling [81].

The late time expansion for holographic Bjorken flow in $\mathcal{N}=4$ SYM was first studied analytically in [26,82], and then computed to high orders in [1,28]. With the aim of extending this program to a transseries expansion we first outline some basic notation to be used in this chapter. We will find the transseries solution describing the energy density of the holographic dual to take the following form,

$$\epsilon\left(u,\boldsymbol{\sigma}\right)=g_{*}\Lambda^{4}\sum_{\boldsymbol{n}\in\mathbb{N}_{0}^{\infty}}\boldsymbol{\sigma}^{\boldsymbol{n}}\,\mathrm{e}^{-\boldsymbol{n}\cdot\boldsymbol{A}\,u}\,\Phi_{\boldsymbol{n}}\left(u\right)\ ,\quad\Phi_{\boldsymbol{n}}\left(u\right)=u^{-\beta_{\boldsymbol{n}}}\sum_{m=0}^{+\infty}\epsilon_{m}^{(\boldsymbol{n})}\,u^{-m}\,,\tag{2.1}$$

where $\Phi_{\boldsymbol{n}}\left(u\right)$ is an infinite sum given by coefficients $\epsilon_{m}^{(\boldsymbol{n})}$ where $\epsilon_{0}^{(\boldsymbol{n})}\neq0$, $\beta_{\boldsymbol{n}}$ is a parameter known as the *characterist exponent*, and the expansion parameter u will be the inverse gradient correction as given in subsection (1.1.2) by $u=\left(\Lambda\tau\right)^{2/3}$ for proper time τ and dimensionful scale Λ, and g_{*} is the constant set by the equation of state, which for $\mathcal{N}=4$ SYM will be $g_{*}=\frac{3N_{c}^{2}\pi^{2}}{8}$. Following Ref. [28] we will set $\Lambda=\pi^{-1}$. The *exponential weights* appearing in Eq. (2.1) are expressed as an infinite dimensional vector of complex numbers. While it need not be the case in general, we will anticipate the result that these exponential weights appear in complex conjugate

pairs for $\mathcal{N}=4$ SYM by writing this vector as,

$$\boldsymbol{A} = \left(A_1, \overline{A_1}, A_2, \overline{A_2}, \cdots\right) \ . \tag{2.2}$$

The sum in Eq. (2.1) runs over every possible value of the infinite dimensional vector

$$\boldsymbol{n} = (n_1, n_{\bar{1}}, n_2, n_{\bar{2}}, \cdots) \ , \tag{2.3}$$

where the components n_i and $n_{\bar{i}}$ of $\boldsymbol{n}$ are non-negative integers. The product $\boldsymbol{n}\cdot\boldsymbol{A}$ then simply picks out some combination of the exponential weights for the argument of the exponential function for a given $\boldsymbol{n}$ from the sum. Lastly we define,

$$\boldsymbol{\sigma}^{\boldsymbol{n}} \equiv \sigma_1^{n_1}\, \sigma_{\bar{1}}^{n_{\bar{1}}}\, \sigma_2^{n_2}\, \sigma_{\bar{2}}^{n_{\bar{2}}}\, \cdots \tag{2.4}$$

as a product of complex constants σ_i known as *transseries parameters*. These coefficients are abitrary and encode the initial data of our system far from equilibrium.[1]

To build some intuition for Eq. (2.1) we first consider the series resulting from the $\boldsymbol{n}=(0,0,0,\cdots)$ term. This contribution is the least suppressed by the exponential weights and takes the form,

$$\epsilon_{\text{hydro}}\,(u) \equiv \Phi_{\mathbf{0}}\,(u) = u^{-\beta_{\mathbf{0}}} \sum_{m=0}^{+\infty} \epsilon_m^{(\boldsymbol{n})}\, u^{-m} \, . \tag{2.5}$$

This perturbative series (at large u) will be called the *hydrodynamic series* or *hydrodynamic sector*, taking the same form as Eq. (1.16) where in $n=4$ spacetime dimensions we will have $\beta_{\mathbf{0}}=2$.

Next we consider the case where $\boldsymbol{n}=\boldsymbol{e}_i$ is 1 in some component i and zero for all other components. In such a case the energy density receives a contribution of the form,

$$\delta\epsilon(u) \sim \sigma_i u^{\beta_{\boldsymbol{e}_i}} e^{-A_i u}\, \Phi_{\boldsymbol{e}_i}(u)\,, \tag{2.6}$$

which is similar to the non-hydrodynamic contribution seen in Eq. (1.23). We name these non-perturbative contributions *fundamental sectors*, and note that σ_i can naturally be identified with their normalization. These constants however are not independent, as imposing that the energy density be real will imply that $\sigma_{\bar{i}} = \overline{\sigma}_i$. Note

[1] For our considerations there will be an additional overall normalization set by our choice of $\epsilon_0^{\mathbf{0}}$, but this does not change anything qualitative in what we have presented.

that implicitly by Eqs. (2.2) and (2.3) we have defined $\boldsymbol{e}_k$ and $\overline{\boldsymbol{e}}_k$ to have components which are only non-zero in slots $2k-1$ and $2k$ respectively.

Lastly Eq. (2.1) includes terms where $\boldsymbol{n}$ corresponds to a linear combination of basis vectors $\boldsymbol{e}_i$ which we will refer to as *mixed sectors*. These non-hydrodynamic contributions are completely determined by the fundamental and hydrodynamic sectors and contain no new data. They can be viewed as the non-linear backreaction to the excitation of a fundamental sector.

As found by [28] when originally computing the hydrodynamic sector of $\mathcal{N}=4$ SYM in Bjorken flow, the coefficients diverge as $\epsilon^{\mathbf{0}}_m \sim m!$ for large m and the sector is classified formally as a Gevrey-1 series. At first glance this may seem a surprise, that far be it from having an extended regime of applicability, the hydrodynamic series instead has zero radius of convergence. This asymptotic behaviour however is typical of transseries solutions as given by Eq. (2.1), and can be sensibly examined through Ecalle's theory of resurgence [5]. A striking property of such expansions is that the large order behaviour of coefficients in each sector can be used to recover information about other sectors in the theory.

We organize this chapter as follows: in Section 2.2 we construct a transseries solution for the gravitational dual to the Bjorken evolution of $\mathcal{N}=4$ SYM plasma. In Section 2.3 we analyse the resurgent structure of the resulting coefficients and explicitly show that we can reconstruct coefficients from the leading non-hydrodynamic sector purely from the coefficients of the hydrodynamic sector. In Section 2.4 we construct the hydrodynamic series for a family of Gauss-Bonnet gravity duals to include the effects of intermediate coupling in our set up. Using these series we estimate the location of the attractor solution for realistic values of the coupling. Finally in Section 2.5 we summarise our main results and discuss future applications of this work.

2.2 The holographic transseries solution

Holographic duals of Bjorken-like flows in $\mathcal{N}=4$ have been explored by finding boost invariant solutions of the dual gravity theory [65, 82–85]. This is achieved by imposing an Eddington-Finkelstein type ansatz for the metric of the 5-D space satisfying boost invariance and transverse homogeneity, which limits to an asymptotically AdS_5 spacetime on the boundary.[2] Our ansatz takes the form,

$$ds^2 = -A(r,\tau)d\tau^2 + 2drd\tau + S(r,\tau)^2\left(e^{-2B(r,\tau)}dy^2 + e^{B(r,\tau)}dx_\perp^2\right), \tag{2.7}$$

where (τ, y, x_1, x_2) reduce to the proper time, rapidity and transverse spatial dimensions on this $r\to\infty$ conformal boundary. While this gauge cannot describe the dual space-time at $\tau = 0$ [86], it is a convenient form to describe the dynamics for any $\tau > 0$ as Einstein's equations follow the compact sequential form [66, 87],

$$S'' = -\frac{1}{2}S\left(B'\right)^2, \tag{2.8}$$

$$S\dot{S}' = 2S^2 - 2\dot{S}S', \tag{2.9}$$

$$S\dot{B}' = -\frac{3}{2}\left(\dot{S}B' + \dot{B}S'\right), \tag{2.10}$$

$$A'' = -3\dot{B}B' - 4 + 12\frac{\dot{S}S'}{S^2}, \tag{2.11}$$

$$\ddot{S} = \frac{1}{2}\left(\dot{S}A' - \dot{B}^2S\right), \tag{2.12}$$

where $f' = \partial_r f$ and $\dot{f} = \left(\partial_\tau + \frac{1}{2}A(r,\tau)\partial_r\right)f$. Note that these two derivative operators do not commute, and that for any metric function X we denote $\dot{X}' \equiv \left(\dot{X}\right)'$, i.e. the r-derivative here is always applied last. The form of the equations given by Eqs. (2.8)–(2.12) will reoccur through the following chapters, but in order to make the connection with [1, 28] we will make the re-definitions,

$$A(r,\tau) = r^2\tilde{A}(r,\tau) \tag{2.13}$$

$$B(r,\tau) = \frac{1}{3}\left(\log\left(\frac{r^2}{(r\tau+1)^2}\right) + d(r,\tau) - \frac{1}{2}b(r,\tau)\right) \tag{2.14}$$

$$S(r,\tau) = r^{2/3}(1+r\tau)^{1/3}\exp\left(\frac{1}{3}d(r,\tau)\right) \tag{2.15}$$

[2] Einstein's equations given here with cosmological constant $\Lambda = -6$ are given by $R_{\mu\nu} + 4g_{\mu\nu} = 0$.

to express Eq. (2.7) in a form convenient for the large-τ expansion,

$$ds^2 = -r^2 \tilde{A}\, d\tau^2 + 2 d\tau dr + (r\tau + 1)^2 e^b dy^2 + r^2 e^{-\frac{1}{2}b+d} dx_\perp^2 \ . \tag{2.16}$$

For Eq. (2.16) to reduce to a flat, boost-invariant solution at the boundary we enforce the conditions

$$\lim_{r\to\infty} \tilde{A}(r,\tau) = 1 \ , \qquad \lim_{r\to\infty} b(r,\tau) = 0 \ , \qquad \lim_{r\to\infty} d(r,\tau) = 0 \ . \tag{2.17}$$

As explained in Subsection 1.1.2, for ideal Bjorken flow the local effective temperature of the plasma at the 4-dimensional Minkowski space boundary should behave as $T \sim \tau^{-\frac{1}{3}}$ at late times. We therefore fix the combination $s = \frac{1}{r}\tau^{-\frac{1}{3}}$ so that in the late time limit the naive location of the horizon in the s coordinate will remain finite. Noting that gradient corrections behave as $\frac{1}{\tau T} \sim \tau^{-\frac{2}{3}}$, we fix $u = \tau^{\frac{2}{3}}$ and expand the metric functions in inverse powers of the inverse gradient u. Fixing a horizon at $s_h = 1$ these coordinates will span $0 < s < 1$ and $u > 0$ with late times corresponding to large u.

Keeping in mind that we hope to extract the full transseries solution, we consider an ansatz for the metric functions of the form

$$\tilde{A}(r,\tau) = \sum_{\boldsymbol{n}\in\mathbb{N}_0^\infty} \Omega_{\boldsymbol{n}}(u) \sum_{i=0}^{\infty} u^{-i} A_i^{(\boldsymbol{n})}(s) \ , \tag{2.18}$$

$$b(r,\tau) = \sum_{\boldsymbol{n}\in\mathbb{N}_0^\infty} \Omega_{\boldsymbol{n}}(u) \sum_{i=0}^{\infty} u^{-i} b_i^{(\boldsymbol{n})}(s) \ , \tag{2.19}$$

$$d(r,\tau) = \sum_{\boldsymbol{n}\in\mathbb{N}_0^\infty} \Omega_{\boldsymbol{n}}(u) \sum_{i=0}^{\infty} u^{-i} d_i^{(\boldsymbol{n})}(s) \ . \tag{2.20}$$

where

$$\Omega_{\boldsymbol{n}}(u) \equiv u^{-\boldsymbol{n}\cdot\boldsymbol{\alpha}}\, \mathrm{e}^{-\boldsymbol{n}\cdot\boldsymbol{A}\, u} \ . \tag{2.21}$$

As already described in the introduction $\boldsymbol{n} = (n_1, n_{\bar{1}}, n_2, n_{\bar{2}}, \cdots) \in \mathbb{N}_0^\infty$ is an infinite dimensional vector of non-negative, integer components which will be used to define the space of solutions. We will use the field equations to determine the quantities $\boldsymbol{A} = \left(A_1, \overline{A_1}, A_2, \overline{A_2}, \cdots\right)$ and $\boldsymbol{\alpha}$ which correspond to particular non-hydrodynamic

sectors.[3] We will denote the hydrodynamic sector by $\mathbf{0}$ and define unit vectors $\boldsymbol{e}_k$ which have all zero entries except the $2k-1$ entry which will be set equal to 1. $\overline{\boldsymbol{e}}_k$ is similarly defined to have only the $2k$ entry non-zero. Under this definition scalar products with $\boldsymbol{A}$ select the corresponding exponential weights, so that $\boldsymbol{e}_k \cdot \boldsymbol{A} = A_k$, and $\overline{\boldsymbol{e}}_k \cdot \boldsymbol{A} = \overline{A_k}$.

After substituting our ansatz into Eqs. (3.15) to (3.19), the linear independence of $\Omega_{\boldsymbol{n}}(u)$ will result in an infinite hierarchy of equations. These equations can again be expanded in inverse powers of u to find linear ODEs for the functions $A_i^{(\boldsymbol{n})}$, $b_i^{(\boldsymbol{n})}$ and $d_i^{(\boldsymbol{n})}$. We use residual gauge invariance to set the radial coordinate r to keep the horizon fixed at $s=1$ at every order, which sets $A_i^{(\boldsymbol{n})}(s=1)=0$. By imposing regularity in the bulk and flatness at the boundary for each metric function we are able to find solutions at each order.

2.2.1 Hydrodynamic and non-hydrodynamic sectors

The case of $\boldsymbol{n}=\mathbf{0}$ will be referred to as the hydrodynamic sector. Any power of $\Omega_{\boldsymbol{n}\neq\mathbf{0}}(u)$ that enters into the equations of motion will remain linearly independent from terms proportional to $\Omega_{\mathbf{0}}(u)$. Therefore $A_i^{(\mathbf{0})}$, $b_i^{(\mathbf{0})}$ and $d_i^{(\mathbf{0})}$ can be found independent of the solutions to any other sector. The zero-th order solution (in our chosen gauge) that preserves flatness and bulk regularity will be given by a boosted blackbrane written as [83],

$$d_0^{(\mathbf{0})}(s) = 0 \ , \quad A_0^{(\mathbf{0})}(s) = 1 - s^4 \ , \quad b_0^{(\mathbf{0})}(s) = 0 \ . \tag{2.22}$$

The cases of $\boldsymbol{n}=\boldsymbol{e}_k$ and $\boldsymbol{n}=\overline{\boldsymbol{e}}_k$ are called the fundamental sectors.[4] Equations linear in $\Omega_{\boldsymbol{e}_k}(u)$ can depend on only the hydrodynamic sector and solutions within its own fundamental sector, and again has no influence from higher sectors. The zero-th order solution in each case is given by,

$$d_0^{(\boldsymbol{e}_k)}(s) = 0 \ , \quad A_0^{(\boldsymbol{e}_k)}(s) = 0 \ , \quad b_0^{(\boldsymbol{e}_k)}(s) = Z_{\boldsymbol{e}_k}(s) \ , \tag{2.23}$$

[3] Note that we will assume that each component of $\boldsymbol{A}$ is not an integer multiple of another component.

[4] In the discussion that follows one can exchange $\boldsymbol{e}_k$ for $\overline{\boldsymbol{e}}_k$ where appropriate.

where $Z_{\boldsymbol{e}_k}(s)$ satisfies

$$\left(s(1-s^4)\partial_s^2 - (3+s^4-2\,\mathrm{i}\,\boldsymbol{e}_k\cdot\boldsymbol{\omega}\,s)\partial_s - 3\,\mathrm{i}\,\boldsymbol{e}_k\cdot\boldsymbol{\omega}\right) Z_{\boldsymbol{e}_k}(s) = 0\ , \tag{2.24}$$

and where we have defined $\boldsymbol{\omega} = -\frac{2\mathrm{i}}{3}\boldsymbol{A}$. We can recognize Eq. (2.24) as the Quasi-normal Mode (QNM) equation given in infalling EF coordinates at zero momentum [88, 89]. Imposing flatness and regularity in $Z_{\boldsymbol{e}_k}(s)$ turns Eq. (2.24) into an eigenvalue problem with an infinite number of solutions $\boldsymbol{\omega}$. We take the eigenvalues $\boldsymbol{\omega}$ with negative real part to correspond to the unit vector $\boldsymbol{e}_k$, and those with positive real part to correspond to $\overline{\boldsymbol{e}}_k$, with index k ordering them naturally by the negative imaginary part of each eigenvalue. The infinite dimensional vectors $\boldsymbol{e}_k$ and $\overline{\boldsymbol{e}}_k$ can now be understood as spanning the space of QNM frequencies. Retrospectively one may have expected the gapped QNMs to be related to the non-hydrodynamic modes of the dual theory, as these are the modes which do not vanish at small momentum.

Each eigenfunction $Z_{\boldsymbol{e}_k}(s)$ is determined up to an arbitrary integration constant associated with the choice of $Z_{\boldsymbol{e}_k}(s=1)$, which we will later identify as the transseries parameter. This freedom comes from the fact that (along with imposing flatness at the boundary) we only require $Z_{\boldsymbol{e}_k}(s)$ to be regular in the bulk, allowing a family of solutions which satisfy this condition. We can interpret each associated sector as an independent non-hydrodynamic excitation. The vector $\boldsymbol{\alpha}$ is fixed through a similar eigenvalue problem at order $i=1$. Our numerically computed values of $\boldsymbol{\alpha}$ and $\boldsymbol{A}$ satisfy $\boldsymbol{\alpha} = \frac{\boldsymbol{A}}{6}$ with high precision.[5]

Finally we consider the mixed sectors where $\boldsymbol{n} \neq \boldsymbol{e}_k$. Once we have fixed $\boldsymbol{\omega}$ in Eq. (2.24), if we replaced $\boldsymbol{e}_k$ by a general vector $\boldsymbol{n}$, then this equation would have no non-trivial solutions obeying the chosen boundary conditions for $\boldsymbol{n} \neq \boldsymbol{e}_k$. All

[5] A heuristic argument for this value is suggested by Refs. [28,83]. At late times $\Omega_{\boldsymbol{e}_k}(u)$ is expected take the form of a decaying mode with frequency ω_k in an adiabatically evolving plasma of effective temperature $T \sim \epsilon^{1/4}$. We hope to capture this dependence in $\Omega_{\boldsymbol{e}_k}(u)$ which we write as,

$$\Omega_{\boldsymbol{e}_k}(u) \sim \exp\left(\mathrm{i}\,\omega_k \int d\tau\, T\right) = \exp\left(\mathrm{i}\,\frac{3}{2}\omega_k\left(u - \frac{1}{6}\log u + \mathcal{O}(u^{-1})\right)\right), \tag{2.25}$$

where the dependence on $T(\tau)$ in the argument of the exponential has been set by conformality. From here we can read off $\boldsymbol{A} = \frac{3\mathrm{i}}{2}\boldsymbol{\omega}$ and $\boldsymbol{\alpha} = \frac{\boldsymbol{A}}{6}$ for each individual mode.

functions $A_i^{(\boldsymbol{n})}$, $b_i^{(\boldsymbol{n})}$ and $d_i^{(\boldsymbol{n})}$ for $\boldsymbol{n} \neq \boldsymbol{e}_k, \overline{\boldsymbol{e}}_k$ and $i \geq 0$ will be fully determined by solutions in the hydrodynamic and the fundamental sectors, and so will contain no free integration constants. In this way these sectors can be viewed as a cascade of interactions of the fundamental modes rather than independent solutions.

2.2.2 Series solution and numerical implementation

Subsequent equations of motion for $i \geq 1$ where $\boldsymbol{n} = \boldsymbol{0}$, $\boldsymbol{e}_k$ or $\overline{\boldsymbol{e}}_k$, (and for $i \geq 0$ where $\boldsymbol{n} \neq \boldsymbol{e}_k$ and $\boldsymbol{n} \neq \overline{\boldsymbol{e}}_k$) can be found by directly substituting Eqs. (2.18) to (2.20) into Eqs. (3.15) to (3.17). They can be written respectively as

$$\mathcal{L}^d_{\boldsymbol{n}} d_i^{(\boldsymbol{n})} = j_i^{d,\boldsymbol{n}} \,, \tag{2.26}$$

$$\mathcal{L}^A_{\boldsymbol{n}} A_i^{(\boldsymbol{n})} = j_i^{A,\boldsymbol{n}} \,, \tag{2.27}$$

$$\mathcal{L}^b_{\boldsymbol{n}} b_i^{(\boldsymbol{n})} = j_i^{b,\boldsymbol{n}} \,, \tag{2.28}$$

where $j_i^{d,\boldsymbol{n}}$, $j_i^{A,\boldsymbol{n}}$ and $j_i^{b,\boldsymbol{n}}$ are source terms, which are sequentially given in terms of solutions at lower orders in i, and solutions at the same order which are determined when solving the equations in sequential order from (2.26) to (2.28). The linear operators above have relatively simple forms,

$$\mathcal{L}^d_{\boldsymbol{n}} = \partial_s^2 \,, \tag{2.29}$$

$$\mathcal{L}^A_{\boldsymbol{n}} = s\partial_s - 4 \,, \tag{2.30}$$

$$\mathcal{L}^b_{\boldsymbol{n}} = s(1-s^4)\partial_s^2 - (3 + s^4 - 2i\,\boldsymbol{n}\cdot\boldsymbol{\omega}\, s)\partial_s - 3i\,\boldsymbol{n}\cdot\boldsymbol{\omega} \,. \tag{2.31}$$

In our chosen gauge, Eq. (3.19) can be written as a constraint at $s = 1$,

$$d_i^{(\boldsymbol{n})}(1) = J_i^{(\boldsymbol{n})} \,, \tag{2.32}$$

with $J_i^{(\boldsymbol{n})}$ a number determined by lower order solutions. Eq. (2.11) is redundant, being implied by the other four equations.

The implementation of the numerical methods used in this paper are a continuation of the techniques used in Ref. [28]. To integrate Eqs. (2.26) to (2.28) we

use Chebyshev spectral methods [90] with 400 grid points over the $s \in [0,1]$ radial coordinate with a minimum of 240 digits of numerical precision.[6]

As mentioned before, in our gauge we have chosen the warp factor $A(r,t)$ to vanish at the naive location of the horizon ($s=1$) which results in the boundary condition that $A_i^{(\boldsymbol{n})}(s=1)=0$. Imposing the constraint given by Eq. (2.32), and standard flatness and regularity conditions (that all functions $d_i^{(\boldsymbol{n})}$, $A_i^{(\boldsymbol{n})}$ and $b_i^{(\boldsymbol{n})}$ vanish at $s=0$ and are regular at $s=1$) fully determines the system for $i \geq 1$ for the hydrodynamic sector, $i \geq 2$ for the fundamental sectors, and $i \geq 0$ for the mixed sectors.

A non-obvious implementation is that of $i=1$ for the fundamental non-hydrodynamic sectors, where the parameter $\boldsymbol{\alpha}$ must be tuned so as to allow a solution for $b_1^{(\boldsymbol{e_k})}$ which vanishes at $s=0$. For $\boldsymbol{\alpha}=\frac{\boldsymbol{A}}{6}$ this condition is satisfied for any finite value of $b_1^{(\boldsymbol{e_k})}(s=1)$ at the horizon. For $i \geq 1$, the value of $b_i^{(\boldsymbol{e_k})}$ at the horizon ($s=1$) must be chosen so as to fix $b_{i+1}^{(\boldsymbol{e_k})}(s=0)=0$. This was employed in our code via a shooting method.

2.2.3 Energy density of the dual theory

Unlike the stress tensor computed for the static blackbrane given in Eq. (1.54) the geometry under consideration here has τ dependent asymptotics. This means that Eq. (1.54) will not be applicable here and we must instead repeat the computation of Eq. (1.52) in our new set-up. Performing an expansion about $r=\infty$ we can always choose a gauge allowing us to write the near boundary expansion in the form,

$$A(r,\tau)=r^2\left(1-\frac{f(\tau)}{r^4}+\ldots\right), \quad b(r,\tau)=\frac{g(\tau)}{r^4}+\ldots, \quad d(r,\tau)=\frac{h(\tau)}{r^4}+\ldots, \tag{2.33}$$

where the ellipses indicate higher orders in $1/r$ which will not be needed, and $f(\tau)$, $g(\tau)$ and $h(\tau)$ are arbitrary functions related by the equations of motion. As shown in Subsection 1.1.2, imposing the symmetries of conformal Bjorken flow and the conservation of the stress tensor leads to a $T_{\mu\nu}$ expressible in terms of a single function $f(\tau)$. We need only fix the T_{00} component of the energy momentum tensor and Eqs.

[6] In each case the computation could be done on a typical laptop to high orders within several hours.

(1.10) and (1.11) will determine the transverse and longitudinal pressure. Applying the near boundary expansion of Eq. (2.33) we can relate the bulk geometry to the expectation value of the boundary stress tensor (see Eq. (1.54)) to be

$$\begin{aligned} T_{\mu\nu} &= \text{diag}\left(\epsilon, \tau^2 p_L, p_T, p_T\right)_{\mu\nu} , \\ &= \frac{3N_c^2}{8\pi^2}\,\text{diag}\left(f(\tau), -\tau^3 f'(\tau) - \tau^2 f(\tau), f(\tau) + \frac{1}{2}\tau f'(\tau), f(\tau) + \frac{1}{2}\tau f'(\tau)\right)_{\mu\nu} . \end{aligned} \tag{2.34}$$

Re-expressing our solution in terms of $u = \tau^{\frac{2}{3}}$ and $s = \frac{1}{r}\tau^{-\frac{1}{3}}$ we can write,

$$f(\tau) = \sum_{\boldsymbol{n}\in\mathbb{N}_0^\infty} \boldsymbol{\sigma}^{\boldsymbol{n}}\, \Omega_{\boldsymbol{n}}(u) \left(u^{-2} \sum_{i=0} f_i^{(\boldsymbol{n})} u^{-i}\right) \tag{2.35}$$

where the coefficients $f_i^{(\boldsymbol{n})}$ can be read from our gravity solution as

$$f_i^{(\boldsymbol{n})} = -\frac{1}{4!}\frac{d^4}{ds^4} A_i^{(\boldsymbol{n})}(s=0)\,. \tag{2.36}$$

The factor of $\boldsymbol{\sigma}^{\boldsymbol{n}}$ (see Eq. (2.4)) is introduced into Eq. (2.35) so that the dependence on the choice of initial condition is explicit in the energy density. For generic $\boldsymbol{n}$, some number of the first coefficients $f_i^{(\boldsymbol{n})}$ in the sum (2.36) will be zero. For convenience we define $\epsilon_0^{(\boldsymbol{n})}$ to be the first non-zero coefficient of $f_i^{(\boldsymbol{n})}$ (with $\epsilon_i^{(\boldsymbol{n})}$, $i > 0$ given by the subsequent coefficients), and absorb the shift of the index into the definition of the characteristic exponent, which will be given by $\beta_{\boldsymbol{n}}$. One then arrives at the final formula for the energy density in the form of a transseries, given in Eq. (2.1), which we repeat here for convenience,

$$\epsilon\,(u, \boldsymbol{\sigma}) = g_* \Lambda^4 \sum_{\boldsymbol{n}\in\mathbb{N}_0^\infty} \boldsymbol{\sigma}^{\boldsymbol{n}}\, \mathrm{e}^{-\boldsymbol{n}\cdot\boldsymbol{A}\, u}\, \Phi_{\boldsymbol{n}}\,(u) \quad , \quad \Phi_{\boldsymbol{n}}\,(u) = u^{-\beta_{\boldsymbol{n}}} \sum_{m=0}^{+\infty} \epsilon_m^{(\boldsymbol{n})}\, u^{-m}\,. \tag{2.37}$$

The coefficients $\epsilon_k^{(\boldsymbol{n})}$ were computed in [2] and are included in that submission for sectors $\Phi_{\boldsymbol{n}}$ with $\boldsymbol{n} = \boldsymbol{e}_1$, $\boldsymbol{e}_2$, $2\boldsymbol{e}_1$, $(\boldsymbol{e}_1 + \overline{\boldsymbol{e}}_1)$, along with their corresponding exponential weights A_i and characteristic exponents $\beta_{\boldsymbol{n}}$. For the hydrodynamic sector $\boldsymbol{n} = \boldsymbol{0}$ coefficients for the hydrodynamic expansion were taken from [1].

The normalisations for the hydrodynamic series $\Phi_{\boldsymbol{0}}$ and for each fundamental sectors $\Phi_{\boldsymbol{e}_k}$, $\Phi_{\overline{\boldsymbol{e}}_k}$ (associated to each k^{th} QNM frequency) are not fixed, and have

been chosen such that

$$\epsilon_0^{(\mathbf{0})}=1,\quad \epsilon_0^{(\boldsymbol{e}_k)}=1,\quad \epsilon_0^{(\overline{\boldsymbol{e}}_k)}=1,\quad k\in\mathbb{N}\,. \tag{2.38}$$

With this choice of normalisation, the mixed sectors have no freedom in their respective coefficients. The list of sectors which were computed are as follows:

- The first 250 coefficients of the *fundamental* sector $\Phi_{\boldsymbol{e}_1}$, and $\beta_{\boldsymbol{e}_1}=-\frac{A_1}{6}+3$ with $A_1=\mathrm{i}\,\frac{3}{2}\,\omega_1$, where $\omega_1\approx 3.1195-\mathrm{i}\,2.7467$ is the lowest nonhydro QNM frequency.

- The first 200 coefficients of the *fundamental* sector $\Phi_{\boldsymbol{e}_2}$, and $\beta_{\boldsymbol{e}_2}=-\frac{A_2}{6}+3$ with $A_2=\mathrm{i}\,\frac{3}{2}\,\omega_2$ where $\omega_2\approx 5.1695-\mathrm{i}\,4.7636$ is the second lowest nonhydro QNM frequency.

- The first 100 coefficients of the *mixed* sector $\Phi_{2\boldsymbol{e}_1}$, with $\beta_{2\boldsymbol{e}_1}=-2\frac{A_1}{6}+4=2\beta_{\boldsymbol{e}_1}-2$.

- The first 100 coefficients of the *mixed* sector $\Phi_{\boldsymbol{e}_1+\overline{\boldsymbol{e}}_1}$, with $\beta_{\boldsymbol{e}_1+\overline{\boldsymbol{e}}_1}=-\frac{A_1}{6}-\frac{\overline{A_1}}{6}+4=\beta_{\boldsymbol{e}_1}+\beta_{\overline{\boldsymbol{e}}_1}-2$.

Note that the sectors $\Phi_{\overline{\boldsymbol{e}}_1}$, $\Phi_{\overline{\boldsymbol{e}}_2}$, and $\Phi_{2\overline{\boldsymbol{e}}_1}$ are just complex conjugates of the sectors $\Phi_{\boldsymbol{e}_1}$, $\Phi_{\boldsymbol{e}_2}$ and $\Phi_{2\boldsymbol{e}_1}$ respectively. Their characteristic exponents $\beta_{\boldsymbol{n}}$ and exponential weights $\boldsymbol{A}$ are similarly related.[7]

2.3 Resurgence in $\mathcal{N}=4$ SYM

For each sector studied in [2] the coefficients for the energy density grew as $\epsilon_k^{\boldsymbol{n}}\sim k!$ at large orders, showing each series to be asymptotic.[8] A well known method for removing this factorial growth is through a Borel transform, which maps a divergent

[7] Curiously, the characteristic exponent appears to follow the pattern $\beta_{\boldsymbol{n}}=-\frac{\boldsymbol{n}\cdot\boldsymbol{A}}{6}+\boldsymbol{n}\cdot\mathbf{1}+\beta_{\mathbf{0}}$, with $\mathbf{1}=(1,1,1,\cdots)$, but we did not prove this to be so.

[8] In our computations we present a finite number of terms in each series, meaning that strictly our series as given is finite. However when we say that these series do not converge we have inferred that the growing behaviour of the coefficients will not change with increasing order, and presume that the full infinite sum would not converge.

series in the variable $u \gg 1$ to a series in the Borel variable ξ via $u^{-\alpha} \mapsto \frac{\xi^{\alpha-1}}{\Gamma(\alpha)}$. The series $\Phi_{\boldsymbol{n}}$ (see Eq. (2.1)) is mapped to

$$\mathcal{B}\left[\Phi_{\boldsymbol{n}}\right](\xi) = \xi^{\beta_{\boldsymbol{n}}-1} \sum_{k=0}^{+\infty} \frac{\epsilon_k^{(\boldsymbol{n})}}{\Gamma(k+\beta_{\boldsymbol{n}})} \xi^k \,. \tag{2.39}$$

The resulting series has a finite radius of convergence which we can utilize to define an analytic continuation. There are several motivations for following such a procedure. The Borel transform of a Gervey-1 series gives us direct access to useful information concerning the other sectors of the theory, and the analytic continuation of the transform can be used to resum the original series through an inverse Borel transform. We will delay further discussion on the topic of resummation until Subsection 2.4.2 but a brief introduction to asymptotic series and the Borel transform can be found in Appendix A.1. In our work we will use diagonal Padé approximants to analytically continue each finite series, an approximation scheme which rewrites the power series as the ratio of two series, better allowing the function to represent singularities in the complex plane.

Performing the Borel transform and finding the Padé approximant for each series we display the poles structures in Fig. 2.1 for the hydrodynamic sector $\Phi_{\mathbf{0}}$ (top left plot), the fundamental sectors $\Phi_{\boldsymbol{e}_1}$, $\Phi_{\boldsymbol{e}_2}$ (top right and middle left plots) and the mixed sectors $\Phi_{2\boldsymbol{e}_1}$ and $\Phi_{\boldsymbol{e}_1+\bar{\boldsymbol{e}}_1}$ (middle left and bottom plots), where the condensation of poles is taken to be indicative of a branch point singularity. We will refer to these figures as the Borel planes of each sector. In Fig. 2.1 we indicate the exponential weights of fundamental sectors in solid circles, for mixed sectors in purple diamonds, and the expansion point of each series as a hollow circle. From the alignment of these branch points with the locations of the exponential weights, it is clear that each sector contains information relating to other sectors in the theory. Later in this chapter will show explicitly how one can recover coefficients of $\Phi_{\boldsymbol{e}_1}$ using only the knowledge of the exponential weight and $\Phi_{\mathbf{0}}$.

Due to numerical error and a finite number of terms in each series, there are several poles (grey dots) which do not correspond to an exponetial weight. As we

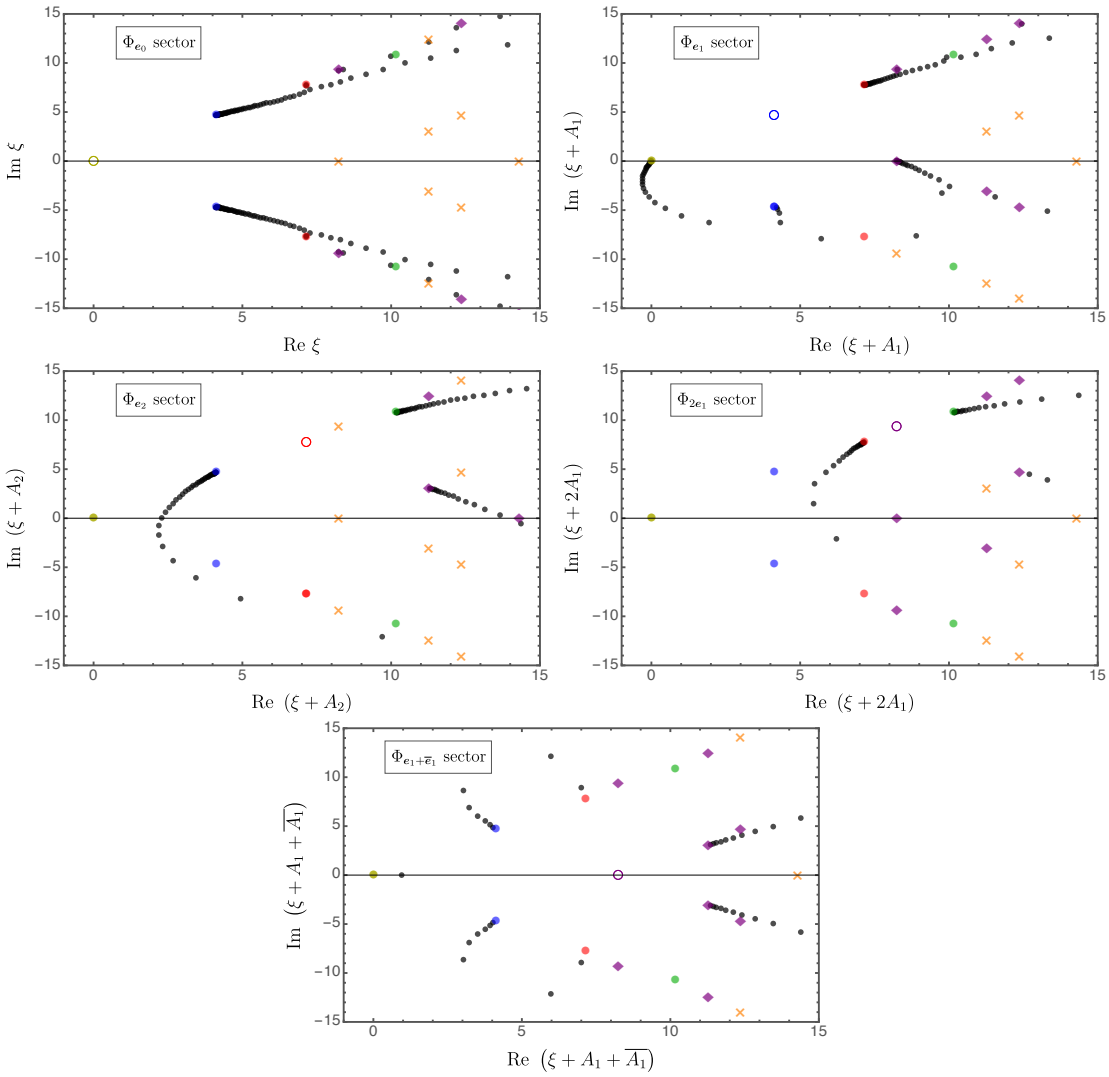

Figure 2.1: The singularity structure (grey dots) in the complex ξ-plane (Borel plane) associated to the Borel transforms of sectors $\Phi_{\boldsymbol{n}}$, with $\boldsymbol{n} = \mathbf{0}$, $\boldsymbol{e}_1$, $\boldsymbol{e}_2$, $2\boldsymbol{e}_1, \boldsymbol{e}_1 + \overline{\boldsymbol{e}}_1$ taken from [2]. The Borel planes have been shifted to be represented on a common axis, with the expansion points shown by a hollow circle and the hydrodynamic expansion located at the origin (in dark yellow). The exponential weights given in Subsection 2.2.3 have been superimposed on each Borel plane and are divided into fundamental sectors (solid circles) and mixed sectors (purple diamonds). The fundamental sectors include: A_1 and $\overline{A_1}$ (blue), A_2 and $\overline{A_2}$ (red), A_3 and $\overline{A_3}$ (green). The yellow crosses indicate non-hydrodynamic sectors which are not directly visible in the Borel plane for a given sector about which we have expanded.

increase the number of terms in our approximation we find the locations of these spurious poles go to infinity and the branch cuts become more defined. Note that it is typical when studying transseries solutions to choose variables which eliminate the integration constant associated with the perturbative sector. This is not the case when studying $\epsilon(u)$ which has an integration constant (or transseries parameter) associated with the hydrodynamic sector, and is the reason why a branch cut appears at the hydrodynamic sector in the Borel plane for sector $\Phi_{\boldsymbol{e}_1}$.[9]

2.3.1 Extracting coefficients for the first non-hydrodynamic sector

Through direct computation we have shown that the energy density exhibits a transseries structure, at least for the first few non-hydrodynamic sectors given by Eq. (2.1). In addition Fig. 2.1 provides strong evidence that this transseries is resurgent, ie. that the coefficients of different sectors are related enabling us to reconstruct solutions of one sector from another. While it may appear unintuitive that the perturbative hydrodynamic sector should contain information about modes that become applicable in a different regime of u, both sectors are governed by the same equations of motion and so are intimately related.

For a resurgent transseries the coefficients of different sectors are generically related in a predictable way by a large order relation. For our hydrodynamic sector the coefficients $\epsilon_k^{(\mathbf{0})}$ will be given by[10]

$$\begin{aligned}\epsilon_k^{(\mathbf{0})} \underset{k\gg 1}{=} & -\frac{\mathsf{S}_{\mathbf{0}\to\boldsymbol{e}_1}}{2\pi\mathrm{i}}\frac{\Gamma(k+\beta_{\mathbf{0}}-\beta_{\boldsymbol{e}_1})}{A_1^{k+\beta_{\mathbf{0}}-\beta_{\boldsymbol{e}_1}}}\chi_{\mathbf{0}\to\boldsymbol{e}_1}-\frac{\mathsf{S}_{\mathbf{0}\to\overline{\boldsymbol{e}}_1}}{2\pi\mathrm{i}}\frac{\Gamma(k+\beta_{\mathbf{0}}-\beta_{\overline{\boldsymbol{e}}_1})}{\left(\overline{A_1}\right)^{k+\beta_{\mathbf{0}}-\beta_{\overline{\boldsymbol{e}}_1}}}\chi_{\mathbf{0}\to\overline{\boldsymbol{e}}_1} \\ & -\frac{\mathsf{S}_{\mathbf{0}\to\boldsymbol{e}_2}}{2\pi\mathrm{i}}\frac{\Gamma(k+\beta_{\mathbf{0}}-\beta_{\boldsymbol{e}_2})}{A_2^{k+\beta_{\mathbf{0}}-\beta_{\boldsymbol{e}_2}}}\chi_{\mathbf{0}\to\boldsymbol{e}_2}-\frac{\mathsf{S}_{\mathbf{0}\to\overline{\boldsymbol{e}}_2}}{2\pi\mathrm{i}}\frac{\Gamma(k+\beta_{\mathbf{0}}-\beta_{\overline{\boldsymbol{e}}_2})}{\left(\overline{A_2}\right)^{k+\beta_{\mathbf{0}}-\beta_{\overline{\boldsymbol{e}}_2}}}\chi_{\mathbf{0}\to\overline{\boldsymbol{e}}_2} \\ & -\frac{\mathsf{S}_{\mathbf{0}\to 2\boldsymbol{e}_1}}{2\pi\mathrm{i}}\frac{\Gamma(k+\beta_{\mathbf{0}}-\beta_{2\boldsymbol{e}_1})}{(2A_1)^{k+\beta_{\mathbf{0}}-\beta_{2\boldsymbol{e}_1}}}\chi_{\mathbf{0}\to 2\boldsymbol{e}_1}-\frac{\mathsf{S}_{\mathbf{0}\to 2\overline{\boldsymbol{e}}_1}}{2\pi\mathrm{i}}\frac{\Gamma(k+\beta_{\mathbf{0}}-\beta_{2\overline{\boldsymbol{e}}_1})}{\left(2\overline{A_1}\right)^{k+\beta_{\mathbf{0}}-\beta_{2\overline{\boldsymbol{e}}_1}}}\chi_{\mathbf{0}\to 2\overline{\boldsymbol{e}}_1} \\ & +\cdots .\end{aligned} \tag{2.40}$$

[9] We have checked that the pressure anisotropy (defined by $R=\frac{p_T-p_L}{\epsilon/3}$) as a function of the dimensionless combination τT will have no such cut.

[10] Eq. (2.40) has been checked numerically in [2].

where we further define the sum

$$\chi_{\boldsymbol{m}\to\boldsymbol{n}}(k)=\sum_{h=0}^{+\infty}\frac{\Gamma(k+\beta_{\boldsymbol{m}}-\beta_{\boldsymbol{n}}-h)}{\Gamma(k+\beta_{\boldsymbol{m}}-\beta_{\boldsymbol{n}})}\left((\boldsymbol{n}-\boldsymbol{m})\cdot\boldsymbol{A}\right)^{h}\epsilon_{h}^{(\boldsymbol{n})}\,, \tag{2.41}$$

and each factor $\mathsf{S}_{\mathbf{0}\to\boldsymbol{n}}$ is known as a Borel residue, a proportionality constant relating the coefficients of each sector given intrinsically by a theory data. To verify that our transseries is resurgent we will use Eq. (2.40) to extract coefficients from the first fundamental sector $\Phi_{\boldsymbol{e}_1}$ from the hydrodynamic gradient expansion given by $\Phi_{\mathbf{0}}$.

In similar theories various established methods have been used to extract the coefficients of fundamental sectors from the a large-order behaviour of the perturbative sector [91, 92]. However in those cases the method of extraction relied heavily on the specific structure of the Borel plane. Here we will use a general approach which relies on the properties of the Borel transform alone, and does not require any analytic continuation or resummation [2, 5].

If we consider the hydrodynamic series $\Phi_{\mathbf{0}}(u)$ whose coefficients $\epsilon_k^{(\mathbf{0})}$ are given by Eq. (2.40) one can show that the Borel transforms of $\Phi_{\mathbf{0}}$ and $\Phi_{\boldsymbol{e}_1}$ are related by

$$\mathcal{B}\left[u^{\beta_{\boldsymbol{e}_1}}\,\Phi_{\mathbf{0}}\right](\xi)\big|_{\xi=A_1}=\mathsf{S}_{\mathbf{0}\to\boldsymbol{e}_1}\,\mathcal{B}\left[u^{\beta_{\boldsymbol{e}_1}}\,\Phi_{\boldsymbol{e}_1}\right](\xi-A_1)\,\frac{\log(\xi-A_1)}{2\pi\,\mathrm{i}}+\text{reg.}\,, \tag{2.42}$$

where "reg." indicates all terms which are regular at $\xi=A_1$, and $\mathcal{B}\left[u^{\beta_{\boldsymbol{e}_1}}\,\Phi_{\boldsymbol{e}_1}\right](\xi-A_1)$ is a regular function with a finite radius of convergence about A_1. An explicit proof of this statement is given in Appendix A.1.1. While it is tempting to consider how one might extract $\Phi_{\boldsymbol{e}_1}$ from $\Phi_{\mathbf{0}}$ using Eq. (2.42), we can find an even more convenient relation.

By direct computation one can find that shifting $\beta_{\boldsymbol{e}_1}$ by any integer multiple will introduce poles into Eq. (2.42), but will always preserve a logarithmic structure. As shown in Appendix A.1.1 if we instead shift $\beta_{\boldsymbol{e}_1}$ by a half integer we find

$$\begin{aligned}\mathcal{B}\left[u^{\beta_{\boldsymbol{e}_1}-1/2}\,\Phi_{\mathbf{0}}\right](\xi)\big|_{\xi=A_1}&=\frac{\mathsf{S}_{\mathbf{0}\to\boldsymbol{e}_1}}{2}\,\mathcal{B}\left[u^{\beta_{\boldsymbol{e}_1}-1/2}\,\Phi_{\boldsymbol{e}_1}\right](\xi-A_1)+\text{reg.}\,, \qquad (2.43)\\ &=\frac{\mathsf{S}_{\mathbf{0}\to\boldsymbol{e}_1}}{2\sqrt{\xi-A_1}}\left(\frac{\epsilon_0^{(\boldsymbol{e}_1)}}{\Gamma(1/2)}+\epsilon_1^{(\boldsymbol{e}_1)}\,\frac{(\xi-A_1)}{\Gamma(3/2)}+\epsilon_2^{(\boldsymbol{e}_1)}\,\frac{(\xi-A_1)^2}{\Gamma(5/2)}+\cdots\right).\end{aligned}$$

Finally we can performing a change of variables, $\xi = A_1 - (\zeta - A_1)^2$, to transform the branch cut into a simple pole,

$$\mathcal{B}\left[u^{\beta_{\boldsymbol{e}_1}-1/2}\,\Phi_{\mathbf{0}}\right](\zeta)\big|_{\zeta=A_1} = \frac{\mathsf{S}_{\mathbf{0}\to\boldsymbol{e}_1}}{2\mathrm{i}\,(\zeta-A_1)}\left(\frac{\epsilon_0^{(\boldsymbol{e}_1)}}{\Gamma(1/2)} - \epsilon_1^{(\boldsymbol{e}_1)}\,\frac{(\zeta-A_1)^2}{\Gamma(3/2)} + \cdots\right). \quad (2.44)$$

From this expression we can see that by calculating the Borel transform $\mathcal{B}\left[u^{\beta_{\boldsymbol{e}_1}-1/2}\,\Phi_{\mathbf{0}}(u)\right](\zeta)$ and analysing its residue at $\zeta = A_1$ we can compute the Borel residue $\mathsf{S}_{\mathbf{0}\to\boldsymbol{e}_1}$.[11] Moreover, by subtracting the simple pole from the Borel transform:

$$\mathcal{B}\left[u^{\beta_{\boldsymbol{e}_1}-1/2}\,\Phi_{\mathbf{0}}\right](\zeta)\big|_{\zeta=A_1} - \frac{\mathsf{S}_{\mathbf{0}\to\boldsymbol{e}_1}}{2\mathrm{i}\,(\zeta-A_1)}\,\frac{\epsilon_0^{(\boldsymbol{e}_1)}}{\Gamma(1/2)} = -\epsilon_1^{(\boldsymbol{e}_1)}\,\frac{\mathsf{S}_{\mathbf{0}\to\boldsymbol{e}_1}}{2\mathrm{i}\,\Gamma(3/2)}\,(\zeta-A_1) + \cdots \quad (2.45)$$

and multiplying everything by $(\zeta - A_1)^{-2}$, we can once again use the residue theorem to predict the next coefficient $\epsilon_1^{(\boldsymbol{e}_1)}$ of the fundamental sector $\Phi_{\boldsymbol{e}_1}$. This procedure can be repeated to arbitrarily high orders provided one has the required numerical precision to do so.

We have used this method to compute the first few coefficients of $\Phi_{\boldsymbol{e}_1}$ from $\Phi_{\mathbf{0}}$. In Fig. 2.2 we display the normalised error of the predicted coefficients relative to those produced by the numerical gravity calculation for the first few coefficients. This error is given by

$$\Delta_{\mathbf{0}}\epsilon_m^{(\mathbf{1})} \equiv \frac{\epsilon_m^{(\mathbf{1})}\,|_{\mathbf{0}-\text{predicted}} - \epsilon_m^{(\mathbf{1})}\,|_{\text{numerical}}}{\epsilon_m^{(\mathbf{1})}\,|_{\text{numerical}}}\,,\ m \geq 1, \quad (2.46)$$

where we define $\epsilon_m^{(\mathbf{1})}\,|_{\text{numerical}}$ as the coefficients of $\Phi_{\boldsymbol{e}_1}$ determined from the gravity calculation of Section 2.2, and $\epsilon_m^{(\mathbf{1})}\,|_{\mathbf{0}-\text{predicted}}$ are our coefficients predicted from the resurgence analysis of the $\Phi_{\mathbf{0}}$ sector. In particular we compute the Borel residue to be,

$$\mathsf{S}_{\mathbf{0}\to\boldsymbol{e}_1} \approx -0.01113 + 0.03050\,\mathrm{i}\,, \quad (2.47)$$

where this constant has been determined to much higher accuracy with the full expression contained in [2]. In that paper a similar approach was also used to recover the coefficients of $\Phi_{\boldsymbol{e}_2}$, $\Phi_{2\boldsymbol{e}}$ and $\Phi_{\boldsymbol{e}_1+\bar{\boldsymbol{e}}_1}$ from the $\Phi_{\mathbf{0}}$ sector, as well as to find the corresponding Borel residues between those sectors.

[11] In fact we only have access to the combination $\mathsf{S}_{\mathbf{0}\to\boldsymbol{e}_1}\,\epsilon_0^{(\boldsymbol{e}_1)}$, but we have chosen to normalise the fundamental sectors such that their first non-zero coefficient is 1.

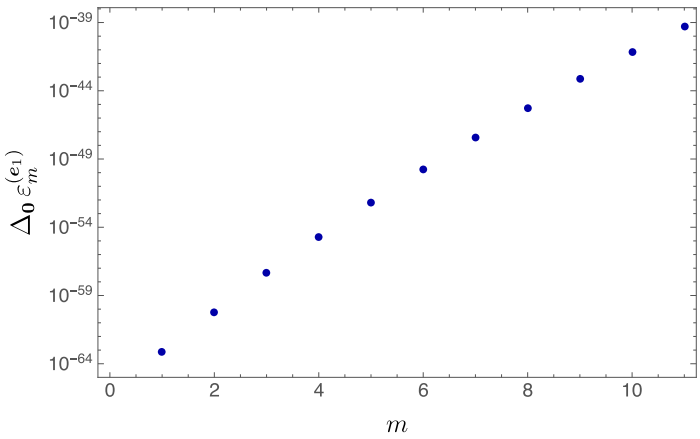

Figure 2.2: Comparison of the predicted results from resurgence techniques and the numerical coefficients obtained from solving Einstein equations in Section 2.3. In the above plots we show this comparison for the fundamental sector Φ_{e_1} as predicted by the large-order behaviour of the coefficients of the perturbative sector $\Phi_{\mathbf{0}}$ given by Eq. (2.46). Figure taken from [2]

2.4 Resurgence in Gauss-Bonnet Holography

In the previous section we have demonstrated that one can recover coefficients of non-hydrodynamic (in gradient) sectors of the theory using the coefficients of the hydrodynamic sector. In this section we extend our analysis in two ways: through using Borel resummation to recover non-hydrodynamic solutions as a function of gradient, and by including the effects of intermediate coupling for a more phenomenologically relevant picture of QGP dynamics. Through our resummaton we estimate the approximate location of the attractor solution in the regime of large gradients.

2.4.1 Gauss-Bonnet Holography and Boost Invariant flow

Starting from the infinite coupling limit, finite coupling corrections are studied via the gauge/gravity duality by introducing higher curvature terms in the dual gravitational theory [93,94]. We will however not study the perturbative corrections to $\mathcal{N} = 4$ SYM theory, but instead consider Gauss-Bonnet gravity, a toy model for finitely coupled holographic systems which has generated significant interest.

While the dual field theory to Gauss-Bonnet gravity is unknown, in this holographic construction on can extract static (thermodynamic) and transport properties

of the dual field theory, as well as the relaxation of small non-thermal perturbations [81,95], its off-equilibrium dynamics [96,97] and corrections to its hydrodynamic expansion [98]. The action of this theory includes both quadratic and quartic curvature terms, governed by a single parameter λ_{GB}; but exhibits classical equations of motion which remain quadratic in derivatives of the metric and as such avoids the Ostrogradsky instability allowing a non-perturbative treatment of the higher derivative terms. The comparison of the analyses described above and the results obtained from finite coupling corrections of $\mathcal{N}=4$ SYM show that for negative λ_{GB} these two theories share many common qualitative aspects, which makes Gauss-Bonnet holography an interesting laboratory with which to explore finite coupling effects in holographic theories.

However one finds that causality, positivity of energy and hyperbolicity considerations constrain the range of values of λ_{GB} to be $-7/36 < \lambda_{GB} \leq 9/100$ [99–106] (see [95] for a detailed discussion on these limitations)[12]. Nevertheless, since these constraints concern the ultraviolet behaviour of the theory, we may still consider values of λ_{GB} beyond this region to explore its infrared dynamics, such as the approach towards hydrodynamics of the theory, as already done in [81, 95].

The Gauss-Bonnet gravity action is given by

$$S = \frac{1}{16\pi G_5}\int d^5x\,\sqrt{-g}\left(R + \frac{12}{L^2} + \frac{\lambda_{GB}L^2}{2}\left(R_{\mu\nu\rho\sigma}R^{\mu\nu\rho\sigma} - 4R_{\mu\nu}R^{\mu\nu} + R^2\right)\right), \tag{2.48}$$

where G_5 is the five dimensional Newton constant, L is the AdS radius of the $\lambda_{GB}=0$ theory, and λ_{GB} is a dimensionless coupling which controls the magnitude of the higher derivative corrections. Without loss of generality, in the rest of this work we will set $L=1$. As in the $\lambda_{GB}\to 0$ limit of $\mathcal{N}=4$ SYM, this theory exhibits a family of static blackbrane solutions dual to a thermal ensemble of an associated gauge theory plasma. Following an approach similar to Subsection 1.3.3 we can extract an equation

[12]The analysis of three point functions of gravitons in high-derivatives theories has led the authors of [103] to suggest that these theories are pathological for any strength of the higher derivative couplings unless a complete tower of stringy states is also considered. See however [104] for a critique of this argument.

of state for each dual field theory [93, 94]

$$\epsilon = \frac{3}{8}\frac{\pi^2 N_c^2}{L_c^3}T^4\,, \quad L_c^2 = \frac{1+\sqrt{1-4\lambda_{GB}}}{2}\,. \tag{2.49}$$

While Eq. (2.49) has been computed for an equilibrium solution we can, as in earlier sections, use it as an out-of-equilibrium definition of the local effective temperature in terms of ϵ. In addition one can compute various transport coefficients in the hydrodynamic regime, such as the ratio of shear viscosity to entropy density [107],

$$\frac{\eta}{s} = \frac{1-4\lambda_{GB}}{4\pi}\,. \tag{2.50}$$

From Eq. (2.50) one can identify larger negative values of λ_{GB} with a lower interaction strength in the theory. Second order transport coefficients of this theory have also been analysed in [95].

Following the program of Section 2.2 we again consider an ansatz of the form

$$ds^2 = -r^2\tilde{A}d\tau^2 + 2d\tau dr + (r\tau+1)^2 e^b dy^2 + r^2 e^{-\frac{1}{2}b+d}dx_\perp^2\,. \tag{2.51}$$

where after fixing variables $u = \tau^{2/3}$ and $s = \frac{1}{r}\tau^{-\frac{1}{3}}$ we substitute a series ansatz similar to Eqs. (2.18)–(2.20),

$$\tilde{A}(r,\tau) = \sum_{i=0}^{\infty} u^{-i}A_i^{(\mathbf{0})}(s)\,, \quad b(r,\tau) = \sum_{i=0}^{\infty} u^{-i}b_i^{(\mathbf{0})}(s)\,, \quad d(r,\tau) = \sum_{i=0}^{\infty} u^{-i}d_i^{(\mathbf{0})}(s)\,. \tag{2.52}$$

In [1] we did not attempt to find a transseries solution of the form Eq. (2.35) but instead confined ourselves to the hydrodynamic sector ($\boldsymbol{n} = \mathbf{0}$). Imposing AdS asymptotics at the ($s = 0$) boundary, and fixing the horizon at $s = 1$, the leading order solution will be given by

$$A_0^{(\mathbf{0})} = \frac{1}{2\lambda_{GB}}\left(1-\sqrt{1-4\lambda_{GB}(1-s^4)}\right)\,, \quad b_0^{(\mathbf{0})} = -2\log\left(L_c\right)\,, \quad c_0^{(\mathbf{0})} = -2\log\left(L_c\right)\,. \tag{2.53}$$

We can examine that as expected the $\lambda_{GB} \to 0$ limit of Eq. (2.53) reduces to the 5-D blackbrane solution given by Eq. (2.23). Following the same procedure outlined in Section 2.2 we can compute the subsequent corrections to the metric order-by-order in

a large u expansion.[13] As in Subsection 2.2.3 one can use the standard tools of holographic renormalisation to extract the dual field theory quantities at the boundary, which was performed for Gauss-Bonnet gravity in [108, 109]. While the calculation is nearly identical to Subsection 2.2.3 and only yields a λ_{GB}-dependent adjustment to the normalization, for clarity we will briefly outline modifications below.

The diagonal stress tensor $T_{ab} = \text{diag}\,(\epsilon,\, \tau^2 p_L,\, p_L, p_L)$ given by,

$$T_{ab} = \frac{3N_c^2}{8\pi^2}\frac{(2L_c^2-1)}{L_c^3}\text{diag}\left(f(\tau), -\tau^3 f'(\tau) - \tau^2 f(\tau), f(\tau) + \frac{1}{2}\tau f'(\tau), f(\tau) + \frac{1}{2}\tau f'(\tau)\right)_{\mu\nu} . \tag{2.54}$$

where we read the function $f(\tau)$ from the warp factor as,

$$\tilde{A}(\tau, r) = 1 - \frac{f(\tau)}{r^4} + \dots . \tag{2.55}$$

In the now familiar variables $u = \tau^{\frac{2}{3}}$ and $s = \frac{1}{r}\tau^{-\frac{1}{3}}$ we can read the function $f(\tau)$ from our gravity solution as,

$$f(\tau) = \left(u^{-2}\sum_{i=0} f_i^{(\mathbf{0})} u^{-i}\right) , \quad f_i^{(\mathbf{0})} = -\frac{1}{4!}\frac{d^4}{ds^4}A_i^{(\mathbf{0})}(s=0) . \tag{2.56}$$

The energy density coefficients can be related to the coefficients in Eq. (2.56) via the normalization of Eq. (2.54),

$$\epsilon_i^{\mathbf{0}} = \frac{3N_c^2}{8\pi^2}\frac{(2L_c^2-1)}{L_c^3} f_i^{\mathbf{0}} . \tag{2.57}$$

As outlined above we computed the first 380 orders of this expansion for infinitely coupled $\mathcal{N} = 4$ SYM, the results of which were used previously in Section 2.3. Given that the Gauss-Bonnet equations of motion contain many more terms, the computation of higher order coefficients becomes much more numerically demanding than for the case of $\lambda_{GB} = 0$. Similarly, the square root singularity hidden behind the horizon of the blackbrane in Eq. (2.53) moves closer to the horizon as we take λ_{GB} to larger negative values. The presence of this non-analyticity requires a larger

[13] While in this chapter we define $u = \tau^{\frac{2}{3}}$ to yield an expansion of the form of Eq. (2.35), the authors of [1] use the inverse $u = \tau^{-\frac{2}{3}}$ and expand in small u.

number of points in our Chebyshev grid to maintain numerical accuracy at high gradients. Due to these difficulties a computation was only feasible for a much lower number of coefficients. The analysis in this section is based on the determination of $N_{\text{coeff}} = (94, 86, 80, 66)$ coefficients for $\lambda_{GB} = (-0.1, -0.2, -0.5, -1)$ respectively. These coefficients as defined in Eq. (2.57) can be found in [1].

Lastly, in this section we will be concerned with the approach of our Bjorken-like system towards local thermal equilibrium and so will find it useful to express our results in terms of the anisotropy,

$$R \equiv \frac{p_T - p_L}{\epsilon/3}\,, \tag{2.58}$$

which tracks the system as it relaxes, vanishing in equilibrium. We normalize R by the conformal equilibrium given by $\frac{\epsilon}{3}$ so that at $R \sim 1$ the gradient corrections to the pressure will be on the order of the equilibrium pressure. For a conformal theory the anisotropy R becomes a function of the dimensionless gradient,

$$w = \tau\, T(\tau)\,, \tag{2.59}$$

where $T(\tau)$ here is a local effective temperature defined by the same Eq. (2.49), where now ϵ and T are now understood to be out of equilibrium quantities dependent on τ. Then R admits an expansion in inverse powers of w in the hydrodynamic limit as

$$R = w^{-1} \sum_{k=0} r_k w^{-k}\,, \tag{2.60}$$

$$= 8\,(\eta/s)\, w^{-1} + w^{-1} \sum_{k=1} r_k w^{-k}\,, \tag{2.61}$$

where in the last line of this equation we have pulled out of the sum the leading term at large w (small gradients) which is controlled by the viscosity to entropy density ratio, $r_0 = 8\,(\eta/s)$. We will refer to this term as *first order* hydrodynamics.

2.4.2 Borel planes and resummation

As was in the case of $\lambda_{GB} = 0$, each hydrodynamic series does not converge but has coefficients that diverge factorially. Applying a similar analysis as described in

Section 2.3, namely computing the Borel transforms and corresponding padé approximants of each series via Eq. (2.39), we can find Borel planes for our representative choices of λ_{GB}. Because the steps outlined in Section 2.3 were defined with respect to a series in u rather than w, we clarify that for a series of the form given in Eq. (2.60), the Borel transform following similar conventions will be given by,[14]

$$\mathcal{B}\left[R\right](\xi) = \sum_{k=0}^{\infty} \frac{r_k}{\Gamma\left(k+1\right)} \xi^k \,. \tag{2.62}$$

where practically we set all coefficients r_k with $k > (N_{coeff} - 1)$ to zero. We have previously mentioned the use of Padé approximants for analytically continuing a series with a finite radius of convergence and will expound on this point here. The finite radius of convergence indicates that the Borel transform of the anisotropic function possesses singularities in the complex-ξ plane. The Borel transform and the original series are related via a Laplace transform. In order to perform this integral, we will need to first analytically continue the Borel transform beyond its radius of convergence. A standard method to do this is to approximate the Borel transform via a Padé approximant as

$$\mathcal{B}\left[R\right](\xi) \approx \mathcal{BP}\left[R\right](\xi) \equiv \frac{\sum_{j=0}^{N} n_i \xi^j}{1 + \sum_{i=1}^{M} d_i \xi^i} \,, \tag{2.63}$$

where all $N + M + 1$ coefficients are fixed by demanding that the power series of the Padé agrees with Eq. (2.62). The choice of N and M are arbitrary, with the constraint that $N + M = N_{\text{coeff}}$. All the analysis of this work is based on symmetric Padé approximants, with $N = M = N_{\text{coeff}}/2$, where we check the stability of our results by varying N.

By construction the Padé approximant allows for the emergence of poles in the complex ξ plane, permiting the function to be well defined outside of the radius of convergence of the Borel transform. In Fig. (2.3) we show the positions of the poles of the Padé approximant for different values of λ_{GB} taken from [1], using ξ as our Borel

[14]The variable ξ used here is now conjugate to w and technically different to the what has been used in Section 2.3, but because $\lim_{u\to\infty} w \sim u$, this will lead to no qualitatively important changes.

parameter as we did in Fig. (2.1). In the upper left panel we show the pole structure for $\mathcal{N} = 4$ SYM which was shown in Section 2.3, a similar figure was previously computed in [28, 31] with 240 coefficients. The rest of the panels show our results for different negative values of $\lambda_{GB} = -0.1, -0.2, -0.5, -1$.

As we learned in Section 2.3, these singularities are a consequence of the existence of non-hydrodynamic sectors in the theory. Tuning λ_{GB} to larger negative values we see the emergence of a branch cut along the horizontal axis, indicating the existence of a purely dissipative mode in addition to the characteristic discrete complex modes of $\mathcal{N} = 4$ SYM. This is consistent with the expectation from the QNM spectrum of Gauss-Bonnet gravity. The emergence of a purely decaying mode is also characteristic of $\mathcal{N} = 4$ SYM with a finite coupling correction, where the 't Hooft coupling dependence of those poles is qualitatively similar to the λ_{GB} dependence of the poles here (provided $\lambda_{GB} < 0$) [81]. We therefore tentatively infer that repeating the analysis with $\mathcal{N} = 4$ SYM at finite coupling will yield the same behaviour.

To explicitly show the relation between the quasi-normal mode spectrum and the Borel plane singularities in Fig. (2.3) we plot the positions of these characteristic frequencies after an appropriate $\frac{3i}{2}$ rescaling (see Subsection (2.2.1)). In this figure the positions of the singularities associated with the first purely imaginary and complex QNM's (with smallest imaginary part, i. e. the smallest damping rate) are given by blue solid circles, with the singularities associated with the second and third complex QNM's (with the next two smallest imaginary parts) shown by red and green respectively. The QNM frequency which appears on the real axis for finite λ_{GB} is shown in orange.

Having analytically continued the Borel transform through Eq. (2.63) we will now attempt to answer one of the central questions of this chapter: how can we make sense of the diverging hydrodynamic gradient expansion, and how can we resum this

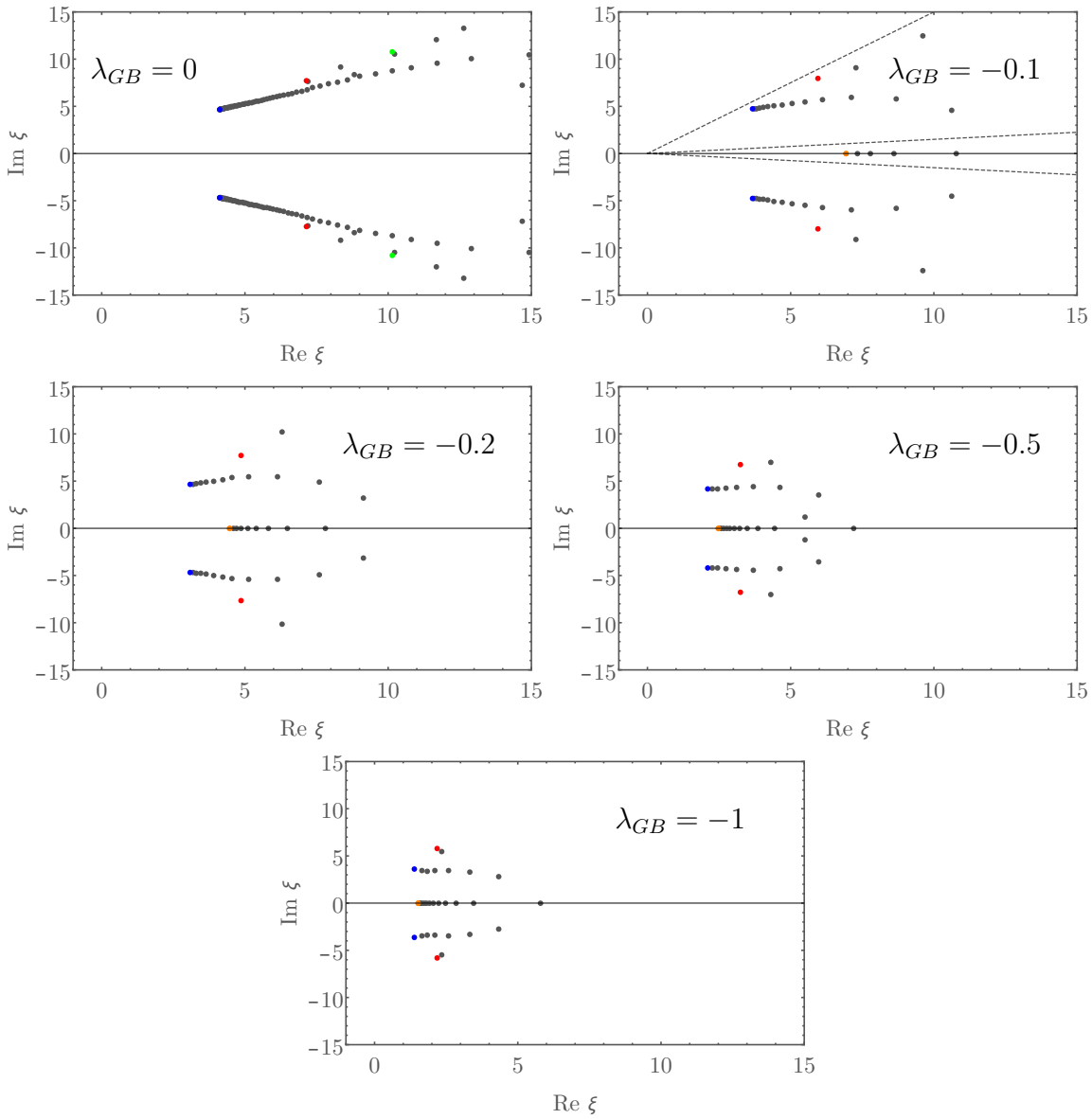

Figure 2.3: Plot of the Borel planes for selected values of λ_{GB} taken from [1]. The straight dashed lines in the upper left channel shows the contours of integration used in Eq. (2.64) given by θ^+, 0^+ and 0^- in decreasing slope order. Similar contours are used for all other cases. The solid grey circles indicate poles of the Padé approximant of $\mathcal{B}[R](\xi)$, the Borel transform associated with the anisotropy function $R(w)$ for different values of λ_{GB}. The expected positions of singularities predicted from the quasi-normal mode frequencies closest to the origin, both for complex (blue) and purely dissipative modes (orange), are marked by solid circles. The subsequent 2^{nd} and 3^{rd} QNM frequencies are marked by blue and green.

series? To do so we will adopt the machinery of the inverse Borel transformation,

$$R_\theta(w) \equiv \int_0^{e^{i\theta}\infty} d\xi e^{-w\xi}\, \mathcal{BP}\left[R\right](\xi)\,, \tag{2.64}$$

where $\theta \in (-i\pi/2, i\pi/2)$ is a parameter we can choose arbitrarily. Applying Eq. (2.64) term by term to Eq. (2.62) yields the original asymptotic expansion of Eq. (2.60). However, the presence of singularities in $\mathcal{BP}\left[R\right](\xi)$ shows that different choices of θ yield answers differing by a residue. We require $R_\theta(w)$ to be an analytic continuation for every complex value of w or ξ, impling that all choices of θ should have yielded an identical result. The resolution of this apparent contradiction is that a gradient expansion given by Eq. (2.60) does not represent the full solution to the equations of motion but rather, as in Eq. (2.37), will require a transseries of the form

$$R\left(w, \boldsymbol{\sigma}\right) = \sum_{\boldsymbol{n}\in\mathbb{N}_0^\infty} \boldsymbol{\sigma}^{\boldsymbol{n}}\, \mathrm{e}^{-\boldsymbol{n}\cdot\boldsymbol{A}\, w}\, \Phi_{\boldsymbol{n}}\left(w\right)\ , \quad \Phi_{\boldsymbol{n}}\left(w\right) = w^{-\beta_{\boldsymbol{n}}} \sum_{k=0}^{+\infty} r_k^{(\boldsymbol{n})}\, w^{-k}\,, \tag{2.65}$$

where non-perturbative contributions are incorporated by terms with non-zero exponential weights $\boldsymbol{A} = 3/2i\boldsymbol{\omega}$ and associated characteristic exponents $\beta_{\boldsymbol{n}}$ [28,31,91]. As defined in Section 2.1 the transseries parameters $\boldsymbol{\sigma}^{\boldsymbol{n}}$ correspond to choices of initial data. Following an analysis similar to Subsection (2.3.1) one can explicitly show that the residue of each branch cut will be proportional to a non-hydrodynamic sector of the theory, but for simplicity we will instead offer a heuristic argument below.

We know that in principle we should be able to define an ambiguity free resummation of the Borel plane. Consider the Borel plane for $\lambda_{GB} = 0$ given in the top left panel of Fig. (2.3). Suppose we were to perform two distinct Borel resummations along different contours: one along the real axis $R_{0^+}(w)$ and another just above the first branch cut $R_{\theta^+}(w)$ so as to cross no other branch cuts. The only way for the resummation of the full solution to be ambiguity free is if a term in the transseries of Eq. (2.65) can be chosen with some fixed coefficient to cancel the extra contribution we got from our different choice of contour [91, 110]. But the difference between each contour is just $R_{\theta^+}(w) - R_{0^+}(w)$ which by complex analysis can be computed via the

residue theorem. Therefore we can find the other transseries sectors from the Borel plane up to some proportionality constant by computing the residues of the complex plane.

In the top right panel of Fig. (2.3) for the $\lambda_{GB} = 0$ case we have drawn (from top to bottom) representative contours for θ^+, 0^+ and 0^- respectively. Denoting by R_{θ^+}, R_{0^+} and R_{0^-} the results of integrating Eq. (2.64) over each of these contours, we define the discontinuities

$$iD_1(w) = R_{0^+} - R_{0^-}, \quad D_2(w) = R_{\theta^+} - R_{0^+}. \tag{2.66}$$

D_1 is real and coincides with the imaginary part of R_{0^+} while D_2 is complex. Note that we could have defined an equivalent discontinuity by reflecting both θ^+ and 0^+ to the lower half; however, this discontinuity is simply the complex conjugate of $D_2(w)$. D_1 and D_2 will both approximately coincide with the dominant non-hydrodynamic contributions in Eq. (2.65), where by dominant we mean that these modes are the least suppressed by the non-perturbative multiplicative factor of $e^{-\boldsymbol{n}\cdot\boldsymbol{A}w}$. From the point of view of holography, these modes are given by the quasinormal mode frequencies with lowest negative imaginary part. Computing this contour integral may inadvertently incoporate contributions from other transseries sectors, but because these terms will be exponentially suppressed with respect to the leading term this detail is negligible.

How do we extend hydrodynamics in this theory beyond the gradient expansion? Performing the resummation given in Eq. (2.64) for any contour from 0 to ∞ unavoidably receives contributions from the full transseries so that one can no longer seperate the hydrodynamic and non-hydrodynamic sectors. In choosing a contour we have implicitly selected some particular initial conditions, equivalent to a specific selection of the constants $\boldsymbol{\sigma}$ in Eq. (2.65). This resummation will however be stable with respect the number of terms included in the expansion given by N_{coeff}, while Eq. (2.60) was not. For this reason we begin by computing a resummation along the 0^+ contour, and subtracting $iD_1(w)$ to impose that the anisotropy be real, to identify

the curve $\mathrm{Re}\,[R_{0^+}(w)]$.

The rapidly decaying nature of the non-hydrodynamic modes of the theory has lead various authors to conclude that one may identify a special trajectory as an attractor solution to which all other initial conditions. Such a solution has been found in Müller-Israel-Stewart theory [32] and numerically in $\mathcal{N}=4$ SYM [71] but we stress that there is nothing particularly special about the choice of initial conditions selected by our Borel resummation scheme. While we will not attempt to reconstruct a specific attractor solution, we can instead estimate its location. By combining the resummation $\mathrm{Re}\,[R_{0^+}(w)]$, and approximating further non-hydrodynamic sectors by D_1 and D_2 we can describe the late time behaviour of the anisotropy as

$$R^{(\mathrm{full})} = \mathrm{Re}\,[R_{0^+}(w)] + a_1 D_1(w) + a_2 \mathrm{Re}\,[D_2(w)] + a_3 \mathrm{Im}\,[D_2(w)]\ , \tag{2.67}$$

where D_2 and its complex conjugate have been added in real combinations, and the coefficients a_i allow choices of different initial conditions.

In Fig. (2.4) we explore the effect of different initial conditions on the time evolution of boost invariant expansion of different theories. Here we plot $R^{(\mathrm{full})}$ for each λ_{GB}, where a thick, black curve denotes the choice $a_i = 0$, and the colourful curves give the anisotropy with randomly chosen coefficients $|a_i| \leq 1$. While no particular choice of a_i has special significance, in the regime where the variation due to initial data is small we can claim to have estimated the location of an attractor solution, in that large changes to the initial data will not push the final trajectory far away from this curve.[15]

In Fig. (2.4) we have rescaled the horizontal axis by $4\pi\frac{\eta}{s}$ so as to align the anisotropy for each λ_{GB} at large w. We also plot on each panel a red dashed curve indicating the first order hydrodynamic approximation $R^{(1^{\mathrm{st}})}(w) = 8\,(\eta/s)\,w^{-1}$, and

[15] We have taken $a_i \sim \mathcal{O}(1)$ as a natural choice, but qualitatively similar results should hold for larger values. We have checked that our choice leads to a spread in anisotropy paramater comparable to that induced by the different initial conditions in $\mathcal{N}=4$ SYM reported in [74].

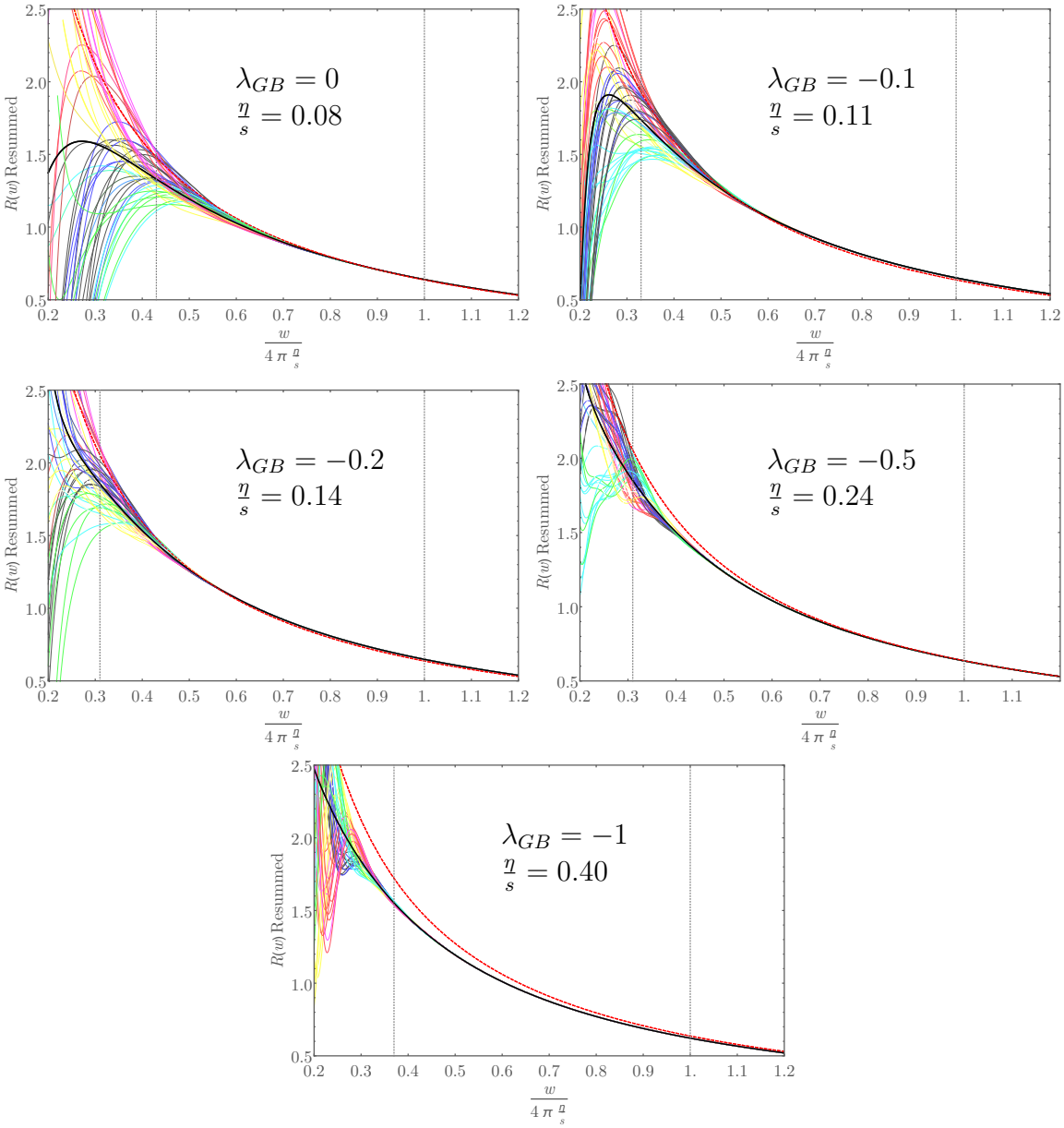

Figure 2.4: Resummed anisotropies as function of the viscosity-rescaled inverse gradient for different values of λ_{GB}. The thick solid black lines are the result of the resummation $\mathrm{Re}\,[R_{0^+}(w)]$ found by performing the integral of Eq. (2.64) along the 0^+ contour, with thin coloured lines corresponding to $R^{(\mathrm{full})}$ of Eq. (2.67) chosen with arbitrary coefficients. The red dashed line corresponds to the first order hydrodynamic prediction ($R^{(1^{\mathrm{st}})}$) and the vertical dotted line on the LHS of each panel indicates the rescaled hydrodynamization time $\frac{w_{\mathrm{hyd}} s}{4\pi\eta}$ indicating where $\mathrm{Re}\,[R_{0^+}(w)] = (1 \pm 0.1)\, R^{(1^{\mathrm{st}})}\Big|_{w_{\mathrm{hyd}}}$. Every curve is insensitive up to 2% to the choice of the Padé order N used for $w > 0.3$. For the case of $\mathcal{N} = 4$ there is no visible change for the entire region plotted.

dashed vertical lines are included at the transitional value of $\frac{w^*}{4\pi\eta/s}$ where,

$$\left|\frac{\mathrm{Re}\left[R_{0^+}(w^*)\right] - R^{(1^{\mathrm{st}})}(w^*)}{\mathrm{Re}\left[R_{0^+}(w^*)\right]}\right| \approx 0.1\,, \tag{2.68}$$

which we estimate as an approximate *hydrodynamization time*. We find that for each λ_{GB} we can identify a common curve that all trajectories relax to even in the region where the anisotropy is larger than 1. This is outside the naive regime of applicability of truncated hydrodynamics, where higher order contributions to the gradient expansion should potentially be large, as viscous contributions to the pressure become comparable to the equilibrium pressure.

Astonishingly even in this region first order hydrodynamics appears to provide an accurate description of the resummation to within 10%, a manifestation of hydrodynamization without isotropization as discussed in [65]. Further by inspection of Fig. (2.4) we see that in all holographic calculations the result of the resummation provides a good proxy to the attractor at the hydrodynamization time in that we do not see much variation due to the initial conditions at this time. We note however as expected that this common curve diverges from truncated hydrodynamics as the coupling becomes weaker (with larger negative λ_{GB}).

There are two major conclusions to draw from this: i) that there is a region outside the naive regime of applicability of hydrodynamics where the dynamics of Bjorken flow are described by some universal behaviour with little sensitivity to initial conditions, and ii) that these dynamics somehow are fairly well described by naive first order truncated hydrodynamics. This means that if one were to have applied truncated first order hydrodynamics to model the Bjorken system from the beginning, the results would have been correct to within 10% even in the presence of large gradients, and consistent with a fast hydrodynamization time. The model of Bjorken flow is most relevant to the QGP at the center of a heavy ion collision. One would hope that in less symmetric settings a comparable analysis might yield similar results.

2.5 Discussion and outlook

In this chapter we studied a transseries solution for a family of gauge theories undergoing Bjorken expansion. Through the AdS/CFT correspondence the problem of plasma equilibration was described as a dynamical blackbrane evolving toward its static state. The dissipative character of the blackbrane horizon translated into the dissipative properties of the late-time asymptotic solution, with quasinormal modes of this moving horizon corresponding to a tower of non-hydrodynamic modes which would rapidly decay during a short transient phase. Transseries solutions therefore naturally model the loss of the initial state, consistent with the process of thermalization.

The explicit identification of non-hydrodynamic modes with the quasinormal mode spectrum suggests that a generalisation of the gradient expansion through the fluid-gravity duality [111] should exist, systematically mapping exponentially suppressed corrections in the bulk to non-hydrodynamic modes in the dual Yang-Mills theory even without imposing the symmetries of Bjorken flow. This idea is further explored in Chapter 4 without Bjorken symmetry, by studying the contribution of non-hydrodynamic modes at finite momentum to the production of entropy.

Demonstrating the resurgent properties of our transseries solution we used novel techniques to partially recover the series of the leading fundamental sector using only the coefficients of the hydrodynamic sector. In principle one could fully reconstruct all sectors of the theory using only the hydrodynamic sector, the only limiting factor being the number of coefficients. Eqs. (2.26)–(2.28) can be integrated exactly for the hydrodynamic sector given by $\boldsymbol{\omega} = \mathbf{0}$ so it would be interesting to find an analytic form for $\epsilon_m^{(\mathbf{0})}$, essentially solving the theory for all sectors.

By resumming the series for a representative selection of the finite coupling parameter λ_{GB} we estimated the typical evolution a hot QGP-like plasma would follow during equilibration. In doing so we constrained the location of an attractor solution, to which all trajectories rapidly converge. This common curve was present in a region

where the anisotropy was at order 1 where viscous corrections are large, placing it outside the regime of hydrodynamics. Despite this, the curve was well approximated by first order hydrodynamics in this region indicating that first order hydro may coincidentally be sufficient to describe this medium far from equilibrium.

While not true in general, asymptotic series routinely exhibit similar behaviour, intuitively when due to the cancellation of their higher order coefficients which oscillate in sign. It is difficult to know apriori at what order one should optimally truncate the series for the most accurate description of hydrodynamics at large gradients. In our analysis we found no obvious general rule between choosing first and second order hydrodynamics, ideal hydrodynamics however was never a good description at large gradients.

Chapter 3

Holographic Bjorken flow at large-D

In Chapter 2 we successfully studied the equilibration process for of a class of gauge theory plasmas and the applicability of hydrodynamics in those systems by applying the transseries expansion in the parameter of small gradients. While we could compute the transseries coefficients to arbitrary orders the analysis was largely numerical and therefore limited.

In this chapter we organize our transseries around the large limit of a new parameter, the number of transverse dimensions, in order to avoid explicitly taking this small gradient limit. For holographic theories this limit will allow us more analytic control in determining the hydrodynamic and non-hydrodynamic sectors. The results presented here outline the analysis given in [3].

3.1 Introduction and motivation

As seen previously in this thesis, holography is a powerful tool that allows us to explore the strongly-coupled regime of non-Abelian gauge theories by mapping their dynamics onto classical gravity in anti-de Sitter (AdS) space. While the gravity dual is significantly easier to analyse than it's strongly interacting field theory counterpart, Einstein's field equations are non-linear and remain in general difficult to solve. Even in cases with a high degree of symmetry such as the Bjorken set up (see Chapter 2) time dependent dynamics far from equilibrium typically require the use of intensive

numerics [87].

In recent years a new strategy has emerged to solve these equations using the number of spacetime dimensions (D) as an expansion parameter [112, 113]. In particular the large-D expansion has been extensively applied to problems in holography [114–138]. Using the set-up of [116, 118, 119, 137] the large-D expansion been shown to be identical to second order hydrodynamics, with higher order viscous terms relegated to subleading D-corrections. In these analyses however the velocity fields of the associated membrane were chosen to be parametrically small (in D). In our analysis we will apply this technique to the relativistic set-up of boost invariant evolution, and as such will need to tailor our expansion to properly describe the kinematics of Bjorken flow.

In this chapter, we present the holographic dual to Bjorken flow for an infinitely coupled $\mathcal{N} = 4$ SYM plasma up to and including order $1/D^3$ terms in the perturbative expansion. We go on to compute the non-perturbative (in D) corrections and find the familiar form of a transseries at leading order in the $1/D$ expansion. In both cases the perturbative and non-perturbative sectors of the large-D expansion match the hydrodynamic and non-hydrodynamic sectors of the small gradient transseries expansion studied in Chapter 2, a connection ultimately stemming from the behaviour of gapped quasinormal modes of the AdS-blackbrane that scale linearly with large D. Moreover we are able to perform these complementary calculations analytically, which were inaccessible using only the small gradient expansion. As a remark we note that $\mathcal{N} = 4$ SYM is a conformal theory that exists in only $3+1$ dimensions, and we do not claim to study $\mathcal{N} = 4$ SYM in higher dimensions. Instead we are approximating the AdS_5 gravitational dual with AdS_D, taking $D \to \infty$ to conveniently order the series.

3.1.1 Second order hydrodynamics at large-D

In order to gauge whether our perturbative large-D solution reproduces standard hydrodynamics, we will first analyse Bjorken-flow for second order hydrodynamics in an arbitrary number of spacetime dimensions $n = D-1$. Recall from Subsection 1.1.2

that conformal Bjorken flow is the solution of relativistic hydrodynamics with the assumptions of boost invariance and the absense of transverse dynamics, obeying a conservation equation and equation of state given by,

$$\tau\dot{\epsilon}(\tau)+\left(\frac{n}{n-1}\right)\epsilon(\tau)+\Delta p_L=0\,, \tag{3.1}$$

with $\Delta p_L=\Pi^y_y$. Evaluating the different gradient structures in Eq. (1.13), the equation for Bjorken flow in n spacetime dimensions and up to second order in gradients is [27]

$$\tau\frac{\dot{\epsilon}}{\epsilon}+\frac{n}{n-1}-2\nu\frac{1}{\tau}\frac{\eta}{\epsilon}-2\nu^2\frac{\eta\tau_\pi}{\tau^2\epsilon}+4\nu^2\frac{n-3}{n-2}\frac{\lambda_1}{\tau^2\epsilon}=0\,, \tag{3.2}$$

with $\nu=(n-2)/(n-1)$, where η is the viscosity and τ_Π and λ_1 are second order transport coefficients. When taking the limit of large transverse dimensions we will need to consider how different thermodynamic quantities scale with n. For the case of a field theory dual to a blackbrane in AdS_D with $D=n+1$ the equilibrium energy density is given by $\epsilon_{\rm eq}=g_*\tilde{\epsilon}_{\rm eq}$ with

$$\tilde{\epsilon}_{\rm eq}=\left(\frac{4\pi T}{n}\right)^n\,. \tag{3.3}$$

and $g_*=\frac{(n-1)}{16\pi}\frac{L^{n-1}}{G_D}$, where G_D is the effective D-dimensional Newton constant, which is related to the number of degrees of freedom of the dual gauge theory. Since g_* is a D-dependent multiplicative factor we will redefine all thermodyamic quatities to conveniently factor it out ($s=g_*\tilde{s}$, $p=g_*\tilde{p}$, ...). We can note from Eq. (3.3) that taking the large n limit with either $\tilde{\epsilon}_{\rm eq}$ or T held fixed will lead to parametrically different results. For an easy comparison to the previous chapters we will keep $\tilde{\epsilon}$ fixed in our holographic analysis at large n. To anticipate this choice we will write Eq. (3.2) in terms of the dimensionless gradient $w_\epsilon\equiv\tau\tilde{\epsilon}^{1/n}$, analogous to the $w\equiv\tau T$ variable introduced in Eq. (2.59). Here we are using w_ϵ purely as a tool to conveniently write down the hydrodynamic conservation equation, which will later be useful to extract transport coefficients from our holographic solution.

From an AdS_D blackbrane solution one can compute the values of the shear viscosity to entropy density ratio, as well as the second order transport coefficients τ_Π

and λ_1 for arbitrary n [22, 23],[1]

$$\eta/s = 1/4\pi\,, \quad \lambda_1 = \frac{n}{8\pi}\frac{\eta}{T}\,, \quad \eta\tau_\Pi = 2\lambda_1\,(1-\beta)\,, \quad \beta = \int_1^\infty dx \frac{x^{(n-2)}-1}{x(x^n-1)}\,. \tag{3.4}$$

which together with the thermodynamic relation allows us to write,

$$\tau\frac{\dot{\tilde{\epsilon}}}{\tilde{\epsilon}} + \frac{n}{n-1} - \frac{2\nu}{n-1}\frac{1}{w_\epsilon} + \frac{2\nu^2}{n-1}\left(\beta - \frac{1}{n-2}\right)\frac{1}{w_\epsilon^2} = 0\,. \tag{3.5}$$

By comparing this expression with the conservation equation (3.1), boost invariant flow consistent with a truncation to second order in inverse normalized gradients is given by the ratio

$$\frac{\Delta p_{\rm L}}{\epsilon} \approx \left.\frac{\Delta p_{\rm L}}{\epsilon}\right|_{\rm hyd_2} \equiv -\frac{2\nu}{n-1}\frac{1}{w_\epsilon} + \frac{2\nu^2}{n-1}\left(\beta - \frac{1}{n-2}\right)\frac{1}{w_\epsilon^2}\,. \tag{3.6}$$

Hydrodynamics beyond second order in gradients leads to additional inverse powers of w_ϵ.

We now will find solutions of the hydrodynamic Eq. (3.5) through the large-D limit. As shown in Eq. (1.14) the local equilibrium energy density for $w_\epsilon \to \infty$ is given by $\tilde{\epsilon}_{eq} = \Lambda^n\,(\Lambda\tau)^{\frac{n}{1-n}}$ where Λ is a dimensionful constant defined by Eq. (1.15). In the large n limit becomes

$$\tilde{\epsilon}^\infty_{\rm eq} = \lim_{n\to\infty}\frac{\Lambda^n}{(\Lambda\tau)^{\frac{n}{n-1}}} = \frac{\Lambda^n}{(\Lambda\tau)}\,. \tag{3.7}$$

We then choose an ansatz in the form of a power series in inverse n,

$$\tilde{\epsilon}(\tau) = \tilde{\epsilon}^\infty_{\rm eq}\left(1 + \sum_{i=1}^\infty \frac{1}{n^i}c_i^{\rm hyd_2}\right)\,. \tag{3.8}$$

Solving Eq. (3.5) order by order in $1/n$ and imposing that we do not correct the normalization of the energy density with the integration constant we find,

$$c_1^{\rm hyd_2} = \frac{1}{2\Lambda^2\tau^2} - \frac{2}{\Lambda\tau} - \log(\Lambda\tau)\,, \tag{3.9}$$

$$c_2^{\rm hyd_2} = \frac{1}{8\Lambda^4\tau^4} - \frac{1}{\Lambda^3\tau^3} + \frac{\frac{1}{2}\log(\Lambda\tau)+1}{\Lambda^2\tau^2} - \frac{2}{\Lambda\tau} + \frac{1}{2}(\log(\Lambda\tau)-2)\log(\Lambda\tau)\,, \tag{3.10}$$

$$\begin{aligned} c_3^{\rm hyd_2} &= \frac{1}{48\Lambda^6\tau^6} - \frac{1}{4\Lambda^5\tau^5} + \frac{\frac{3}{8}\log(\Lambda\tau)+\frac{1}{4}}{\Lambda^4\tau^4} + \frac{\frac{4}{3}-2\log(\Lambda\tau)}{\Lambda^3\tau^3}\,, \\ &+\frac{3\log(\Lambda\tau)(\log(\Lambda\tau)+6)-4\pi^2-6}{12\Lambda^2\tau^2} - \frac{2}{\Lambda\tau} - \frac{1}{6}\log(\Lambda\tau)((\log(\Lambda\tau)-6)\log(\Lambda\tau)+6)\,. \end{aligned} \tag{3.11}$$

[1] Note that we have normalised the shear tensors as in [27] which differs by a factor of 2 from the normalisation of [23].

The expressions above can be interpreted through a comparison to the small gradient expression presented in Eq. (1.16) given by $\tilde{\epsilon}(\tau) = \tilde{\epsilon}_{eq}(\tau)\left(1 + \epsilon_1 u^{-1} + \epsilon_2 u^{-2} + ...\right)$ for $u^{-1} = (\Lambda\tau)^{-\frac{n-2}{n-1}} \sim \frac{1}{\Lambda\tau} + \frac{1}{n}\frac{\log(\Lambda\tau)}{\Lambda\tau} + \mathcal{O}(n^{-2})$. Here powers of $(\Lambda\tau)^{-1}$ are the result of powers of u^{-1}, with the $\log(\Lambda\tau)$ terms correcting the exponent at each order in $1/n$.

However, the functions present in Eqs. (3.9)–(3.11) only capture the gradient corrections due to second order hydrodynamics at large-D. In the following section we will compute the stress tensor for the holographic theory, and use this comparison to read off higher gradient coefficients at large-D. For future notational convenience this comparison is most easily made through the conservation equation (3.5) in the form

$$\tau\frac{\dot{\tilde{\epsilon}}}{\tilde{\epsilon}} + \frac{n}{n-1} + \sum_{i=1}^{\infty}\frac{\theta^{(i)}}{w_{\epsilon}^{i}} = 0 \ , \tag{3.12}$$

where the $\theta^{(i)}$ are the linear combinations, appropriate for Bjorken flow, of the i-th order transport coefficients. In the large-D limit, these transport coefficients can be further expanded in inverse powers of n

$$\theta^{(i)} = \sum_{j}\theta_{j}^{(i)}\frac{1}{n^{j}} \ . \tag{3.13}$$

To close this section we summarize the results to follow. In Section 3.2 we describe the holographic set-up for arbitrary spacetime dimension in the gravity dual D, and find the perturbative bulk solution analytically at large D. Using our solution we extract the transport coefficients relevant for Bjorken flow to $\mathcal{O}(1/D^3)$. In Section 3.3 we show analytically how non-perturbative fluctuations in the $1/D$ expansion emerge in this boost-invariant setup and find their contribution to the energy density. By comparing to a small gradient transseries for arbitrary D we identify these non-perturbative (in D) solutions with the non-hydrodynamic modes of Chapter 2. Finally, in Section 3.4 we comment on the relationship between the large-D and hydrodynamic expansions in this setup as well as on the implications our findings have on the non-convergence of the large-D expansion.

3.2 Large-D limit of Bjorken Flow

In holography, the analysis of Bjorken flow in n spacetime dimensions is performed by searching for solutions of the Einstein equations in $D = n + 1$ dimensions in an asymptotically AdS_D spacetime. Following the analysis presented in Section 2.2 for $D = 5$ dimensions, we parameterize the dual spacetime to Bjorken flow with the following Eddington-Finkelstein-like ansatz,

$$ds^2 = -A(r,\,\tau)\,d\tau^2 + 2d\tau dr + S(r,\,\tau)^2\left(e^{-(n-2)B(r,\tau)}dy^2 + e^{B(r,\tau)}dx_\perp^2\right)\,, \tag{3.14}$$

where boost invariance and transverse homogenuity impose that the metric functions do not depend on the spacetime rapidity y or transverse dimensions $x_\perp$. In this gauge the Einstein's equations[2] result in a simple set of equations following a similar form to Eqs. (2.8)– (2.12) that we found in the case of $n = 4$ boundary dimensions,

$$S'' = -\frac{n-2}{4}S\left(B'\right)^2\,, \tag{3.15}$$

$$S\dot{S}' = \frac{n}{2}S^2 - (n-2)\dot{S}S'\,, \tag{3.16}$$

$$S\dot{B}' = -\frac{n-1}{2}\left(\dot{S}B' + \dot{B}S'\right)\,, \tag{3.17}$$

$$A'' = -n(n-3) - (n-2)(n-1)\left(\frac{1}{2}\dot{B}B' - 2\frac{\dot{S}S'}{S^2}\right)\,, \tag{3.18}$$

$$\ddot{S} = \frac{1}{2}\dot{S}A' - \frac{n-2}{4}\dot{B}^2 S\,, \tag{3.19}$$

where $f' = \partial_r f$ and $\dot{f} = \left(\partial_\tau + \frac{1}{2}A(r,\tau)\partial_r\right)f$. Where, as before, the derivative operators do not commute, and we denote $\dot{X}' \equiv \left(\dot{X}\right)'$. With the ansatz (3.14), AdS_D-space – dual to the vacuum of the gauge theory – takes a non-trivial form, which depends explicitly on proper time, τ. The three metric functions in this case are given by

$$A_{\rm V} = r^2, \quad B_{\rm V} = \frac{2}{n-1}\log\left(\frac{r}{1+r\tau}\right), \quad S_{\rm V} = r^{\frac{n-2}{n-1}}\left(1+r\tau\right)^{\frac{1}{n-1}}\,. \tag{3.20}$$

To simplify the holographic analysis of the strongly coupled expansion, we find it convenient to factor out this non-trivial dependence of the metric functions which do

[2]In more familiar notation, the equations we solve are $R_{\mu\nu} = -(D-1)g_{\mu\nu}$ with the cosmological constant set such that an anti-de Sitter solution has radius of curvature equal to one.

not lead to dynamics in the dual field theory. Consequently, we redefine the fields as

$$\tilde{A} \equiv \frac{A}{A_{\rm V}}, \quad \tilde{B} \equiv (n-2)\,(B - B_{\rm V})\,, \quad \tilde{S} \equiv \frac{S}{S_{\rm V}}. \tag{3.21}$$

This redefinition simplifies, in particular, the near boundary behaviour of the different metric functions. Exploiting the residual gauge dependence in Eq. (3.14), it is always possible to choose a gauge in which our metric functions take the convenient form near the AdS_D boundary as $r \to \infty$

$$\tilde{A} = 1 - \frac{1}{r^n}\left(\tilde{\epsilon}(\tau) + \mathcal{O}\left(\frac{1}{r}\right)\right), \tag{3.22}$$

$$\tilde{B} = \frac{1}{r^n}\left(-\frac{n}{n-1}\Delta\tilde{p}_L(\tau) + \mathcal{O}\left(\frac{1}{r}\right)\right), \tag{3.23}$$

$$\tilde{S} = 1 + \frac{1}{r^{n+1}}\left(s_1(\tau) + \mathcal{O}\left(\frac{1}{r}\right)\right), \tag{3.24}$$

where $\tilde{\epsilon}$ and $\Delta\tilde{p}_L$ are the energy density and pressure anisotropy of the dual gauge theory. These two boundary values are not independent, since they are related via the conservation equation and equation of state, given together by Eq. (3.1). In holography this condition comes from the constraints imposed by Eq. (3.19).

For large numbers of spacetime dimensions, the quickly changing function r^{-n} in the boundary expansion Eq. (3.22) reveals two distinct regions in the gravitational analysis. Using the definition (1.15) of the scale Λ,[3] these two regions are

- The Near Horizon Region: $r \sim \Lambda$, or $\log r/\Lambda \ll 1$. In this region, in the large-n limit, the factor $\tilde{\epsilon}(\tau)/r^n$ is order 1 and the gravitational field becomes strong. As expected from the presence of a non-zero density in the boundary theory, in this region the gravity dual develops a horizon at $r^n \sim 1/\tilde{\epsilon}$.

- The Near Boundary Region: $(r/\Lambda)^n \gg 1$. In this region, the combination $\tilde{\epsilon}(\tau)/r^n$ is small and the effect of the energy density may be considered as a small perturbation over the AdS_D space.

[3]For convenience we repeat this here as,

$$\Lambda = \lim_{\tau\to\infty} \tau^{\frac{1}{n-2}} \left(\tilde{\epsilon}(\tau)\right)^{\frac{1}{n\nu}}, \quad \nu = \frac{n-2}{n-1}\,. \tag{3.25}$$

The treatment of these two regions requires different approximations, which can be matched at the intermediate region $1/n \ll \log r/\Lambda \ll 1$, where both the regions defined above overlap. In the following subsection we will analyse the gravitational dynamics in those two regions.

3.2.1 The Near horizon region

We start the analysis of the dual geometry for the region close to the horizon, where gravity interacts strongly and it is necessary to find a non-linear solution of Einstein's equations. This can in general be a complicated task at finite D requiring numerical solutions. However, as in other analyses [114–138], in the limit of large-D Einstein's equations simplify tremendously and allow us to instead find analytic solutions.

In the near horizon region we take advantage of the fact that $r \sim \Lambda$ to define

$$R = \left(\frac{r}{\Lambda}\right)^n , \tag{3.26}$$

which remains fixed as we vary the value of $D = n + 1$. In terms of this variable, the intermediate region where we will perform the matching with the Near Boundary region occurs at $R \gg 1$. We expand each metric function in inverse powers of $1/n$ of the form,

$$\tilde{A}(\tau, R) = \sum_{i=0}^{\infty} \frac{1}{n^i} A_i(\tau, R) , \tag{3.27}$$

$$\tilde{B}(\tau, R) = \sum_{i=0}^{\infty} \frac{1}{n^i} B_i(\tau, R) , \tag{3.28}$$

$$\tilde{S}(\tau, R) = \sum_{i=0}^{\infty} \frac{1}{n^i} S_i(\tau, R) , \tag{3.29}$$

after which we can greatly simplify Einstein's equations by taking the large-D limit at fixed R, and determine the different metric coefficients order by order. As already anticipated, the large-D approximation simplifies the R-dependence of the corresponding differential equations, which can be solved analytically. Imposing consistency with the near boundary expansion (3.22)-(3.24), to leading order in $1/n$ we find

$$A_0 = 1 - \frac{1}{R}\bar{a}_0^{\rm NH} , \quad B_0 = 0 , \quad S_0 = 1 , \tag{3.30}$$

where $\bar{a}_0^{\rm NH}$ satisfies the differential equation

$$(1+\tau\Lambda)\,\partial_\tau \bar{a}_0^{\rm NH} - \Lambda \bar{a}_0^{\rm NH} = 0\,, \tag{3.31}$$

which has a simple solution as

$$\bar{a}_0^{\rm NH} = \frac{\alpha_0}{1+\tau\Lambda}\,, \tag{3.32}$$

where α_0 is an arbitrary constant.

The similarity between the leading order in the near boundary expansion (3.22) and the leading order solution (3.30) suggests that the function $\bar{a}_0^{\rm NH}$ may be identified with the leading order energy density $\tilde{\epsilon}$. However, this identification is incorrect, as may be inferred from Eq. (3.31), which differs from the large-n and ideal hydrodynamic limit of the conservation equation (3.1). As we will see in Subsection 3.2.2, the characteristic $(1+\tau\Lambda)$ dependence of $\bar{a}_0^{\rm NH}$ does not imply that the energy density in the dual field theory at this order in n possesses an infinite series in gradients $1/\tau$ at late times. This strange dependence is instead a consequence of the fact that the proper time as measured in the near horizon region is different to the proper time of the boundary theory, which is the where we originally made the identification to define τ for the dual theory.

However for large τ the leading $1/\tau$ dependence agrees with the behaviour of the boundary energy density. Anticipating this result, and in order to lighten notation, the definition (1.15) of the scale Λ imposes

$$\alpha_0 = 1\,. \tag{3.33}$$

Following the same procedure above, the next order in the $1/n$-expansion is given by

$$A_1 = -\frac{\bar{a}_1^{\rm NH}(\tau)}{R} - \frac{1}{(1+\tau\Lambda)^2}\frac{\log R}{R}\,, \tag{3.34}$$

$$B_1 = 0\,, \tag{3.35}$$

$$S_1 = 0\,, \tag{3.36}$$

with

$$\bar{a}_1^{\rm NH} = -\frac{\log\left(1+\tau\Lambda\right)+\alpha_1}{(1+\tau\Lambda)} \tag{3.37}$$

where α_1 is an arbitrary constant, which we fix to $\alpha_1 = 0$ by demanding that the overall scale of the energy density Λ does not receive corrections in $1/n$. Similarly, to second order we find,

$$A_2 = -\frac{\bar{a}_2^{\rm NH}(\tau)}{R} + \frac{(\tau\Lambda+(1+\tau\Lambda)\log\left(1+\tau\Lambda\right))}{(1+\tau\Lambda)^3}\frac{\log R}{R} + \frac{\tau\Lambda-1}{2(1+\tau\Lambda)^3}\frac{(\log R)^2}{R} \tag{3.38}$$

$$B_2 = \frac{\tau\Lambda\left(\log\left(1+\frac{1}{(1+\tau\Lambda)R-1}\right)\log\left(\frac{1}{(1+\tau\Lambda)R}\right)-\mathrm{Li}_2\left(\frac{1}{(1+\tau\Lambda)R}\right)\right)}{(1+\tau\Lambda)^2\log\left(1+\tau\Lambda\right)}\,, \tag{3.39}$$

$$S_2 = 0\,, \tag{3.40}$$

where $\mathrm{Li}_2(z)$ is the polylogarithm of order 2 and

$$\bar{a}_2^{\rm NH}(\tau) = \frac{1}{2(1+\tau\Lambda)^3}\left((1+\tau\Lambda)^2(\log\left(1+\tau\Lambda\right))^2 - 2(2+4\tau\Lambda+(\tau\Lambda)^2)\log\left(1+\tau\Lambda\right)\right)\,, \tag{3.41}$$

where, as before, we have set an arbitrary integration constant by demanding that there are no n-corrections to Λ. analysing the expansion to third order yields long expressions for the metric functions, which we have stored in Appendix B.1. Here we only quote the large-R behaviour of the blackening function A_3, necessary to perform the matching with the near boundary region in Subsection 3.2.2, which is given by,

$$\begin{aligned} A_3 \approx\ & \frac{-\bar{a}_3^{\rm NH}(\Lambda\tau)+\frac{4\Lambda\tau(\log(\Lambda\tau+1)+1)}{(\Lambda\tau+1)^4}}{R} \\ & +\frac{\log(R)\left(2\Lambda\tau(\Lambda\tau+6)+\log(\Lambda\tau+1)\left(10\Lambda\tau+(\Lambda\tau+1)^2(-\log(\Lambda\tau+1))+4\right)\right)}{2R(\Lambda\tau+1)^4} \\ & -\frac{\log^2(R)\left((\Lambda^2\tau^2-1)\log(\Lambda\tau+1)+\Lambda\tau(\Lambda\tau-5)\right)}{2R(\Lambda\tau+1)^4} - \frac{(\Lambda\tau(\Lambda\tau-4)+1)\log^3(R)}{6R(\Lambda\tau+1)^4}\,, \end{aligned} \tag{3.42}$$

with,

$$\begin{aligned} \bar{a}_3^{\rm NH}(\tau) = & -\frac{18\Lambda\tau+\pi^2(3\Lambda\tau-1)+6}{9(\Lambda\tau+1)^4} - \frac{\log^3(\Lambda\tau+1)}{6\Lambda\tau+6} + \frac{(\Lambda\tau+2)\log^2(\Lambda\tau+1)}{(\Lambda\tau+1)^2} \\ & -\frac{(\Lambda\tau+2)(\Lambda\tau(\Lambda\tau+5)+2)\log(\Lambda\tau+1)}{(\Lambda\tau+1)^4}\,. \end{aligned} \tag{3.43}$$

We have also checked that the function $\tilde{S}-1$ does not remain zero for all orders, receiving its first non-trivial contribution at S_4. Since this fourth-order expression is needed

to determine A_3 and B_3, its expression can also be found in Appendix B.1. Additionally, to show the consistency of the large-D and large-τ expansions, in Appendix B.2 we explicitly compute the low order metric functions in the gradient expansion of Eqs. (2.18), (2.19) and (2.20) from Section 2.2 for arbitrary dimensions $D = n + 1$. Expanding the result at large n and fixed R in the near horizon region shows both expressions to be compatible. Finally, to extract the dual field theory stress tensor from these expansions we must match these results to the metric functions computed in the near boundary region.

3.2.2 Matching with the near boundary region

We now perform a similar calculation in the near boundary region where $\left(\frac{\Lambda}{r}\right)^n \ll 1$. As already mentioned, while in the near-horizon region gravity interacts strongly, in this region we can view the effect of the horizon as a small perturbation on an AdS_D background. To make the approximation apparent, we will redefine the fields in this region as

$$A(\tau, r) = r^2 \left(1 - \frac{a(r,\tau)}{r^n}\right) , \tag{3.44}$$

$$B(\tau, r) = \frac{2}{n-1} \log\left(\frac{r}{1+r\tau}\right) + \frac{1}{n-2}\frac{b(r,\tau)}{r^n} , \tag{3.45}$$

$$S(\tau, r) = r \left(\frac{1+r\tau}{r}\right)^{\frac{1}{n-1}} \left(1 + \frac{s(r,\tau)}{r^{n+1}}\right) . \tag{3.46}$$

Since gravity is weak in this limit, we linearize the equations dropping all terms that are quadratic or higher in a, b, and s leaving a set of linear PDEs. In the large-D

limit we can expand each function as power series in $1/n$,[4]

$$a(\tau,r)=\sum_{i=0}^{\infty}\frac{a_i^{\rm NB}(\tau_{\rm B},r)}{n^i}\,,\quad b(\tau,r)=\sum_{i=0}^{\infty}\frac{b_i^{\rm NB}(\tau_{\rm B},r)}{n^i}\,,\quad s(\tau,r)=\sum_{i=2}^{\infty}\frac{s_i^{\rm NB}(\tau_{\rm B},r)}{n^i}\,, \tag{3.48}$$

where we have pre-emptively introduced a convenient time variable $\tau_{\rm B}=\tau+r^{-1}$ to simplify the analysis. Note that $\tau_{\rm B}$ agrees with the gauge theory proper-time at the boundary. The leading non-zero solutions can be found as,

$$a_0^{\rm NB}(\tau_{\rm B},r)=a_0^{\rm NB}(\tau_{\rm B})\,, \tag{3.49}$$

$$b_0^{\rm NB}(\tau_{\rm B},r)=a_0^{\rm NB}(\tau_{\rm B})+\tau_{\rm B}a_0^{\rm NB\prime}(\tau_{\rm B})\,, \tag{3.50}$$

$$s_2^{\rm NB}(\tau_{\rm B},r)=\tau_{\rm B}^{-1}a_0^{\rm NB}(\tau_{\rm B})+a_0^{\rm NB\prime}(\tau_{\rm B})\,, \tag{3.51}$$

where the function $a_0^{\rm NB}(\tau_{\rm B})$ remains undetermined by the equations of motion, instead it will be constrained by matching our solution to Eq. (3.30) in the near horizon region. Making this identification in the overlap region where we fix $R\gg 1$ and large n we can find,

$$a_0^{\rm NB}(\tau+1)=\bar{a}_0^{\rm NH}(\tau)=\frac{\alpha_0}{1+\tau\Lambda}\,, \tag{3.52}$$

from which we identify $a_0^{\rm NB}(\tau)=\tilde{\epsilon}_{\rm eq}^{\infty}(\tau)$ where $\tilde{\epsilon}_{\rm eq}^{\infty}(\tau)$ is the large-D limit of ideal Bjorken flow given by Eq. (3.7). We can generate higher order solutions in $1/n$ for the near boundary region without too much effort so we will not state the resulting functions for $b_i^{\rm NB}$ and $s_i^{\rm NB}$ but will instead display the solution for $a_i^{\rm NB}$ which will be necessary to extract the energy density. Up to order $1/n^3$ we find,

$$\begin{aligned}a(\tau,r)\;=\;&a_0^{\rm NB}(\tau_{\rm B})+\frac{1}{n}\left(a_1^{\rm NB}(\tau_{\rm B})+\Delta a_1^{\rm NB}(\tau_{\rm B},r)\right)\\&+\frac{1}{n^2}\left(a_2^{\rm NB}(\tau_{\rm B})+\Delta a_2^{\rm NB}(\tau_{\rm B},r)\right)+\frac{1}{n^3}\left(a_3^{\rm NB}(\tau_{\rm B})+\Delta a_3^{\rm NB}(\tau_{\rm B},r)\right)\,,\end{aligned} \tag{3.53}$$

[4] In [2] we solved the near boundary problem in an even more direct way by taking linear combinations of the equations of motion to find a fourth order equation for $a(r,\tau)$,

$$\begin{aligned}&-\tfrac{(n-2)(n-1)((n-3)r\tau+n)a^{(0,1)}(r,\tau)}{r^5(r\tau+1)}+\tfrac{2(n-2)(2(n-3)r\tau+2n-3)a^{(1,1)}(r,\tau)}{r^4(r\tau+1)}-\tfrac{(n-5)(n-3)(n-2)a^{(1,0)}(r,\tau)}{r^3}\\&+\tfrac{\left(-5n-\frac{3}{r\tau+1}+15\right)a^{(2,1)}(r,\tau)}{r^3}+\tfrac{(n-3)(3n-14)a^{(2,0)}(r,\tau)}{r^2}+\tfrac{(13-3n)a^{(3,0)}(r,\tau)}{r}+\tfrac{2a^{(3,1)}(r,\tau)}{r^2}+a^{(4,0)}(r,t)=0\,.\end{aligned} \tag{3.47}$$

However we find it instructive to present an alternative analysis here which can be easily generalized in more complicated scenarios, where finding a similar equation is unfeasible.

where the functions $a_i^{\rm NB}(\tau_{\rm B})$ are only functions of $\tau_{\rm B}$ which, as explicitly shown above, can be determined after matching them to the near horizon solutions. The functions $\Delta a_i^{\rm NB}(\tau_{\rm B}, r)$ are fixed by the $a_i^{\rm NB}(\tau_{\rm B})$ as

$$\Delta a_1^{\rm NB}(\tau_{\rm B}, r) = \frac{(3-4r\tau_{\rm B})a_0^{\rm NB\prime}(\tau_{\rm B}) + \tau_{\rm B} a_0^{\rm NB\prime\prime}(\tau_{\rm B})}{2r^2\tau_{\rm B}}\,, \tag{3.54}$$

$$\begin{aligned}\Delta a_2^{\rm NB}(\tau_{\rm B}, r) = {} & \frac{(3-4r\tau_{\rm B})a_1^{\rm NB\prime}(\tau_{\rm B})}{2r^2\tau_{\rm B}} - \frac{3\left(8r^2\tau_{\rm B}^2 - 8r\tau_{\rm B}+1\right)a_0^{\rm NB\prime}(\tau_{\rm B})}{8r^4\tau_{\rm B}^3} + \frac{a_1^{\rm NB\prime\prime}(\tau_{\rm B})}{2r^2} \\ & \frac{a_0^{\rm NB(3)}(\tau_{\rm B})(3-4r\tau_{\rm B})}{4r^4\tau_{\rm B}} + \frac{a_0^{\rm NB(4)}(\tau_{\rm B})}{8r^4} + \frac{\left(16r^2\tau_{\rm B}^2 - 24r\tau_{\rm B}+3\right)a_0^{\rm NB\prime\prime}(\tau_{\rm B})}{8r^4\tau_{\rm B}^2}\,,\end{aligned} \tag{3.55}$$

$$\begin{aligned}\Delta a_3^{\rm NB}(\tau_{\rm B}, r) = {} & \frac{a_0^{\rm NB(5)}(\tau_{\rm B})(3-4r\tau_{\rm B})}{16r^6\tau_{\rm B}} + \frac{a_0^{\rm NB(6)}(\tau_{\rm B})}{48r^6} + \frac{a_1^{\rm NB(4)}(\tau_{\rm B})}{8r^4} + \frac{a_2^{\rm NB\prime\prime}(\tau_{\rm B})}{2r^2} \\ & \frac{a_1^{\rm NB(3)}(\tau_{\rm B})(3-4r\tau_{\rm B})}{4r^4\tau_{\rm B}} + \frac{3a_0^{\rm NB(4)}(\tau_{\rm B})\left(4r^2\tau_{\rm B}^2 - 8r\tau_{\rm B}+1\right)}{16r^6\tau_{\rm B}^2} + \frac{a_0^{\rm NB(3)}(\tau_{\rm B})(3r\tau_{\rm B}-1)}{4r^6\tau_{\rm B}^3} \\ & + \frac{(3-4r\tau_{\rm B})a_2^{\rm NB\prime}(\tau_{\rm B})}{2r^2\tau_{\rm B}} - \frac{3\left(8r^2\tau_{\rm B}^2 - 8r\tau_{\rm B}+1\right)a_1^{\rm NB\prime}(\tau_{\rm B})}{8r^4\tau_{\rm B}^3} \\ & + \frac{3\left(16r^4\tau_{\rm B}^4 - 64r^3\tau_{\rm B}^3 + 60r^2\tau_{\rm B}^2 - 12r\tau_{\rm B}-1\right)a_0^{\rm NB\prime}(\tau_{\rm B})}{16r^6\tau_{\rm B}^5} \\ & \frac{\left(-32r^4\tau_{\rm B}^4 + 192r^3\tau_{\rm B}^3 - 180r^2\tau_{\rm B}^2 + 36r\tau_{\rm B}+3\right)a_0^{\rm NB\prime\prime}(\tau_{\rm B})}{16r^6\tau_{\rm B}^4} + \frac{\left(16r^2\tau_{\rm B}^2 - 24r\tau_{\rm B}+3\right)a_1^{\rm NB\prime\prime}(\tau_{\rm B})}{8r^4\tau_{\rm B}^2}\,.\end{aligned} \tag{3.56}$$

Since the functions $\Delta a_i^{\rm NB}(\tau_{\rm B}, r)$ vanish at the boundary, the $1/n$ expansion of the normalized energy density $\tilde{\epsilon}$ given in Eq. (3.22) can be read off from the functions $a_i^{\rm NB}(\tau)$ as,

$$\tilde{\epsilon}(\tau) = a_0^{\rm NB}(\tau) + \frac{1}{n}a_1^{\rm NB}(\tau) + \frac{1}{n^2}a_2^{\rm NB}(\tau) + \frac{1}{n^3}a_3^{\rm NB}(\tau)\,. \tag{3.57}$$

As shown explicitly in Eq. (3.52) we can match the boundary solution Eq. (3.53) to the near horizon solutions of Eqs. (3.30)-(3.41) after replacing $r = \Lambda R^{1/n}$ and

taking the large n limit with $R \gg 1$ to find,

$$a_0^{\rm NB}(\tau) = \tilde{\epsilon}_{\rm eq}^{\infty}(\tau)\,, \tag{3.58}$$

$$a_1^{\rm NB}(\tau) = \tilde{\epsilon}_{\rm eq}^{\infty}(\tau)\, c_1^{\rm hyd_2}(\tau)\,, \tag{3.59}$$

$$a_2^{\rm NB}(\tau) = \tilde{\epsilon}_{\rm eq}^{\infty}(\tau)\left(\frac{\theta_2^{(3)}}{3\Lambda^3\tau^3}+\frac{\theta_2^{(4)}}{4\Lambda^4\tau^4}+c_2^{\rm hyd_2}(\tau)\right)\,, \tag{3.60}$$

$$\begin{aligned} a_3^{\rm NB}(\tau) = \tilde{\epsilon}_{\rm eq}^{\infty}(\tau)\Bigg(&\frac{\frac{1}{6}\left(\theta_2^{(3)}-3\theta_2^{(4)}\right)+\frac{\theta_3^{(5)}}{5}}{\Lambda^5\tau^5}+\frac{-8\theta_2^{(3)}+9\theta_2^{(4)}\log(\Lambda\tau)+3\left(\theta_2^{(4)}+\theta_3^{(4)}\right)}{12\Lambda^4\tau^4}+\\ &+\frac{2\theta_2^{(3)}\log(\Lambda\tau)+\theta_2^{(3)}+\theta_3^{(3)}}{3\Lambda^3\tau^3}+\frac{\frac{\theta_2^{(4)}}{8}+\frac{\theta_3^{(6)}}{6}}{\Lambda^6\tau^6}+c_3^{\rm hyd_2}(\tau)\Bigg)\,, \end{aligned} \tag{3.61}$$

where, as before, $\tilde{\epsilon}_{\rm id}^{\infty}(\tau)$ is given by Eq. (3.7), the functions $c_1^{\rm hyd_2}(\tau)$, $c_2^{\rm hyd_2}(\tau)$ and $c_3^{\rm hyd_2}(\tau)$ are predicted from the second order hydrodynamics Eqs. (3.9)-(3.11), and the coefficients $\theta_2^{(i)}$ and $\theta_3^{(i)}$ are transport coefficients defined in Eq. (3.12) where the superscript i indicates which gradient correction w_ϵ^{-i} they multiply, and the subscript j gives the order in the $1/n$ expansion. The expansion for the transport coefficients corresponding to second order hydrodynamics are given below,

$$\theta_1^{(1)}=-2\,,\quad \theta_2^{(1)}=0\,,\quad \theta_3^{(1)}=2\,, \tag{3.62}$$

$$\theta_1^{(2)}=1\,,\quad \theta_2^{(2)}=-3\,,\quad \theta_3^{(2)}=\frac{-12-2\pi^2}{3} \tag{3.63}$$

which are consistent with the coefficients of the w_ϵ^{-i} terms in Eq. (3.6). As is apparent from Eqs. (3.58) and (3.59), our large-D computation coincides exactly with the prediction of second order hydrodynamics for the first order in $1/n$. At higher orders in $1/n$ we constrain the value of further coefficients given by,

$$\theta_2^{(3)}=3\,,\qquad \theta_3^{(3)}=\frac{-9+4\pi^2}{3}\,, \tag{3.64}$$

$$\theta_2^{(4)}=-2\,,\qquad \theta_3^{(4)}=6\,, \tag{3.65}$$

$$\theta_3^{(5)}=-\frac{25}{4}\,, \tag{3.66}$$

$$\theta_3^{(6)}=7\,. \tag{3.67}$$

The energy density $\tilde{\epsilon}(\tau)$ given in Eq. (3.57) appears to be perturbative at large τ containing no modes reminiscent of the transseries structure that appeared in Chapter

2. This observation implies that at this order in the n expansion, we have effectively eliminated all non-hydrodynamic modes from the time evolution of the system. This behaviour is in fact expected as in other large-D analyses where for small velocity set-ups, second order hydrodynamics becomes an exact description of the system dynamics [116, 118, 119, 137]. Going beyond $1/n$-order, the system's evolution is no longer described by second order hydrodynamics, but nevertheless as shown in Eq. (3.60) and Eq. (3.61) is given by a finite sum in the inverse of the normalized gradient w_ϵ. In fact, Eqs. (3.58)-(3.61) may be viewed as the prediction of 6-th order hydrodynamics, for which the deviation of the longitudinal pressure with respect to its equilibrium value obtains contributions up to w_ϵ^{-6}

$$\frac{\Delta P_{\rm L}}{\epsilon} \approx \frac{\Delta P_{\rm L}}{\epsilon}\bigg|_{\rm hyd_2} + \sum_{i=3}^{6} \frac{\theta^{(i)}}{w_\epsilon^i}\,, \tag{3.68}$$

where we have used Eq. (3.6). Since no terms with inverse powers of w_ϵ greater than 6 appear in our holographic result, Eq. (3.60) and Eq. (3.61) specify the result of the gradient expansion up to $\mathcal{O}(n^{-4})$ for all higher order transport coefficients.

3.3 Non-Perturbative Modes and Large-D Trans-series

When constructing the large-D expansion in the preceding section we saw that the non-perturbative modes, reminiscent of the non-hydrodynamics explored is Chapter 2, did not contribute to the energy density in this limit. At finite D we should expect the metric to undergo different paths of evolution corresponding to choices of initial data which are not completely captured by hydrodynamic evolution. We could expect that our previous expansion missed these non-perturbative modes and that they potentially follow a now familiar transseries structure.

Therefore we will study perturbations on the asymptotically AdS geometry that that evolve on short timescales of order $1/(n\,\Lambda)$. As we will see, this is the typical scale of variation of the characteristic relaxation modes of black branes, known as quasi-normal modes (QNMs), which were first analysed at large-D in [139,140]. To describe

the dynamics of those fast fluctuations we will employ WKB-like techniques, which can also be used to describe the spectrum of QNMs, as demonstrated in Appendix B.3.

3.3.1 Non-perturbative contributions in $1/D$ for the near boundary region

We begin by analysing solutions in the near boundary region. Similar to the analysis of Subsection 3.2.2, we linearize Einstein's equations about the vacuum AdS solution with metric functions given by equations (3.44) to (3.46). We consider the now an ansatz of the form,

$$b(r,\tau) = \left(b_0^{\rm WKB}(r,\tau) + ...\right)\Omega(r,\tau)\,, \tag{3.69}$$

$$a(r,\tau) = \left(\frac{1}{n}a_1^{\rm WKB}(r,\tau) + ...\right)\Omega(r,\tau)\,, \tag{3.70}$$

$$s(r,\tau) = \left(\frac{1}{n^2}s_2^{\rm WKB}(r,\tau) + ...\right)\Omega(r,\tau)\,. \tag{3.71}$$

where we choose,

$$\Omega(r,\tau) = \left(\frac{r}{\Lambda}\right)^{n/2} e^{-in\hat{\omega}\Lambda\left(\tau+\frac{1}{r}\right)}\, e^{n\sigma(r)}\,. \tag{3.72}$$

This form of $\Omega(r,\tau)$ is suggestive and intended to mimic the non-hydrodynamic behaviour of $\Omega_{\boldsymbol{n}}(u)$ in Eq. (2.21) in Section 2.2. The dimensionless parameter $\hat{\omega}$ is an undetermined constant that will be fixed in Subsection 3.3.3. To leading order in n one finds that $\sigma'(r) = \pm\frac{\sqrt{r^2-4(\hat{\omega}\Lambda)^2}}{2r^2}$. Choosing the normalizable ("$-$") branch of the square root we find the solutions,

$$\sigma(r) = \frac{1}{2}\left(\frac{\sqrt{r^2-4(\hat{\omega}\Lambda)^2}}{r} - \log\left(\sqrt{\frac{r^2}{\Lambda^2}-4\hat{\omega}^2}+\frac{r}{\Lambda}\right)\right)\,, \tag{3.73}$$

$$a_1^{\rm WKB}(r,\tau) = \frac{ir\left(\sqrt{r^2-4(\hat{\omega}\Lambda)^2}+r\right)}{2\hat{\omega}\Lambda(1+r\tau)\left(\sqrt{r^2-4(\hat{\omega}\Lambda)^2}-2i\hat{\omega}\Lambda\right)} b_0^{\rm WKB}(r,\tau)\,, \tag{3.74}$$

$$s_2^{\rm WKB}(r,\tau) = \frac{2r^2}{(1+r\tau)\left(\sqrt{r^2-4(\hat{\omega}\Lambda)^2}+r-2i\hat{\omega}\Lambda\right)} b_0^{\rm WKB}(r,\tau)\,. \tag{3.75}$$

We can note that these solutions are not regular as $\hat{\omega}\to 0$, as the entire WKB solution fails in this limit. At the next order in inverse n we find that we can further constrain

$b_0^{\rm WKB}(r,\tau)$ by,

$$b_0^{\rm WKB}(r,\tau) = h_0(\Lambda\tau_\Omega)\frac{\Lambda^n r}{\sqrt{1+r\tau}\sqrt[4]{\frac{r^2}{\Lambda^2}-4\hat{\omega}^2}}\,, \tag{3.76}$$

with $\tau_\Omega = \tau + \frac{1+\frac{i\sqrt{r^2-4(\hat{\omega}\Lambda)^2}}{2\hat{\omega}\Lambda}}{r}$ and $h_0(\tau_\Omega)$ an undetermined function of τ_Ω.

Pre-emptively we will extract the corresponding contribution to the energy density by expanding Eq. (3.74) close to the boundary and comparing the result to Eq. (3.22). The energy density associated with the fluctuation is given by,

$$\delta\tilde{\epsilon}(\tau) = \frac{i\Lambda^n}{n\hat{\omega}}\left(\frac{e}{2}\right)^{\frac{n}{2}}\frac{h_0\left(\tau\Lambda+\frac{i}{2\hat{\omega}}\right)}{(\Lambda\tau)^{3/2}}e^{-in\hat{\omega}\Lambda\tau}+\mathcal{O}(n^{-2})\,. \tag{3.77}$$

The form of the expansion in Eqs. (3.69) to (3.71) above can be viewed in analogy with Quantum Mechanics as a WKB expansion in n, and will not be valid for values of r which correspond to stationary points of $\sigma(r)$, given by the condition $n\,\sigma'(r)^2 = \sigma''(r)$. This point, which can already be inferred through the singular structure of Eq. (3.76) is given by $r = 2\hat{\omega}\Lambda$. It is standard in such situations to "zoom in" on this region by linearizing the equations of motion about the stationary point. Expanding around $r = 2\hat{\omega}\Lambda$ we find that the "phase of the wave-function" has the expansion

$$\sigma(r) = -\frac{1}{2}\log(2\hat{\omega}\Lambda) - \frac{(r-2\hat{\omega}\Lambda)^{3/2}}{6\hat{\omega}\Lambda^{3/2}} + O(r-2\hat{\omega}\Lambda)^{5/2}\,, \tag{3.78}$$

motivating the definition of a new coordinate to absorb a factor of n,

$$x \equiv \left(\frac{r}{2\hat{\omega}\Lambda}-1\right)n^{2/3}\,, \tag{3.79}$$

in terms of which an expansion of $e^{n\sigma(r)}$ about $r = 2\hat{\omega}\Lambda$ with fixed x at large n will be regular. In precisely this region where $|x| \ll 1$, the conditions for the validity of WKB do not hold, and we find a *stationary point* solution which will be later matched to the WKB region when $|x| \gg 1$.

Linearizing Eqs. (3.44) to (3.46) about $x = 0$ with an ansatz of the form,

$$b(r,\tau) = \left(b_0^{\rm SP}(x,\tau)+n^{-1/3}b_1^{\rm SP}(x,\tau)+...\right)r^{n/2}e^{-in\hat{\omega}\Lambda\left(\tau+\frac{1}{r}\right)}\,, \tag{3.80}$$

$$a(r,\tau) = \frac{1}{n}\left(a_1^{\rm SP}(x,\tau)+n^{-1/3}a_2^{\rm SP}(x,\tau)+...\right)r^{n/2}e^{-in\hat{\omega}\Lambda\left(\tau+\frac{1}{r}\right)}\,, \tag{3.81}$$

$$s(r,\tau) = \frac{1}{n^2}\left(s_2^{\rm SP}(x,\tau)+n^{-1/3}s_3^{\rm SP}(x,\tau)+...\right)r^{n/2}e^{-in\hat{\omega}\Lambda\left(\tau+\frac{1}{r}\right)}\,, \tag{3.82}$$

we find an Airy function equation for $b_0^{\rm SP}$, and simple algebraic relations for $a_1^{\rm SP}$ and $s_2^{\rm SP}$ that relate them to $b_0^{\rm SP}$.

$$b_0^{\rm SP}(x,\tau) = g_0(\tau)\,{\rm Ai}\left(\frac{x}{\sqrt[3]{2}}\right)\,, \tag{3.83}$$

$$a_1^{\rm SP}(x,\tau) = -\frac{g_0(\tau)}{1+2\hat{\omega}\Lambda\tau}\,{\rm Ai}\left(\frac{x}{\sqrt[3]{2}}\right)\,, \tag{3.84}$$

$$s_2^{\rm SP}(x,\tau) = \frac{(2+2i)\hat{\omega}\Lambda g_0(\tau)}{1+2\hat{\omega}\Lambda\tau}\,{\rm Ai}\left(\frac{x}{\sqrt[3]{2}}\right)\,, \tag{3.85}$$

where $g_0(\tau)$ is an arbitrary function of τ. Solutions at subleading orders can be easily generated but they will not be used in the following discussion and so we omit them here. Our WKB and stationary point solutions have a region of over overlap when $x \gg 1$ where they can be matched with each other. Comparing the results of Eqs. (3.69) and (3.80) in this overlap region at leading order in n gives,

$$h_0(\Lambda\tau) = \frac{(2\hat{\omega})^{n/2}}{\sqrt[6]{16n}}\sqrt{\frac{\Lambda\tau}{\pi}}\,g_0\left(\Lambda\tau - \frac{1}{2\hat{\omega}}\right)\,. \tag{3.86}$$

3.3.2 Non-perturbative contributions in $1/D$ for the near horizon region

We now explore the nature of the transseries sectors in the near horizon region, where the full effects of non-linear gravity are present. Informed by the structure of Eq. (3.72), we make make an ansatz in the near horizon region of the form,

$$\tilde{A}(\tau,R) = \sum_{i=0}^{\infty}\frac{1}{n^i}A_i(\tau,R) + \sum_j \Omega_j^{\rm NH}(\tau)\sum_{i=0}^{\infty}\frac{1}{n^i}A_{ij}(\tau,R) + \dots\,, \tag{3.87}$$

$$\tilde{B}(\tau,R) = \sum_{i=0}^{\infty}\frac{1}{n^i}B_i(\tau,R) + \sum_j \Omega_j^{\rm NH}(\tau)\sum_{i=0}^{\infty}\frac{1}{n^i}B_{ij}(\tau,R) + \dots\,. \tag{3.88}$$

$$\tilde{S}(\tau,R) = \sum_{i=0}^{\infty}\frac{1}{n^i}S_i(\tau,R) + \sum_j \Omega_j^{\rm NH}(\tau)\sum_{i=0}^{\infty}\frac{1}{n^i}S_{ij}(\tau,R) + \dots\,, \tag{3.89}$$

where,

$$\Omega_j^{\rm NH}(\tau) = e^{-in\hat{\omega}_j(1+\tau\Lambda)}\,. \tag{3.90}$$

Here the subscript j anticipates a family of solutions parameterized by $\hat{\omega}_j$ and ellipses denote higher order terms in the transseries which arise as powers of $\Omega_j^{\rm NH}(\tau)$. Eqs.

(3.87)-(3.89) fully represent the large-n analogue to the transseries constructed in Subsection 2.2, exhibiting a perturbative sector given by an expansion in powers of $1/n$, supplemented by non-perturbative contributions of the form $e^{n\hat{\omega}_j \Lambda\tau}$.

From the linear independence of $\Omega_j^{\rm NH}(\tau)$, the functions $A_i(\tau, R)$, $B_i(\tau, R)$ and $S_i(\tau, R)$ can be solved identically to the perturbative series analysed in Subsection 3.2.1. The $\mathcal{O}(\Omega_j^{\rm NH}(\tau))$ contributions given by $A_{ij}(\tau, R)$, $B_{ij}(\tau, R)$ and $S_{ij}(\tau, R)$ describe linearised fluctuations on top of the $1/n$ expanded non-linear background. Inserting the ansatz (3.87)-(3.89), we can find the first few terms of the transseries in the near-horizon region. Many of the lowest order coefficients vanish,

$$A_{0j} = 0\,, \tag{3.91}$$

$$S_{0j} = S_{1j} = 0\,, \tag{3.92}$$

while the metric function $B_{0j}(R, \tau) = Z(\xi, \tau)$ with $\xi = (1 + \Lambda\tau)R$ satisfies,

$$Z'' + \frac{(1 + 2\xi(-1 + i\hat{\omega}))}{\xi(1-\xi)} Z' + \frac{i\hat{\omega}}{\xi(1-\xi)} Z \;\; = \;\; 0\,, \tag{3.93}$$

where $'$ denotes derivatives with respect to ξ. This equation coincides with the large-D limit of the QNM equation of a static blackbrane, which gives the near-horizon behaviour of the spin-2, zero momentum QNM analysed in Appendix B.3. Imposing that $Z(\xi, \tau)$ is regular at $\xi = 1$, one can find a solution to Eq. (3.93) given by,

$$B_{0j}(R, \tau) = f(\tau)\, {}_2F_1(q_+, q_-, q_+ + q_-, 1 - (1 + \Lambda\tau)R)\,, \tag{3.94}$$

with ${}_2F_1$ the ordinary hypergeometric function, $q_\pm = \frac{1}{2}\left(1 - 2i\hat{\omega} \pm \sqrt{1 - 4\hat{\omega}^2}\right)$ and $f(\tau)$ an arbitrary function of τ. Beyond this leading order, the next non-zero corrections in the large-D expansion are A_{1j}, B_{1j} and S_{2j}, which we will not compute in this work.

3.3.3 Matching in the overlap region

In Section 3.2 we matched the perturbative solutions of the near boundary and near horizon regions, and imposed a consistency condition to fix the energy density of the

dual theory. In the very same way we can extract the contribution of these non-perturbative modes to the energy density performing a similar matching analysis. Consequently this procedure will both fix the undetermined function h_0 in Eq. (3.76), and the possible values of the frequency $\hat{\omega}$ which enable consistent solutions.

As we learned in in Subsection 3.3.1, for $\hat{\omega} < 1/2$ the WKB expansion given by Eqs. (3.69)–(3.71) is valid in the overlap region since the stationary point lies beyond the horizon. However, expanding both solutions at large R and large n yields inconsistent asymptotics meaning that no solutions can exist for these values of $\hat{\omega}$. For $\hat{\omega} \geq 1/2$, the WKB solution must be matched to the stationary point solution in the vicinity of $r_{\rm S} = 2\hat{\omega}\Lambda$. A particularly interesting regime is given by $\hat{\omega} \gtrsim 1/2$ where $r_{\rm S}$ is placed at the cusp of the horizon, which corresponds to the smallest frequencies where this type of fluctuation occurs. In this range the near horizon solution Eqs. (3.91)-(3.94) must first be matched to the stationary point solution given by Eqs. (3.80)-(3.82), which in turn can be matched to the WKB solution. In what follows we will expand[5]

$$\hat{\omega} = \frac{1}{2} + n^{-2/3}\delta\omega_1 + n^{-1}\delta\omega_2 + n^{-4/3}\delta\omega_3 + \dots \,. \tag{3.95}$$

A similar but more explicit analysis focused on computing the QNM frequencies of a static blackbrane can be found in Appendix B.3. Note that the fact that $\hat{\omega} - 1/2 \sim \mathcal{O}(n^{-2/3})$ justifies the use of the near boundary approximation, Eqs. (3.80)-(3.82), to describe the dynamics close to the stationary point, since

$$\left(\frac{r_{\rm S}}{\Lambda}\right)^n \approx \left(1 + \delta\omega_1 \frac{2}{n^{2/3}}\right)^n \underset{n\to\infty}{=} e^{2\delta\omega_1 n^{1/3}} \gg 1 \,, \tag{3.96}$$

where $\delta\omega_1$ is positive as $\hat{\omega} \gtrsim 1/2$.

Examining the stationary point solution given by Eq. (3.80) at large R and large

[5]Including a $n^{-1/3}$ contribution to $\hat{\omega}$ prevents a consistent matching between the stationary point solution given by Eq. (3.80) and the WKB solution given by Eq. (3.69).

n we find,

$$\lim_{R\to\infty}\frac{1}{r^n}b(r,\tau)\propto\ g_0(\tau)R^{-\frac{1}{2}+\frac{i}{2}} \tag{3.97}$$
$$\times\left(\begin{array}{l}\text{Ai}\left(-2^{2/3}\delta\omega_1\right)+\dfrac{\text{Ai}\left(-2^{2/3}\delta\omega_1\right)(...)+\frac{\text{Ai}'\left(-2^{2/3}\delta\omega_1\right)\left(-\frac{2ig_0'(\tau)}{g_0(\tau)}-2\delta\omega_2+\log(R)-\frac{i}{1+\Lambda\tau}\right)}{\sqrt[3]{2}}}{\sqrt[3]{n}}\end{array}\right)+O(n^{-2/3})$$

Similarly, near the special value of $\hat{\omega}=\frac{1}{2}+\delta$ with $\delta>0$, Eq. (3.94) has a large R expansion of the form,

$$\lim_{R\to\infty}B_{0j}(R,\tau)=f(\tau)\frac{\Gamma(1-i)}{\Gamma\left(\frac{1}{2}-\frac{i}{2}\right)^2}\left[(1+\Lambda\tau)R\right]^{-\frac{1}{2}+\frac{i}{2}}\left(-2H_{-\frac{1}{2}-\frac{i}{2}}+\log((1+\Lambda\tau)R)\right)+O(\delta)\,, \tag{3.98}$$

where H_m denotes the m^{th} Harmonic number. Immediately by comparing the logarithmic structure of Eqs. (3.97) and (3.98) at fixed orders in n, we can set $-2^{2/3}\delta\omega_1$ to be the zeros of the Airy Function and fix the function $g_0(\tau)$ through,

$$-\frac{2ig_0'(\tau)}{g_0(\tau)}-2\delta\omega_2-\frac{i}{1+\Lambda\tau}=-2H_{-\frac{1}{2}-\frac{i}{2}}+\log(1+\Lambda\tau)\,, \tag{3.99}$$

which yields,

$$g_0(\tau)=\tilde{C}_0(1+\Lambda\tau)^{-\frac{1}{2}+\frac{i}{2}+\frac{i\Lambda\tau}{2}}\exp\left(-\frac{i}{2}(1-2(\delta\omega_2-H_{-\frac{1}{2}-\frac{i}{2}}))\Lambda\tau\right) \tag{3.100}$$

where $\tilde{C}_0$ is an undetermined overall constant related to initial data.[6] Using Eq. (3.86) and Eq. (3.77), the energy density of this associated fluctuation in the boundary theory is

$$\delta\tilde{\epsilon}(\tau)=C_0\Lambda^n\left(\Lambda\tau\right)^{-3/2}\left(\Lambda\tau+i\right)^{\frac{i}{2}(\Lambda\tau+i)}\exp\left[-i\Lambda\tau\left(\frac{n+1}{2}+\delta\omega_1 n^{1/3}+H_{-\frac{1}{2}-\frac{i}{2}}\right)\right]\,, \tag{3.102}$$

where the constant C_0 is related to $\tilde{C}_0$ by constant factors involving n, and $(-2^{2/3}\delta\omega_1)$ is given by a zero of the Airy Ai function.

[6]Comparing the overall time dependence of Eqs. (3.97) and (3.98) will fix,

$$f(\tau)\propto(1+\Lambda\tau)^{\frac{i\Lambda\tau}{2}}\exp\left(-\frac{i}{2}(1-2(\delta\omega_2-H_{-\frac{1}{2}-\frac{i}{2}}))\Lambda\tau\right), \tag{3.101}$$

where the proportionality can be fixed by accounting for an overall constant shift between Eqs. (3.72) and (3.90).

An inspection of Eq. (3.102) clearly shows that these fluctuations are non-perturbative, for times parametrically of the same order as Λ they oscillate rapidly and can not be expressed as a power series in $1/D$. We also find an infinite set of oscillating frequencies $\hat{\omega}_j$ that characterize each mode, given by the countably infinite zeros of the Airy Ai function. As found in for the non-hydrodynamic modes in Subsection 2.2.3, each non-perturbative mode of the large-D expansion comes associated with an arbitrary constant undermined by the equations of motion. Therefore we can codify off-equilibrium states of the dual gauge theory with this infinite set of constants, which relax to the perturbative (in D) equilibrium solution, similarly given by late time hydrodynamics.

While the leading and next to leading oscillation frequencies are purely real, it is interesting to note that the dissipation of the oscillation only occurs at a subleading order in $1/D$, given by

$$H_{-\frac{1}{2}-\frac{i}{2}} \approx -0.290892 - 1.44066i\,, \tag{3.103}$$

which, at this order, is common to all of these fluctuating modes. This uniformity implies that all these fluctuation dissipate at the same time scale, of order $1/\Lambda$. The behaviour is qualitatively different to the non-hydrodynamic modes of the large-τ expansion, which can be graded in their dissipation rates.

At late times, $\tau \gg 1/\Lambda$, Eq. (3.102) may be expressed as a power series in inverse powers of τ, in which the leading order is given by

$$\delta\tilde{\epsilon}(\tau) \underset{\tau\to\infty}{=} \Lambda^n C_0 e^{-i\Lambda\tau\left(\frac{(n+1)}{2}+\delta\omega_1 n^{1/3}+H_{-\frac{1}{2}-\frac{i}{2}}\right)} (\Lambda\tau)^{i\Lambda\tau/2} \frac{1}{(\Lambda\tau)^2}\,. \tag{3.104}$$

This observation will be useful for the analysis of the following subsection where we will compute the transseries expansion for small gradients, and compare that to the results of this section for an interpretation of these non-perturbative (in D) modes.

3.3.4 Comparison to the non-hydrodynamic transseries at arbitrary D

To better understand the origin of the non-perturbative in $1/D$ contributions to the energy density identified above, in this section we compare those results with the gradient expansion at fixed D. As we have seen in Section 3.2, the power expansion in $1/D$ of boost invariant longitudinal expansion is determined by the hydrodynamic limit. From the form of the non-pertubative contribution in Eq. (3.102), it is clear that these modes are both non-perturbative (in D) and non-hydrodynamic. To make the connection between these expansions more concrete we construct a small gradient transseries as we did for the case of infinitely coupled $\mathcal{N}=4$ SYM in Chapter 2, but now for arbitrary D.

To make contact with the notation of Section 2.2 and to facilitate the late-time analysis, we introduce the following field redefinition

$$A = r^2 \bar{A}(\tau, r), \tag{3.105}$$

$$B = \frac{1}{n-1}\left(\log\left(\frac{r^2}{(1+r\tau)^2}\right) + \frac{n-1}{n-2}\left(2\,\bar{d}(\tau,r) - \bar{B}(\tau,r)\right)\right), \tag{3.106}$$

$$S = r^{\frac{n-2}{n-1}}(1+r\tau)^{\frac{1}{n-1}} e^{\bar{d}(\tau,r)}. \tag{3.107}$$

Then at sufficiently late times we can supplement the gradient expansion of the metric functions (3.105)–(3.107) with non-perturbative (in gradients) contributions in the form of a transseries

$$\bar{A}(r,\tau) = \sum_{i=0}^{\infty} u^{-i}\bar{A}_i^{(\mathbf{0})}(s) + \sum_{\boldsymbol{n}\in\mathbb{N}^\infty} \Omega_{\boldsymbol{n}}^{\mathrm{LT}}(u) \sum_{i=0}^{\infty} u^{-i}\bar{A}_i^{(\boldsymbol{n})}(s)\,, \tag{3.108}$$

$$\bar{B}(r,\tau) = \sum_{i=0}^{\infty} u^{-i}\bar{b}_i^{(\mathbf{0})}(s) + \sum_{\boldsymbol{n}\in\mathbb{N}^\infty} \Omega_{\boldsymbol{n}}^{\mathrm{LT}}(u) \sum_{i=0}^{\infty} u^{-i}\bar{b}_i^{(\boldsymbol{n})}(s)\,, \tag{3.109}$$

$$\bar{d}(r,\tau) = \sum_{i=0}^{\infty} u^{-i}\bar{d}_i^{(\mathbf{0})}(s) + \sum_{\boldsymbol{n}\in\mathbb{N}^\infty} \Omega_{\boldsymbol{n}}^{\mathrm{LT}}(u) \sum_{i=0}^{\infty} u^{-i}\bar{d}_i^{(\boldsymbol{n})}(s)\,, \tag{3.110}$$

where we have adopted the notation of Eqs. (2.18)–(2.20) where $u = (\Lambda\tau)^{-\nu}$ with $\nu = \frac{n-2}{n-1}$, $s = \frac{\Lambda}{r}(\tau\Lambda)^{1/(n-1)}$, $\boldsymbol{n}$ is an infinite dimensional vector of positive integers[7],

[7]Note that $\boldsymbol{n}$ is not the number of dual theory spacetime dimensions n.

the sum over $\mathbb{N}_0^\infty$ gives every possible combination of natural number components, and $\Omega^{LT}_{\boldsymbol{n}}(u)$ is a non-perturbative function at large-u. We define $\boldsymbol{e}_k$ as a unit vector with a single value at component k equal to 1.

Computing the metric functions $\bar{A}_i^{(\mathbf{0})}(s)$, $\bar{b}_i^{(\mathbf{0})}(s)$, and $\bar{d}_i^{(\mathbf{0})}(s)$ in the hydrodynamic sector allows us to find the late time energy density,

$$\tilde{\epsilon} \approx \tilde{\epsilon}_{\rm eq}\left(1-\frac{2}{n-1}u^{-1}+\frac{\nu}{n-1}\left(\frac{1}{n}+\beta\right)u^{-2}+\mathcal{O}\left(u^3\right)\,.\right)\,. \tag{3.111}$$

where $\tilde{\epsilon}_{\rm eq}=\Lambda^n\left(\Lambda\tau\right)^{\frac{n}{1-n}}$ as defined above Eq. (3.7). Following the argument used to justify the form of the non-hydrodynamic contributions in Eq. (2.25), we expect $\Omega^{LT}_{\boldsymbol{e}_j}$ to be given by a mode relaxing in an adiabatically changing medium with effective temperature given by $\tilde{\epsilon}$,

$$\begin{aligned}\Omega^{LT}_{\boldsymbol{e}_j} &\sim \exp\left\{-i\int d\tau\bar{\omega}^{(j)}\tilde{\epsilon}^{1/n}\right\} \\ &\approx u^{\frac{2i\bar{\omega}^{(j)}}{(n-2)n}}e^{-i\bar{\omega}^{(j)}\left(\frac{n-1}{n-2}\right)u}\left(1-i\bar{\omega}^{(j)}\left(\frac{1}{n^3-3n^2+2n}-\frac{\beta}{(n-1)n}\right)u^{-1}+\mathcal{O}(u^{-2})\right)\,,\end{aligned} \tag{3.112}$$

with $\bar{\omega}^{(j)}$ a (set of complex) number(s). Defining then $\Omega^{LT}_{\boldsymbol{e}_j}(u)\equiv u^{\frac{2i\bar{\omega}^{(j)}}{(n-2)n}}e^{-i\bar{\omega}^{(j)}\left(\frac{n-1}{n-2}\right)u}$, the leading transseries corrections to the metric functions can be found as,

$$\bar{A}_0^{(\boldsymbol{e}_j)}=0\,,\quad \bar{d}_0^{(\boldsymbol{e}_j)}=0\,, \tag{3.113}$$

with the leading order transseries correction to $\bar{B}$ satisfying the equation

$$\bar{b}_0^{(\boldsymbol{e}_j)\prime\prime}(s)+\frac{\left((n-1)+s^n-2i\bar{\omega}^{(j)}\,s\right)}{s(-1+s^n)}\bar{b}_0^{(\boldsymbol{e}_j)\prime}(s)+\frac{(n-1)i\bar{\omega}^{(j)}}{s(-1+s^n)}\,\bar{b}^{(\boldsymbol{e}_j)}(s)=0\,, \tag{3.114}$$

which coincides with the equation for tensor fluctuations of the blackbrane at zero spatial momentum (see Appendix B.3). This equation characterizes an infinite set of discrete n-dependent QNM frequencies $\bar{\omega}^{(j)}$ with associated arbitrary normalization constant C_j. At subsequent orders in the gradient expansion $\bar{A}_1^{(\boldsymbol{e}_j)}$ will be generically non-zero, meaning that we will receive an additional multiplicative factor of $u^{-2\left(\frac{n-1}{n-2}\right)}$ to the dual theory energy density after holographic renormalization. Further contributions result in an infinite series of in u^{-1} implying that the energy density in the

dual gauge theory can be expressed as a transseries (in gradients) of the form

$$\tilde{\epsilon}(u) = \tilde{\epsilon}_{\rm hyd}(u) + \Lambda^n \sum_j C_j u^{-\frac{2}{n-2}\left(n-1-\frac{i\bar{\omega}^{(j)}}{n}\right)} e^{-i\bar{\omega}^{(j)}\left(\frac{n-1}{n-2}\right)u} \left(1 + \sum_{i=1} \rho_i u^i\right) \tag{3.115}$$

with $\epsilon_{\rm hyd}(u)$ the hydrodynamic expansion (3.111), and ρ_i is a set of fixed coefficients determined by the subsequent orders in the transseries expansion. The complex numbers C_j are, on the contrary, arbitrary and can be selected to encode the initial conditions of the evolution.

Let us now discuss the large-D limit of the expression for the energy density (3.115). As we have seen in the previous section and in Appendix B.3, the QNM spectrum can be computed in a series of inverse fractional powers of n [116, 140]. For the least damped modes, $\bar{\omega}^{(j)} \sim n\hat{\omega}\Lambda$ with $\hat{\omega}$ given in Eq. (3.95). Taking the large-D limit of Eq. (3.115), the contribution of these modes to the energy density leads to

$$\tilde{\epsilon}(u) = \Lambda^n \left(\frac{1}{\tau\Lambda} + \sum_j C_j e^{-i\left(\frac{n+1}{2} + \delta\omega_1^{(j)} n^{1/3} + \delta\omega_2\right)\tau\Lambda} (\tau\Lambda)^{-2+i\tau\Lambda/2} \left(1 + \sum_{i=1} \frac{\rho_i^\infty}{(\Lambda\tau)^i}\right) + ...\right) , \tag{3.116}$$

where the ellipses denote subleading n terms and ρ_i^∞ are the large-D limits of the constants ρ_i. At late times, this expression matches exactly the time dependence of the energy density (3.104) we found in a large n expansion at late times in the previous subsection. However, using our large-D analysis we are able to go beyond the strict late time limit, providing a resummation of all the gradient terms at leading order in n. Equating Eq. (3.116) and Eq. (3.102) yields

$$\left(1 + \frac{i}{\Lambda\tau}\right)^{-\frac{1}{2}+\frac{i\Lambda\tau}{2}} \sim \left(1 + \sum_{i=1} \frac{\rho_i^\infty}{(\Lambda\tau)^i}\right) , \tag{3.117}$$

from which one can extract the leading $1/D$ behviour for the energy density coefficients to all orders in the gradient. At this order in the $1/D$ expansion this tail of coefficients is identical for all non-perturbative modes, but subsequent orders will become dependent on $\omega^{(j)}$. The infinite series of gradient corrections stands in contrast to the perturbative results of Section 3.2, where we found only a finite number of gradient terms at each order in $1/D$.

3.4 Discussion and outlook

In this chapter we explored the dynamics of Bjorken evolution in holographic theories from an expansion in large numbers of dimensions. By packing the space with extra transverse degrees of freedom while enforcing additional symmetry, Einstein's equations yielded simple ODEs at each order in inverse D allowing us greater analytic control.

As we have seen, our perturbative large-D analysis of Bjorken flow was controlled by hydrodynamics. By extending this expansion to order $\mathcal{O}(n^{-3})$ we have extracted the large-D behaviour of a subset of higher-order transport coefficients up to 6-th order in gradients. Denoting these coefficients by $\lambda^{(i)}$, with i the gradient order, these are related to the constants $\theta^{(i)}$, defined in Eq. (3.68), as

$$\lambda^{(i)} = \theta^i \tilde{\epsilon}_{\rm eq}^{1-i/n} \,, \tag{3.118}$$

with the equilibrium energy density given in Eq. (3.3). With this normalisation $\lambda^{(1)} \equiv -2\nu\eta$, $\lambda^{(2)} \equiv -2\nu^2 \left(\eta\tau_\pi - 2(n-3)\lambda_1/(n-2)\right)$ and $\lambda^{(3)}$ is a combination of 14 third-order coefficients in the basis of [141]. Beyond third order the coefficients are not classified. The finite number of inverse powers of τ in our result Eq. (3.61) also implies that in units of $\tilde{\epsilon}_{\rm eq}^{1/n}$ relevant transport coefficients beyond 6-th order are suppressed by at least n^{-4}.

While in principle this expansion could be continued for arbitrarily large orders in $1/D$, the existence of non-perturbative modes found in Section 3.3 indicate that as in Chapter 2 the perturbative series will not converge, as already noted in [116]. These excitations correspond to fast modes, with a typical rate of variation of order $n\Lambda$, parametrically separated from the hydrodynamic regime. From the point of view of time-evolution, the existence of this set of excitations codifies the many possible initial conditions that can be specified for the system. In Subsection 3.3.4 we checked that these solutions correspond to the large-D limit of non-hydrodynamic modes and found that we could identify an infinite series of coefficients for the energy density about this sector at leading order in $1/D$.

The emergence of the hydrodynamic/non-hydrodynamic seperation at large-D is a natural consequence of the way in which we tailored this limit. In Eq. (3.26) in the near horizon region we have expanded each metric function about some $r \sim \Lambda \sim \mathcal{O}(n^0)$ at large n with fixed R, later implying $\tilde{\epsilon} \sim \Lambda^n$ after these functions are consistently matched to the near boundary region. The energy density and temperature of the dual theory are related by Eq. (3.3) as $\tilde{\epsilon} = \left(\frac{4\pi T}{n}\right)^n$. As non-hydrodynamic modes evolve on a time scale set by the effective temperature $\tau_*^{-1} \sim T \sim n\Lambda$, we could have predicted that these dynamics would be parametrically seperated as evidenced by Section 3.3.

Another subtle point is our implicit assumption that the computation is consistent with the late time region through our definition of Λ from Eq. (1.15) as the normalization of the energy density at in the ideal limit of $\tau \to \infty$. This condition sets the integration constants α_i in Eqs. (3.33), (3.37), (3.41) and (3.43). We have checked that by fixing a rescaled $\tau_n = n\,\tau$ in the near horizon region the non-hydrodynamic modes will emerge at perturbative orders in $1/n$. Further investigation should be made to determine whether this scaling could be used to find a special "attractor" solution by imposing an alternative initial condition at early times.

Chapter 4

Black holes near equilibrium

In this chapter we utilize the transseries expansion to demostrate how the dynamics of a near equilibrium black hole can be obtained analytically. Following the prescription set out in Chapter 2 we use the non-perturbative functions of the transseries as an expansion parameter to organize the computation. This chapter is based on [4] and aims to explain the numerical findings of [142].

4.1 Introduction and motivation

In Chapters 2 and 3 we saw how the transseries expansion naturally arises in holographic theories undergoing Bjorken flow while describing the hydrodynamic and non-hydrodynamic modes of the underlying dynamics. In this chapter we will consider an expansion about a far simpler flow, static equilibrium, in order to focus closely on the higher order transseries terms themselves.

Beyond holography, black holes are fascinating objects in of themselves, with implications for astrophysics and quantum gravity. Recently their behaviour out of equilibrium has become experimentally accessible through the detection of gravitational waves from black hole binary collisions [143]. While this is arguably the most interesting regime of general relativity analytic results here are scarce, instead often resorting to intensive numerics. Any analytic inroads we can make to study black holes out of equilibrium are therefore valuable.

In this chaper we describe the out of equilibrium evolution of the horizon. It has

long been known that the horizon area cannot decrease [144], here we show exactly how it increases as a function of its quasinormal modes (QNMs). While we focus on black branes in anti-de Sitter spacetime, the results presented here will apply to spherical evolution of the Schwarzschild black hole, and could potentially be extended beyond spherical symmetry.

A black hole in equilibrium has entropy given by its area [145, 146]. Out of equilibrium this identification is less clear, but analogous to the second law of thermodynamics the black hole area still cannot decrease [144]. In this context one can define various horizons satisfying this law, all of which coincide with the event horizon in equilibrium. Notions of non-equilibrium entropy have been explored holographically for the apparent [52] and event horizon [53]. Dynamical horizons have been studied previously through the fluid gravity correspondence [54]. In these inhomogeneous systems one can define a local entropy current at either the apparent or event horizon with non-negative divergence [55–57]. Such approaches necessarily neglect the contributions of gapped QNMs, which are given precisely by the transseries terms that we will include.

In [142] the area of spatially homogeneous horizons was studied numerically for various geometries equilibrating to static black holes. The authors, Jansen and Magán, found that they could infer an analytic form for the late time behaviour of the horizon area,

$$\delta S(t) \propto e^{2\omega^I t} \left(\cos\left(2\omega^R t\right) + B\right) , \tag{4.1}$$

where ω is the quasinormal mode (QNM) that gives the dominant damped oscillation, the superscripts indicate real and imaginary parts, and the parameter B could be determined from a fit. We present the numerical findings of that study in Fig. (4.1), focusing on the quantities δS_{AH} and δS_{EH}, the difference between the final and instantaneous areas of the apparent horizon and event horizon respectively.

While we should expect the horizon area to always increase ($\delta S'(t) \geq 0$) in the case of [142] it was found that the apparent horizon would saturate this law during this

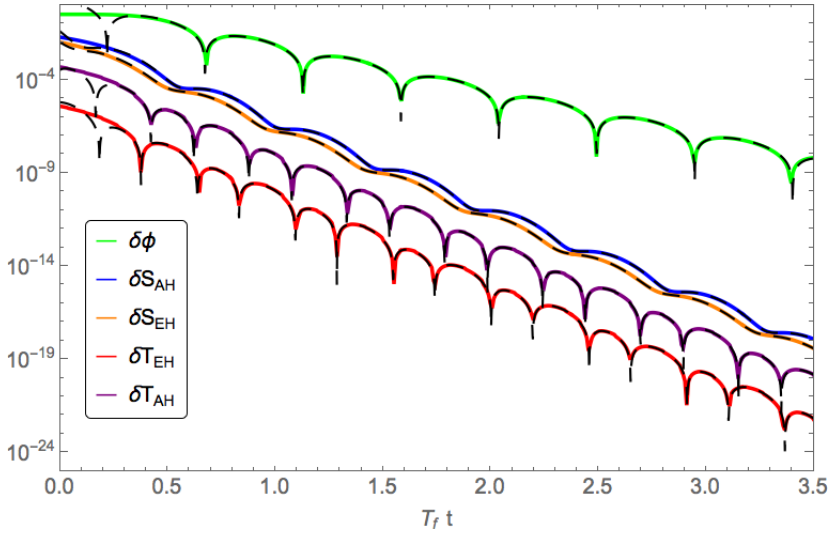

Figure 4.1: Logarithmic plot of the near equilibrium evolution of a black hole in response to a small scalar perturbation in the set up of [142] from where we have taken this Figure. Shown here in solid lines are the scalar field (green), the areas of the apparent and event horizon (blue, orange), and the temperatures of the event and apparent horizon (red, purple), subtracted from the final values they attain at equilibrium. The last two quantities are shifted down by 10^1 and 10^3 respectively for display purposes. For each quantity a dashed black line has been plotted following the form $Ae^{2\omega^I t}\left(\cos\left(2\omega^R t+\delta\right)+B\right)$ where ω^R and ω^I are the real and imaginary parts of the dominant QNM frequency and the remaining parameters are given by a fit.

equilibration period. The parameter B appeared to generically take on its minimum possible value consistent with the area theorem,

$$B_{\rm AH}=\frac{|\omega|}{-\omega^I}\,. \tag{4.2}$$

In contrast the event horizon did not show a similar saturation and instead always increased.

In this chapter we present the findings of [4] which explains this observation and derives an analytic form for the entropy through a transseries expansion. We go on to show that the event horizon entropy will obey Eq. (4.1) with,

$$B_{EH}=\frac{|\omega|}{-\omega^I}\times\frac{|\omega-i\pi T|}{-\left(\omega-i\pi T\right)^I}\,, \tag{4.3}$$

where T is the Hawking temperature in equilibrium. For inhomogeneous evolution the sensible quantity of interest will be the divergence of the entropy current ($\partial_\mu s^\mu$) from which the total entropy can always be computed via a simple integral. While

for homogenous perturbations Eq. (4.1) will hold, we will break spatial homogeneity by allowing fluctuations at any finite momentum.

Independent of the small gradient and large-D expansions explored in Chapters 2 & 3, a transseries can still be viewed as an expansion in the parameter $e^{-i\omega t}$ where ω is a stable QNM frequency with negative imaginary part. As this expansion parameter becomes small at late times we also refer to this series as a late time expansion. At first order this series contains precisely all the QNMs, and contributions from the second order can be viewed as the leading backreaction due to the first order perturbations. In this paradigm the amplitude of these modes need not be small, instead the expansion is sensible provided $\mathrm{Im}(\omega)$ is an order one negative number. The first non-trivial results of our program will occur at second order meaning that our approximation in principle breaks down at times $t \lesssim |3\,\mathrm{Im}(\omega_0)|^{-1}$, where ω_0 is the dominant QNM. However it is often the case that the first order QNM approximation can describe nonlinear general relativity well beyond its expected regime of validity, even with large perturbations [28, 147, 148].

We organise this chapter as follows. In Section 4.2 we set up the problem and define the metric, entropy current and transseries expansion. In Section 4.3 we show an explicit computation to derive our main result Eq. (4.34) for the divergence of the entropy current due to QNM perturbations in the case of Einstein gravity with negative cosmological constant. We further explain how the entropy density can be obtained from this expression in the case of homogeneous perturbations. Finally in Section 4.4 we discuss the implications and extensions of our analysis.

4.2 Setup and summary

We start with the now familiar Eddington-Finkelstein form of the metric which was used in Chapters 2 & 3,

$$\begin{aligned} ds^2 &= -A dt^2 + 2dt\left(dr + F^{(x)}dx + F^{(y)}dy\right) + S^2 g_{ij} dx_\perp^2 \,, \\ g_{ij} &= \begin{pmatrix} e^{-2B}\cosh G & e^{-\frac{1}{2}(B-H)}\sinh G & 0 \\ e^{-\frac{1}{2}(B-H)}\sinh G & e^{B+H}\cosh G & 0 \\ 0 & 0 & e^{B-H} \end{pmatrix} , \end{aligned} \tag{4.4}$$

where all functions depend on (t, r, x) but not on the remaining coordinates $x_\perp$. To make a connection with holographic frameworks in our computation we will work in exclusively $4+1$ dimensions with negative cosmological constant, but a near identical approach can be generalized to include other spaces and higher/lower dimensions. With these considerations Einstein's equations take the form $R_{\mu\nu} = -4g_{\mu\nu}$, where we have set the cosmological constant so that the anti-de Sitter vacuum solution would have a radius of curvature set equal to one. In contrast to Sections 2.2 and 3.2 in Eq. (4.4) we have included off-diagonal components in the metric which will be necessary for the addition of modes with finite momentum. We will further restrict to solutions evolving to a static and homogeneous equilibrium, so that at infinite t the only nonzero functions will be A and S which will depend only on the radial coordinate r. The equilibrium solution for Einstein's equations given above is the AdS-Schwarzschild black brane in $D = 4 + 1$ dimensions,

$$\begin{aligned} &\lim_{t\to\infty} A(r) = r^2\left(1 - \left(\frac{r_h}{r}\right)^4\right) , \quad \lim_{t\to\infty}\Sigma(r) = r \,, \\ &\lim_{t\to\infty} F^{(x)} = \lim_{r\to\infty} F^{(y)} = \lim_{t\to\infty} B = \lim_{t\to\infty} G = \lim_{t\to\infty} H = 0 \,, \end{aligned} \tag{4.5}$$

with equilibrium temperature given by $T = r_h^2 \lim_{t\to\infty} A'(r_h)/(4\pi)$, where r_h is the equilibrium horizon location given by $\lim_{t\to\infty} A(r_h) = 0$, giving $r_h = \pi T$.[1] For small perturbations from equilibrium this ansatz contains a tensor fluctuation through H,

[1] Because in this chapter we are studying perturbations on a static (rather than Bjorken) background we will take our dimensionful scale to be the equilibrium temperature T as opposed to the mass scale Λ used in previous sections. Throughout this chapter T will be taken as an equilibrium quantity, although one could imagine defining an out of equilibrium effective temperature as was done in earlier chapters.

a vector or shear fluctuation through $F^{(y)}$ and a scalar or sound fluctuation through $F^{(x)}$.

4.2.1 Entropy currents

Out of equilibrium the identification of entropy with a horizon surface becomes ambiguous as multiple distinct codimension-2 surfaces exist on which to define one. We will consider two such surfaces, the event horizon (EH) and the apparent horizon (AH). The event horizon is a null surface defined by its normal vector n^M, where M runs over all the coordinates, while the apparent horizon is a spacelike surface on which the geodesic expansion θ vanishes[2],

$$\text{AH} : \theta|_{r_{\text{AH}}} = 0\,, \quad \text{EH} : n_M n^M|_{r_{\text{EH}}} = 0\,. \tag{4.6}$$

In the infinite t limit these surfaces align and are given radially by the zero of the blackening function A.

Our ansatz Eq. (4.4) preserves the residual gauge freedom associated with a choice of radial shift $r \to r + \xi(t, x)$. This is routinely used in numerical evolution schemes to fix the position of a locally determined apparent horizon, while doing the same for a globally determined event horizon is usually not possible. In our setup however this is no issue as we assume knowledge of our final state and expand our solution backwards in time in a controlled way. We will fix this gauge implicitly by imposing either condition of Eq. (4.6) at a fixed constant radius r_{AH} or r_{EH} which is independent of the other coordinates.

For each horizon we can define an entropy current, following [55], through its normal vector v_M, which through our chosen radial gauge is simply $v = \partial_r$. The entropy current is given by,

$$s^\mu = s\frac{v^\mu}{v^t}\,, \tag{4.7}$$

[2]There is a subtlety here in that this definition depends on how the full spacetime is foliated by spacelike surfaces, however here the late time expansion clearly singles out constant time slices as the natural foliation.

where $s = \sqrt{-g}/4$ is the entropy density evaluated at the appropriate horizon, and μ runs over all but the radial coordinate [54, 118]. The divergence of this entropy current is constrained to be non-negative through the area theorems [55],

$$\partial_\mu s^\mu \geq 0\,, \tag{4.8}$$

which is true for both the event and apparent horizon. One can establish a bulk-boundary map for this current identifying the x^μ coordinates on the horizon with the same x^μ coordinates on the boundary as was done in [54, 55].

4.2.2 The transseries expansion with finite momenta

Following the analysis of Chapter 2 and [2] we will show how to construct a transseries solution for the metric out of functions of the form,

$$\Omega_{\boldsymbol{n}}(t,x) = e^{-i\boldsymbol{n}\cdot(\boldsymbol{\omega}\, t - \boldsymbol{k}\, x)}\,, \tag{4.9}$$

where $\boldsymbol{n}$ is an infinite dimensional vector of positive integers, and $\boldsymbol{\omega}$ and $\boldsymbol{k}$ are infinite dimensional vectors of yet undetermined complex numbers. We will show that $\boldsymbol{\omega}$ and $\boldsymbol{k}$ are the QNM frequencies and corresponding momenta for the AdS-blackbrane, known to be found in pairs related through complex conjugation. Anticipating this result we organize these vectors as,

$$\boldsymbol{\omega} = (\omega_0, \omega_{\bar{0}}, \omega_1, \omega_{\bar{1}}, ...)\ , \quad \boldsymbol{k} = (k_0, k_{\bar{0}}, k_1, k_{\bar{1}}, ...)\ , \tag{4.10}$$

where we define infinite dimensional unit vectors $\boldsymbol{e}_i$ and $\bar{\boldsymbol{e}}_i$ which are zero everywhere and 1 in the $(2i-1)$-th and $(2i)$-th components respectively so that $\boldsymbol{e}_i \cdot \boldsymbol{\omega} = \omega_i$ and $\bar{\boldsymbol{e}}_i \cdot \boldsymbol{\omega} = \omega_{\bar{i}}$.[3] Written in this form we have that $\omega_{\bar{i}} = -\bar{\omega}_i$. Since the QNM frequencies of the AdS-blackbrane have negative imaginary part the function $\Omega_{\boldsymbol{n}}(t,x)$ on Eq. (4.9) vanishes exponentially as $t \to \infty$, meaning that our expansion in powers of $\Omega_{\boldsymbol{n}}$ will have an interpretation as a late time expansion. In this chapter we will only consider expansions about the static solution to the order of $\mathcal{O}\left(\Omega_{\boldsymbol{e}_i}\Omega_{\boldsymbol{e}_j}\right)$, with two

[3] We will find however that in the computation to follow that we can replace some vector $\bar{\boldsymbol{e}}_i$ with $\boldsymbol{e}_j$ without changing the mathematics, and will do so for convenience.

interacting modes about equilibrium. While the computation will hold for any choice of i and j, they should be chosen sufficiently low so as to be leading with respect to combinations of order $\mathcal{O}\left(\Omega_{\boldsymbol{e}_i}\Omega_{\boldsymbol{e}_j}\Omega_{\boldsymbol{e}_k}\right)$.

To simplify notation we will pre-emptively rescale $\omega_i = \pi T \lambda_i$, $k_i = \sqrt{\frac{3}{2}}\pi T q_i$, while defining the rescaled coordinate $z = \frac{\pi T}{r}$. In the transseries expansion we write all metric functions g as a series in $\Omega_{\boldsymbol{n}}$,

$$g(r,t,x) = \sum_{\boldsymbol{n}\in\mathbb{N}_0^\infty}^{\infty} \Omega_{\boldsymbol{n}}(t,x)\, g_{\boldsymbol{n}}(z)\,, \tag{4.11}$$

where $\mathbb{N}_0^\infty$ is the set of all infinite dimensional vectors with positive integer components including 0, and where the coefficients $g_{\boldsymbol{n}}$ depend only on the coordinate z while the time evolution is governed by $\Omega_{\boldsymbol{n}}$. Unlike the scenarios studied in Chapters 2 and 3 which came with an associated series needed to compute $g_{\boldsymbol{n}}$, our set up is sufficiently simple so as to extract all relevant information from $g_{\boldsymbol{n}}$ exactly, allowing us to focus solely on the higher order $\Omega_{\boldsymbol{n}}$ contributions themselves. We emphasize that we do not expect all solutions to Einstein's equations to be expressible by this simple ansatz (4.11), but rather aim to understand the dynamics which can be described in this way. We note however that despite these limitations, similar expansions have been successfully used to describe non-linear gravity far from equilibrium in holographic set-ups [28, 147, 148].

With these conventions the equilibrium solution is given by the $\boldsymbol{n} = \boldsymbol{0}$ term in the expansion fixing,

$$\begin{aligned} A_{\boldsymbol{0}}(z) = \frac{\pi T}{z^2}\left(1-z^4\right)\,, \quad S_{\boldsymbol{0}}(z) = \pi T/z\,, \\ F_{\boldsymbol{0}}^{(x)} = F_{\boldsymbol{0}}^{(y)} = B_{\boldsymbol{0}} = G_{\boldsymbol{0}} = H_{\boldsymbol{0}} = 0\,, \end{aligned} \tag{4.12}$$

where in these rescaled z coordinates the equilibrium horizon is placed at $z_h = 1$.

We consider next the "lowest" order modes in Ω_n given by $\boldsymbol{n} = \boldsymbol{e}_i$, which are analogous to the *fundamental modes* modes of Chapter 2. As already stated the QNM spectrum of the AdS-blackbrane consists of complex conjugate pairs which we have ordered in the vector $\boldsymbol{\omega}$. Imposing that all metric functions $g_{\boldsymbol{n}}$ are real we find

that components $\boldsymbol{e}_i$ and $\bar{\boldsymbol{e}}_i$ can not be independent, fixing that $q_{\bar{i}} \equiv -q_i$, $\lambda_{\bar{i}} \equiv -\bar{\lambda}_i$, where $\bar{\lambda}_i$ is the complex conjugate of λ_i, and implying that these modes do not have independent normalizations and must be considered in pairs. Mathematically the first order corrections in $\Omega_{\boldsymbol{e}_i}$ are just linearized perturbations about equilibrium, giving contributions which are identical to a common quasinormal mode analysis. These modes can be written in terms of three gauge invariant combinations known as the tensor, shear and sound channel, with helicities 2, 1 and 0 respectively,[4]

$$\begin{aligned} X_{\boldsymbol{e}_i} &\equiv H_{\boldsymbol{e}_i}\,, \\ Y_{\boldsymbol{e}_i} &\equiv ik_i F^{(y)}_{\boldsymbol{e}_i} + i\omega_i S_{\mathbf{0}}^2 G_{\boldsymbol{e}_i}\,, \\ Z_{\boldsymbol{e}_i} &\equiv 4k_i\omega_i F^{(x)}_{\boldsymbol{e}_i} + 2k_i^2\left(\frac{\bar{f}'}{\bar{\Sigma}'}S_{\boldsymbol{e}_i} - A_{\boldsymbol{e}_i}\right) \\ &\quad + S_{\mathbf{0}}\left(k_n^2\frac{A'_{\mathbf{0}}}{S'_{\mathbf{0}}} - 6\omega_i^2 S_{\mathbf{0}}\right)B_{\boldsymbol{e}_i}\,. \end{aligned} \tag{4.13}$$

Each gauge-invariant mode in Eq. (4.13) satisfies its own decoupled QNM equation, given below explicitly as,

$$z\left(z^4-1\right)X''_{\boldsymbol{e}_i}(z) + \left(z^4 - 2i\lambda_i z + 3\right)X'_{\boldsymbol{e}_i}(z) + \frac{3}{2}X_{\boldsymbol{e}_i}(z)\left(q_i^2 z + 2i\lambda_i\right) = 0\,, \tag{4.14}$$

$$\begin{aligned} &z\left(z^4-1\right)Y''_{\boldsymbol{e}_i}(z) + \left(-\frac{12q_i^2\left(z^4-1\right)z^4}{2\lambda_i^2+3q_i^2\left(z^4-1\right)} + 5z^4 - 2i\lambda_i z - 1\right)Y'_{\boldsymbol{e}_i}(z) \\ &\quad + Y_{\boldsymbol{e}_i}(z)\left(-i\lambda_i + \frac{12q_i^2 z^3\left(-2z^4 + i\lambda_i z + 2\right)}{2\lambda_i^2+3q_i^2\left(z^4-1\right)} + \frac{3q_i^2 z}{2} + 4z^3 + \frac{4}{z}\right) = 0\,, \end{aligned} \tag{4.15}$$

$$\begin{aligned} &z\left(z^4-1\right)Z''_{\boldsymbol{e}_i}(z) + \left(-\frac{8q_i^2\left(z^4-1\right)z^4}{2\lambda_i^2+q_i^2\left(z^4-3\right)} + 5z^4 - 2i\lambda_i z - 1\right)Z'_{\boldsymbol{e}_i}(z) \\ &\quad + Z_{\boldsymbol{e}_i}(z)\left(-i\lambda_i + \frac{8q_i^2 z^3(2+i\lambda_i z)}{2\lambda_i^2+q_i^2\left(z^4-3\right)} + \frac{3q_i^2 z}{2} + 4z^3 + \frac{4}{z}\right) = 0\,. \end{aligned} \tag{4.16}$$

By examining Eq. (4.14) near the horizon and assuming a regular solution we can find the relations,

$$X'_{\boldsymbol{e}_i}(1) = \frac{3\left(2\lambda_i - iq_i^2\right)}{4(\lambda_i+2i)}X_{\boldsymbol{e}_i}(1)\,, \quad X''_{\boldsymbol{e}_i}(1) = -\frac{3\left(-4\lambda_i(\lambda_i-4i) + 3q_i^4 + 12i\lambda_i q_i^2\right)}{16(\lambda_i+2i)(\lambda_i+4i)}X_{\boldsymbol{e}_i}(1)\,. \tag{4.17}$$

Similar constraints will hold for $Y_{\boldsymbol{e}_i}(1)$ and $Z_{\boldsymbol{e}_i}(1)$, and will be useful for simplifications later in this chapter. We also note that in Eq's (4.15) and (4.16) one can scale

[4] In Eq. (4.13) we have used a slightly different definition for $Y_{\boldsymbol{e}_i}$ than what is found in [4] so as to preserve the property $\overline{Y}_{\boldsymbol{e}_i} = Y_{\bar{\boldsymbol{e}}_i}$.

out the asymptotic near boundary behaviour by defining $\tilde{Y}_{\boldsymbol{e}_i}(z) = 1/z^2 Y_{\boldsymbol{e}_i}(z)$ and $\tilde{Z}_{\boldsymbol{e}_i}(z) = 1/z^2 Z_{\boldsymbol{e}_i}(z)$, so that we recover identical equations for $\tilde{Y}_{\boldsymbol{e}_i}(z)$, $\tilde{Z}_{\boldsymbol{e}_i}(z)$ and $H_n(z)$ as $q \to 0$. This is the same equation from which we computed the non-hydrodynamic modes in Section 2.2. Under simple coordinate redefinitions these equations at finite q_i are found to be the same as those studied in [89]. Imposing that the fluctuations die off at $z = 0$ and are ingoing at the $z = 1$ horizon, allow for a countably infinite set of frequencies $\lambda_i(q_i)$, which are all included at first order in $\Omega_{\boldsymbol{e}_i}$. As such we have defined the vector $\boldsymbol{\omega}$ in terms of the components of $\boldsymbol{k}$, which are allowed to vary.

As these fluctuations are linear perturbations around equilibrium they only depend on the equilibrium solution where the horizons coincide, we therefore have that $z_{AH} = z_{EH} = z_h$. The amplitude and phase of a given mode at the horizon will remain undetermined by the QNM equations and can be considered initial data. We parameterise these constants as,

$$X_{\boldsymbol{e}_i}(1) = \mathcal{X}_{\boldsymbol{e}_i} e^{i\alpha^{\mathcal{X}}_{\boldsymbol{e}_i}/2}\,, \tag{4.18}$$

where by the reality of the solution $X_{\bar{\boldsymbol{e}}_i} = \overline{X}_{\boldsymbol{e}_i}$ with analogous definitions holding for $Y_{\boldsymbol{e}_i}$ and $Z_{\boldsymbol{e}_i}$.

Most crucially in our computation we include second order contributions of the form $\mathcal{O}\left(\Omega_{\boldsymbol{e}_i}\Omega_{\boldsymbol{e}_j}\right)$. These terms can be thought of as the interactions of pairs of QNMs, and give the leading backreaction due to the perturbations. In particular the leading contribution in order of magnitude will be given when the $\boldsymbol{e}_i$ modes interact with themselves and their complex conjugate. In this analysis we neglect interactions of three and higher modes, which can in principle be included in a similar way.

An important point in the calculation that follows is that the exponential functions $\Omega_{\boldsymbol{e}_i}$ are linearly independent. From this property we will be able to separate the equations of motion out into independent ODEs in z for the coefficients $g_{\boldsymbol{n}}(z)$, sourced by the first order contributions. These equations further reduce to algebraic relations when evaluated on either the event- or apparent horizon, which allows us to write

the divergence of the entropy currents purely in terms of the horizon values defined in Eq. (4.18).

A final point of consideration is that Eqs. (4.14)–(4.16) in fact define three seperate sets of infinite dimensional vectors, one for each channel, which potentially introduces confusion in deciding which mode $\boldsymbol{e}_i$ refers to in $\boldsymbol{\omega}$. However the analysis proceeds as follows: fixing some $\lambda_i(q_i)$ we expand each metric function g in powers of $\Omega_{\boldsymbol{e}_i}$ as given in Eq. (4.11). In the following sections we derive an expression for $\partial_\mu s^\mu$ which is dependent on the normalizations of the QNMs given by Eq. (4.18). Then fixing the QNM frequency λ_i to be to be an eigenvalue of either Eq. (4.14), (4.15) or (4.16) will force us to set the normalization of the remaining non-normalizable modes to zero. Because this will effectively decouple the channels we will use a different vector $\boldsymbol{\omega}$ for each channel graded by their negative imaginary parts in decreasing order.

4.3 Computation and results

In this section we outline the steps necessary to calculate the divergence of the entropy current, and provide explicit details of the computation. Here there are three key ingredients which will be needed: the raw expression for the divergence of the entropy current $\partial_\mu s^\mu$, a constraint from the equations of motion, and the definition of either the apparent or event horizon. By imposing either horizon condition in Eq. (4.6) order by order, Einstein's equations ($E_{\mu\nu} = 0$) will give relations between the various metric functions at the horizon that allow us to express $\partial_\mu s^\mu$ fully in terms of the QNM frequencies and the horizon values given by Eq. (4.18).

4.3.1 The constraint equation

Einstein's equations $E_{\mu\nu} = 0$ can be readily found from Eq. (4.4), but in particular our only necessary constraint will come from solving the unexpanded E_{rr} for $\partial_r^2\Sigma$, inserting that into E_t^r and expanding the result in a transseries to second order.

After expanding the result in a series in $\Omega_{\boldsymbol{n}}$ and isolating the linearly independent contributions we can find equations constraining $g_{\boldsymbol{e}_i}$ and $g_{\boldsymbol{e}_i+\boldsymbol{e}_j}$.[5] We can find,

$$-\frac{3}{4}A_{\boldsymbol{e}_i}(1)\left(q_i^2-2i\lambda_i\right)+\sqrt{\frac{3}{2}}F^{(x)}_{\boldsymbol{e}_i}(1)(\lambda_i-2i)q_i+3\lambda_i(\lambda_i-2i)\left(\pi T\right)S_{\boldsymbol{e}_i}(1)=0\,, \tag{4.19}$$

$$\begin{aligned}&\frac{1}{2}A_{\boldsymbol{e}_i+\boldsymbol{e}_j}(1)\left(-3(q_i+q_j)^2+6i(\lambda_i+\lambda_j)\right)+2\sqrt{\frac{3}{2}}F^{(x)}_{\boldsymbol{e}_i+\boldsymbol{e}_j}(1)(\lambda_i+\lambda_j-2i)(q_i+q_j)\\&\quad+6\left(\pi T\right)S_{\boldsymbol{e}_i+\boldsymbol{e}_j}(1)(\lambda_i+\lambda_j)(\lambda_i+\lambda_j-2i)+W_{\boldsymbol{e}_i+\boldsymbol{e}_j}=0\,,\end{aligned} \tag{4.20}$$

where we can cover the equivalent expressions for $\bar{\boldsymbol{e}}_i$ and $\bar{\boldsymbol{e}}_j$ by just replacing them in the above equation, and the source term $W_{\boldsymbol{e}_i+\boldsymbol{e}_j}$ is given by,

$$\begin{aligned}W_{\boldsymbol{e}_i+\boldsymbol{e}_j}=&B_{\boldsymbol{e}_i}(1)\left(3B_{\boldsymbol{e}_j}(1)\lambda_i\lambda_j\left(\pi T\right)^2+\sqrt{6}F^{(x)}_{\boldsymbol{e}_i}(1)(\lambda_j-2i)(q_i+q_j)\right)\\&+\sqrt{6}B_j(1)F^{(x)}_{\boldsymbol{e}_i}(1)(\lambda_i-2i)(q_i+q_j)+\frac{i\sqrt{\frac{3}{2}}q_iF^{(x)}_{\boldsymbol{e}_j}(1)A'_{\boldsymbol{e}_i}(1)}{\left(\pi T\right)^2}+\frac{i\sqrt{\frac{3}{2}}q_jF^{(x)}_{\boldsymbol{e}_i}(1)A'_{\boldsymbol{e}_j}(1)}{\left(\pi T\right)^2}\\&-\frac{i\lambda_iF^{(x)}_{\boldsymbol{e}_j}(1)F^{(x)\prime}_{\boldsymbol{e}_i}(1)}{\left(\pi T\right)^2}-\frac{i\lambda_jF^{(x)}_{\boldsymbol{e}_i}(1)F^{(x)\prime}_{\boldsymbol{e}_j}(1)}{\left(\pi T\right)^2}-\frac{iF^{(y)}_{\boldsymbol{e}_j}(1)\lambda_iF^{(y)\prime}_{\boldsymbol{e}_i}(1)}{\left(\pi T\right)^2}-\frac{iF^{(y)}_{\boldsymbol{e}_i}(1)\lambda_jF^{(y)\prime}_{\boldsymbol{e}_j}(1)}{\left(\pi T\right)^2}\\&+\frac{F^{(x)}_{\boldsymbol{e}_i}(1)F^{(x)}_{\boldsymbol{e}_j}(1)\left(2i\lambda_j\left(\lambda_i^2+q_i^2-q_iq_j\right)+\lambda_j^2(q_i(q_j-q_i)+2i\lambda_i)+\lambda_i(\lambda_i-2i)q_j(q_i-q_j)\right)}{2\lambda_i\lambda_j\left(\pi T\right)^2}\\&+\frac{F^{(y)}_{\boldsymbol{e}_i}(1)F^{(y)}_{\boldsymbol{e}_j}(1)(-3q_iq_j+2i(\lambda_i+\lambda_j))}{2\left(\pi T\right)^2}-\sqrt{\frac{3}{2}}F^{(y)}_{\boldsymbol{e}_i}(1)G_{\boldsymbol{e}_j}(1)(\lambda_i-2i)(q_i+q_j)\\&-\sqrt{\frac{3}{2}}F^{(y)}_{\boldsymbol{e}_j}(1)G_{\boldsymbol{e}_i}(1)(\lambda_j-2i)(q_i+q_j)+G_{\boldsymbol{e}_i}(1)G_{\boldsymbol{e}_j}(1)\lambda_i\lambda_j\left(\pi T\right)^2+H_{\boldsymbol{e}_i}(1)H_{\boldsymbol{e}_j}(1)\lambda_i\lambda_j\left(\pi T\right)^2\,.\end{aligned} \tag{4.21}$$

Note that in order to simplify $W_{\boldsymbol{e}_i+\boldsymbol{e}_j}$ in Eq. (4.21) we have substituted Eq. (4.19) as well as set $A_{\boldsymbol{e}_i}(1)=0$ preemptively.[6]

4.3.2 Finding the apparent and event horizon

We will define the entropy current as given by Eq. (4.7), but the meaning of this quantity will depend on how we define $v=\partial_r$ the normal vector to the horizon

[5] The form of these equations will be identical if we exchange $\boldsymbol{e}_i$ for $\bar{\boldsymbol{e}}_j$ vectors.

[6] The condition that $A_{\boldsymbol{e}_i}(1)=0$ holds for both the event and apparent horizon and intuitively follows from the fact that all $g_{\boldsymbol{e}_i}$ metric functions are linear perturbations of the static blackbrane metric, which must leave the horizon location unchanged. The condition will be shown more explicitly to hold in Section 4.3.2.

surface. Using the radial gauge freedom associated with the metric ansatz (4.4) we can fix the horizon at $z = 1$, but whether v_M represents the apparent or event horizon will be decided by the horizon condition Eq. (4.6) we select. For an apparent horizon we impose the zero expansion condition ($\theta\big|_{z=1} = 0$) fixing $z = 1$ at the outer most trapped surface.

Evaluating this condition and isolating linearly independent terms in $\Omega_{\boldsymbol{n}}$ we can extract the following constraints to order $O(\Omega_{\boldsymbol{e}_i}\Omega_{\boldsymbol{e}_j})$,

$$3A_{\boldsymbol{e}_i}(1) - i\sqrt{6}F^{(x)}_{\boldsymbol{e}_i}(1)q_i - 6i\lambda_i\,(\pi T)\,S_{\boldsymbol{e}_i}(1) = 0 \tag{4.22}$$

$$6A_{\boldsymbol{e}_i+\boldsymbol{e}_j}(1) - i2\sqrt{6}F^{(x)}_{\boldsymbol{e}_i+\boldsymbol{e}_j}(1)(q_i+q_j) - 12i\,(\pi T)\,S_{\boldsymbol{e}_i+\boldsymbol{e}_j}(1)(\lambda_i+\lambda_j) + \frac{1}{(\pi T)^2}V_{\boldsymbol{e}_i+\boldsymbol{e}_j} = 0\,, \tag{4.23}$$

where,

$$\begin{aligned} V_{\boldsymbol{e}_i+\boldsymbol{e}_i} =& -i\sqrt{6}\,(\pi T)^2\,(q_i+q_j)(2B_{\boldsymbol{e}_i}(1)F^{(x)}_{\boldsymbol{e}_j}(1) + 2B_{\boldsymbol{e}_j}(1)F^{(x)}_{\boldsymbol{e}_i}(1) - F^{(y)}_{\boldsymbol{e}_i}(1)G_{\boldsymbol{e}_j}(1) - F^{(y)}_{\boldsymbol{e}_j}(1)G_{\boldsymbol{e}_i}(1)) \\ &+ \frac{iq_j}{\lambda_j}\left(F^{(x)}_{\boldsymbol{e}_j}(1)F^{(x)}_{\boldsymbol{e}_i}(1)(q_j-q_i)\right) + \frac{iq_i}{\lambda_i}\left(F^{(x)}_{\boldsymbol{e}_i}(1)F^{(x)}_{\boldsymbol{e}_j}(1)(q_i-q_j)\right) && (4.24) \\ &+ 6(F^{(x)}_{\boldsymbol{e}_i}(1)F^{(x)}_{\boldsymbol{e}_j}(1) + F^{(y)}_{\boldsymbol{e}_i}(1)F^{(y)}_{\boldsymbol{e}_j}(1))\,, && (4.25) \end{aligned}$$

A key feature of the event horizon on the other hand is that the surface must be null. The condition we should use in this case is $v^M v_M\big|_{z=1} = 0$. Following similar steps as outlined above we arrive at an alternative set of conditions,

$$A_{\boldsymbol{e}_i}(1) = 0\,, \tag{4.26}$$

$$A_{\boldsymbol{e}_i+\boldsymbol{e}_j}(1) + \frac{(F^{(x)}_{\boldsymbol{e}_i}(1)F^{(x)}_{\boldsymbol{e}_j}(1) + F^{(y)}_{\boldsymbol{e}_i}(1)F^{(y)}_{\boldsymbol{e}_j}(1))}{(\pi T)^2} = 0\,. \tag{4.27}$$

Note that substituting Eq. (4.22) into Eq. (4.19) yields the expression $A_{\boldsymbol{e}_i}(1) = 0$, as does Eq. (4.26). In both cases this retrospectively justifies the assumption used to simplify Eq. (4.21).

4.3.3 Computing the divergence of the entropy current

We are now ready to combine the pieces above into the calculation of $\partial_\mu s^\mu$. Following the definition of Eq. (4.34) having set $v = \partial_r$, it is easy to find,

$$\begin{aligned}\partial_\mu s^\mu =& \frac{1}{4}\left(\Omega_{\boldsymbol{e}_i} f_{\boldsymbol{e}_i} + \Omega_{\boldsymbol{e}_j} f_{\boldsymbol{e}_j} + \Omega_{\bar{\boldsymbol{e}}_i} f_{\bar{\boldsymbol{e}}_i} + \Omega_{\bar{\boldsymbol{e}}_j} f_{\bar{\boldsymbol{e}}_j}\right) \\ &+\frac{1}{4}\left(\Omega_{2\boldsymbol{e}_i} f_{2\boldsymbol{e}_i} + \Omega_{2\bar{\boldsymbol{e}}_i} f_{2\bar{\boldsymbol{e}}_i} + \Omega_{\boldsymbol{e}_i+\bar{\boldsymbol{e}}_j} f_{\boldsymbol{e}_i+\bar{\boldsymbol{e}}_j} + \Omega_{\bar{\boldsymbol{e}}_i+\boldsymbol{e}_j} f_{\bar{\boldsymbol{e}}_i+\boldsymbol{e}_j}\right) + \mathcal{O}(\Omega_{\boldsymbol{e}_i}\Omega_{\boldsymbol{e}_j}\Omega_{\boldsymbol{e}_k})\,,\end{aligned} \tag{4.28}$$

with,

$$f_{\boldsymbol{e}_i} = -\frac{1}{2} i\,(\pi T)^2\left(\sqrt{6}F^{(x)}_{\boldsymbol{e}_i}(1) q_i + 6\lambda_i\,(\pi T)\,S_{\boldsymbol{e}_i}(1)\right)\,, \tag{4.29}$$

$$f_{\boldsymbol{e}_i+\boldsymbol{e}_j} = -i\,(\pi T)^2\left(\sqrt{6}F^{(x)}_{\boldsymbol{e}_i+\boldsymbol{e}_j}(1)(q_i+q_j) + 6\,(\pi T)\,S_{\boldsymbol{e}_i+\boldsymbol{e}_j}(1)(\lambda_i+\lambda_j)\right) + U_{\boldsymbol{e}_i+\boldsymbol{e}_j}\,, \tag{4.30}$$

where,

$$\begin{aligned}U_{\boldsymbol{e}_i+\boldsymbol{e}_j} =& -i\sqrt{\frac{3}{2}}F^{(x)}_{\boldsymbol{e}_j}(1)\,(\pi T)\,(q_i+q_j)(2B_{\boldsymbol{e}_i}(1)\,(\pi T) + S_{\boldsymbol{e}_i}(1)) \\ &- i\sqrt{\frac{3}{2}}F^{(x)}_{\boldsymbol{e}_i}(1)\,(\pi T)\,(q_i+q_j)(2B_{\boldsymbol{e}_j}(1)\,(\pi T) + S_{\boldsymbol{e}_j}(1)) \\ &+ i\sqrt{\frac{3}{2}}F^{(y)}_{\boldsymbol{e}_i}(1)G_{\boldsymbol{e}_j}(1)\,(\pi T)^2\,(q_i+q_j) + i\sqrt{\frac{3}{2}}F^{(y)}_{\boldsymbol{e}_j}(1)G_{\boldsymbol{e}_i}(1)\,(\pi T)^2\,(q_i+q_j) \\ &- 6i\,(\pi T)^2\,S_{\boldsymbol{e}_i}(1)S_{\boldsymbol{e}_j}(1)(\lambda_i+\lambda_j)\,.\end{aligned} \tag{4.31}$$

The first thing to note is that substituting Eq. (4.19) and either Eq. (4.26) or Eq. (4.22) into Eq. (4.29) results in $f_{\boldsymbol{e}_i} = 0$, meaning that the divergence of the entropy current receives its first non-zero contribution at $O(\Omega_{\boldsymbol{e}_i}\Omega_{\boldsymbol{e}_j})$. This is to be expected, as $\Omega_{\boldsymbol{e}_i}$ and $\Omega_{\bar{\boldsymbol{e}}_i}$ are damped oscillating functions, the sum of which will not be non-negative in general. Because $\partial_\mu s^\mu$ should be positive definite, the leading order contribution should vanish to preserve this feature. The interaction of modes at second order given by an $\Omega_{\boldsymbol{e}_i}\Omega_{\bar{\boldsymbol{e}}_i}$ term in Eq. (4.28) is able to cancel out this oscillation and allow instead a non-trivial correction.

Let us examine the coefficient $f_{\boldsymbol{e}_i+\boldsymbol{e}_i}$ from Eq. (4.28). Substituting the conditions

given by Eqs. (4.20), (4.23) and (4.27) we find,

$$f^{(AH)}_{\boldsymbol{e}_i+\boldsymbol{e}_j} = -\frac{2\,(\pi T)^4\,\lambda_i\lambda_j}{(q_i+q_j)^2+4}\left(X_{\boldsymbol{e}_i}(1)X_{\boldsymbol{e}_j}(1) - \frac{Y_{\boldsymbol{e}_i}(1)Y_{\boldsymbol{e}_j}(1)}{\lambda_i\lambda_j\,(\pi T)^6} + \frac{Z_{\boldsymbol{e}_i}(1)Z_{\boldsymbol{e}_j}(1)}{12\,(\pi T)^8\,(\lambda_i^2-q_i^2)\,(\lambda_j^2-q_j^2)}\right), \tag{4.32}$$

$$f^{(EH)}_{\boldsymbol{e}_i+\boldsymbol{e}_j} = \frac{i\lambda_i\lambda_j\,(\pi T)^4}{\lambda_i+\lambda_j-2i}\left(X_{\boldsymbol{e}_i}(1)X_{\boldsymbol{e}_j}(1) - \frac{Y_{\boldsymbol{e}_i}(1)Y_{\boldsymbol{e}_j}(1)}{\lambda_i\lambda_j\,(\pi T)^6} + \frac{Z_{\boldsymbol{e}_i}(1)Z_{\boldsymbol{e}_j}(1)}{12\,(\pi T)^8\,(\lambda_i^2-q_i^2)\,(\lambda_j^2-q_j^2)}\right), \tag{4.33}$$

for the apparent horizon and event horizon respectively, where we have indicated the distinction with the superscripts (AH) and (EH). Interestingly, Eqs. (4.32) and (4.33) now show that $\partial_\mu s^\mu$ will explicitly depend only on information regarding the linear perturbations about the equilibrium solution, all dependence on the higher order metric functions has dropped out of the computation. Substituting the initial data given by Eq. (4.18) and summing the contributions in Eq. (4.28) we arrive at an expression for the divergence of the entropy current due to the interaction of all pairs of modes. The resulting expression is more complicated than we would like to decipher immediately so we will simply state the result in Appendix C.1 and analyse the leading contribution from the least damped mode below. We can find the leading evolution by setting $j = i = 0$, but to emphasize that the expression is the same for all choices of $i > 0$ we will leave i general in the expressions below. We find,

$$\partial_\mu s^\mu_a = \sum_{\mathcal{H}\in\{\mathcal{X},\mathcal{Y},\mathcal{Z}\}} B^{\mathcal{H}}_a\, e^{2\omega_i^I t}\left(C_a + \cos(2k_i x - 2t\omega_i^R + \delta^{\mathcal{H}}_a)\right) + \mathcal{O}(\Omega_{3\boldsymbol{e}_i}), \tag{4.34}$$

where the subscript a indicates whether we have computed the divergence of the entropy current at the apparent horizon (AH) or event horizon (EH). The remaining quantities given by a constant term C_a computed to be,

$$C_{(EH)} = \frac{|\lambda_i - i|}{1-\lambda_i^I}, \quad C_{(AH)} = 1+q_i^2, \tag{4.35}$$

a normalization $B^{\mathcal{H}}_a$ for each channel and choice of horizon,

$$B^{\mathcal{H}}_a = b^{\mathcal{H}}\begin{cases}\dfrac{1}{(1+q_i^2)} & a = \text{(AH)},\\[2ex] \dfrac{1}{|\lambda_i - i|} & a = \text{(EH)},\end{cases} \quad \text{with} \quad b^{\mathcal{H}} = \begin{cases}\dfrac{1}{8}(\pi T)^4\,|\lambda_i|^2\,\mathcal{X}_i^2 & \mathcal{H}=\mathcal{X}\text{, (tensor)}\\[2ex] \dfrac{\mathcal{Y}_i^2}{8(\pi T)^2} & \mathcal{H}=\mathcal{Y}\text{, (shear)}\\[2ex] \dfrac{|\lambda_i|^2\mathcal{Z}_i^2}{96(\pi T)^4\left|\lambda_i^2-q_i^2\right|^2} & \mathcal{H}=\mathcal{Z}\text{, (sound)}\end{cases}, \tag{4.36}$$

and with phases $\delta_a^{\mathcal{H}}$ given by,

$$\delta^{\mathcal{H}}_{(AH)} = \begin{cases} \alpha_i^{\mathcal{X}} - \arctan\left(\dfrac{2\lambda_i^I\lambda_i^R}{\left(\lambda_i^I\right)^2-\left(\lambda_i^R\right)^2}\right) & \mathcal{H}=\mathcal{X}\,,\ \text{(tensor)} \\ \alpha_i^{\mathcal{Y}} & \mathcal{H}=\mathcal{Y}\,,\ \text{(shear)} \\ \alpha_i^{\mathcal{Z}} - \arctan\left(\dfrac{2\lambda_i^R\lambda_i^I\left(|\lambda_i|^4-q_i^4\right)}{2|\lambda_i|^4q_i^2-\left(\left(\lambda_i^R\right)^2-\left(\lambda_i^I\right)^2\right)\left(|\lambda_i|^4+q_i^4\right)}\right) & \mathcal{H}=\mathcal{Z}\,,\ \text{(scalar)} \end{cases} . \tag{4.37}$$

For clarity we do not list the explicit results for $\delta^{\mathcal{H}}_{(EH)}$ here, but as explained below they can be computed from $\delta^{\mathcal{H}}_{(AH)}$.

There are several interesting observations to make while examining Eq. (4.34). While we have simultaneously included the contributions from all the channels, each channel in Eq. (4.34) decouples completely with no interactions between them at this order. This did not need to be the case as at $\mathcal{O}(\Omega_{2\boldsymbol{e}_i})$ the metric functions are typically sourced by contributions from all channels.

In each case $\partial_\mu s_a^\mu$ takes the form of a decaying exponential modified by an oscillating contribution and a constant term C_a, which is crucial in ensuring that $\partial_\mu s_a^\mu$ remains positive definite. Eq. (4.35) ensures this from the fact that $C_a \geq 1$, with the severity of the oscillations in Eq. (4.34) decreasing as we increase it away from this minimum. C_a is universal across fluctuations in all channels and depends only on whether we evaluate the expression at the apparent or event horizon. We will name this parameter C_a the *oscillation suppression*, distinguishing it from the slightly differently defined damping shift in [142]. A similar but distinct definition of C_a exists in [4] and Appendix C.1 which considers the oscillation suppression associated with interactions of QNMs with different frequencies.

Each term in the sum over $\mathcal{H}$ in Eq. (4.34) has an amplitude $B_a^{\mathcal{H}}$ and phase $\delta_a^{\mathcal{H}}$ that depends on initial data through the normalization of the QNMs given in Eq. (4.18). Through redefinitions of the amplitudes $\mathcal{X}_i$, $\mathcal{Y}_i$ and $\mathcal{Z}_i$ and phases $\alpha_i^{\mathcal{X}}$, $\alpha_i^{\mathcal{Y}}$ and $\alpha_i^{\mathcal{Z}}$ we could absorb any appearance of λ_i and q_i in Eqs. (4.36) and (4.37) into this initial data, meaning that this functional dependence is not particularly interesting. In fact from Eq. (4.36) it is the ratio of the amplitudes for $\partial_\mu s^\mu$ measured at the

apparent and event horizon which remains independent of initial data, and which yields the same result across each channel,

$$\frac{B^{\mathcal{H}}_{(EH)}}{B^{\mathcal{H}}_{(AH)}} = \frac{1+q_i^2}{|\lambda_i - i|}\,. \tag{4.38}$$

Similarly we find the combination,

$$\delta^{\mathcal{H}}_{(EH)} - \delta^{\mathcal{H}}_{(AH)} = \arctan\left(\frac{\lambda_i^R}{1-\lambda_i^I}\right), \tag{4.39}$$

to be independent of the initial phase consistently for each channel. Using Eq. (4.39) one can recover $\delta^{\mathcal{H}}_{(EH)}$ from the phases given in Eq. (4.37). A consequence of this observation is that in a similar set up near equilibrium one could use Eqs. (4.38) and (4.39) to construct the event horizon entropy from the apparent horizon entropy. This may be a useful application as the apparent horizon is typically easier to define than the event horizon.

Interestingly $C_{(EH)}$ for the event horizon is momentum independent while for the apparent horizon it is frequency independent. We also find that at zero momentum $C_{(AH)} = 1$ for the apparent horizon, which saturates the condition that $\partial_\mu s^\mu \geq 0$ given by the area theorem. Using our expression (4.34) in the homogeneous limit of $q_i \to 0$, we can integrate the result to find the entropy density given by Eq. (4.1), with an oscillation suppression (called the damping shift in [142]) given by Eqs. (4.2) and (4.3) for the apparent and event horizon respectively. As such we can analytically confirm the numerical results of [142].

4.4 Discussion and outlook

Through the transseries expansion we have succeeded in computing the leading contribution to the divergence of the entropy current for an equilibrating blackbrane. Expanding about a static background the leading order terms in the expansion were identical to a standard QNM computation. At second order these corrections could be interpreted as the backreactive interactions between the linear fluctuations on the blackbrane. Despite this process being the result of non-linear gravity, we nevertheless found a fully analytic description of the time evolving horizon relying only on the values of the quasinormal mode frequencies and equilibrium temperature.

In principle this computation could be expanded to include interactions of three modes. For tensor perturbations we have checked explicitly that $\partial_\mu s^\mu$ receives no $\mathcal{O}(\Omega_{3\boldsymbol{e}_i})$ contributions. In this case the $\mathcal{O}(\Omega_{2\boldsymbol{e}_i})$ modes reduce to a QNM equation but with frequency $2\omega_i$, which is not itself a QNM frequency. This implies that the equation will have no normalizable solutions, forcing us to set them to zero, in turn causing the third order transseries corrections to vanish. It would be interesting to see if these corrections vanish in general, as this would imply that our expression for $\partial_\mu s^\mu$ is in fact only corrected at fourth order.

We found that the positivity of $\partial_\mu s^\mu$ prevented any non-zero contribution at first order, instead allowing the first non-trivial term to occur at $\mathcal{O}(\Omega_{2\boldsymbol{e}_i})$. This statement has the consequence that the holographic entropy associated with these horizon areas will rapidly equilibrate at half the time scale set by the dominant QNM. When enforcing spatial translation symmetry (setting all momenta to zero) this transseries accurately describes far-from-equilibrium dynamics in holographic theories as all dynamical modes are gapped with graded negative imaginary part on the frequency plane [28, 147, 148]. However this series becomes difficult to organise when including low momentum hydrodynamic modes, where the distinction between $\Omega_{\boldsymbol{e}_i+\boldsymbol{e}_j}$ and $\Omega_{\boldsymbol{e}_i+\ldots+\boldsymbol{e}_n}$ contributions becomes unclear. In such situations it may be preferable to instead use the fluid gravity correspondence for an effective hydrodynamic descrip-

tion of the blackbrane [54, 56]. Because our analysis does not explicitly truncate in gradients, instead resumming them into $\omega(k)$, it may be be useful to determine if any region of overlap exists between these two expansions.

In our set up we have simplified the dynamics by allowing for spatial dependence along only the x-coordinate. While one can do this at linear level without loss of generality, this is too restrictive when describing the interaction of different modes and this condition should be relaxed in future work. From Fig. (4.1) it is clear that quantities such as the temperature follow a similar evolution to the entropy, and it would be interesting to try to compute this following a similar method to what we have studied here.

Chapter 5

Conclusion

In this thesis we have applied the transseries expansion to three systems in classical gravity. Through the gauge/gravity correspondence our analysis has had implications for both the dynamics of strongly coupled field theories as well as for the evolution of black holes themselves.

In Chapter 2 we set out to understand the fast hydrodynamization problem of heavy ion physics, that the quark gluon plasma (QGP) created in such collisions appears to evolve according to hydrodynamics in the large gradient regime where this framework should be inapplicable. To add some insight to this puzzle we examined the gradient expansion for $\mathcal{N} = 4$ SYM matter undergoing boost invariant evolution (Bjorken flow), by recasting the dynamics of this theory at infinite 't Hooft coupling and large N_c into quantities described by Einstein's equations. Extracting the energy density to high orders in this perturbative expansion we found the series to diverge, implying the existence of non-hydrodynamic modes best understood through a transseries solution which we then computed numerically. Due to the nature of resurgent transseries specific relations exist between different independent solutions in the system, known as transseries sectors. We were able to test that these relations hold for the $\mathcal{N} = 4$ SYM transseries by constructing the first 9 coefficients of the leading non-hydrodynamic sector purely from the coefficients of the hydrodynamic sector. In principle such a procedure could be used to extract the coefficients for all sectors if one were to find the hydrodynamic coefficients for this theory analytically.

We extended our scope to include gauge theories at intermediate coupling through the higher derivative toy model known as Gauss-Bonnet gravity. Constructing the diverging hydrodynamic expansions for this family of theories at varied coupling we then used Borel summation to find stable resummations that were not sensitive to the order of the expansion. We argued that these resummations were prescription dependent, with the ambiguity between differing prescriptions being approximately equal to the non-hydrodynamic modes hidden from the original gradient expansion. Adding a random ensemble of relaxing non-hydrodynamic modes to our resummation we could estimate the typical trajectories of an equilibrating gauge theory plasma undergoing Bjorken flow. We found that even in the presence of large gradients, trajectories would typically collapse onto a common curve, referred to as an *attractor*, and that this curve would be well described by first order viscous hydrodynamics. This behaviour is consistent with the apparent unreasonable effectiveness of hydrodynamics observed when describing the QGP.

In Chapter 3 we studied the Bjorken holographic system by instead using the number of boundary dimensions $n = D - 1$ as our large parameter. Imposing the symmetries of Bjorken expansion while packing the space with an arbitrary number of transverse dimensions we were able to find analytic solutions for the metric functions to order $\mathcal{O}(n^{-3})$. The usual large-D set-up proposed by Emparan, Suzuki, and Tanabe results in non-relativistic hydrodynamic equations of motion [112, 113], in order to properly describe the relativistic nature of our system we tailored our expansion for this purpose. As in these systems we found that the perturbative sector of the large-D expansion is governed by hydrodynamics [116, 118, 119, 137]. Using our solution we extracted combinations of transport coefficients to $\mathcal{O}(n^{-3})$ relevant for Bjorken flow up to 6-th order in gradients. Consequently this also showed that higher order contributions in gradient must be suppressed by at least n^{-4}.

Next we studied fluctuations rapidly evolving on this background with a timescale set by the effective temperature $T \sim n\,\tilde{\epsilon}^{1/n}$. These modes were non-perturbative at large-D enabling a transseries structure to emerge similar to the small gradient

transseries of Chapter 2, indicating that a sum including all higher order corrections to the perturbative large D sector will not converge. We computed the contribution to the energy density from these non-perturbative sectors and found them to correspond to the large-D limit of non-hydrodynamic modes in Bjorken flow. From our solution we obtained an infinite set of energy density coefficients associated with each non-perturbative sector to leading order in $1/D$. To conclude we discussed the parametric seperation between hydrodynamic and non-hydrodynamic modes at large-D and suggested a scaling choice which mixes both sectors potentially allowing access to the solution's behaviour at early times.

In Chapter 4 we applied the transseries expansion to study the equilibration of GR solutions towards a branebrane. Due to the simplicity of the set up we could fully determine the non-linear behaviour of the divergence of the entropy current ($\partial_\mu s^\mu$) analytically to second order in the expansion. Despite our calculation being sensitive to the interaction of linear modes across different channels, in our set up the dynamics reduced to a sum of independent, decoupled excitations evolving on top of a static horizon. Early computations suggest that the transseries expansion for $\partial_\mu s^\mu$ will vanish at third order, meaning that the error incorporated by neglecting higher order contributions will typically be exceedingly small. The generic applicability of the transseries also indicates that a similar approach could be used to study black hole equilibration in less symmetric scenarios and for related quantities such as the black hole temperature and out of equilibrium energy density.

One possible direction of further study would be to explore the connection between the fast moving modes of these theories and the non-hydrodynamic modes of the gradient expansion. There may exist some generalization of Hydrodynamics which naturally incorporates these dynamics through a similar transseries expansion. An ambitious goal would be to describe a far-from-equilibrium system via perturbations about a particular attractor solution throughout its evolution, as opposed to only at late times through the near equilibrium hydrodynamic expansion. One should first explore whether this expectation is possible, as further relaxing the symmetries of

Bjorken flow could break this transseries structure. As such, it would be relevant to apply this expansion to less symmetric cases as a sanity check of this conjecture.

An equally interesting problem would be to understand whether the fluid-gravity correspondence could similarly be generalized to include these fast modes. In the cases of both Bjorken flow and static equilibrium it is clear that the non-hydrodynamic modes of the system correspond to quasinormal modes of the corresponding dual gravity theory. In order to check this, one could apply a transseries expansion to the set-up of [57] in place of their grandient expansion.

We noted that in the case of Bjorken flow the perturbative dynamics of the large-D expansion exclusively recovered information of the hydrodynamic sector, while the non-perturbative modes recovered the non-hydrodynamic sector. This is an interesting observation in of itself and should be explored in greater generality. We found that through the large-D expansion we could recover an infinite series in gradients of the leading (in $1/D$) non-hydrodynamic modes. Because the large D expansion appears able to recover all-order information in gradients, this may be a tractable approach for recovering attractor solutions through the gauge-gravity correspondence.

Lastly by applying the transseries expansion to the simple set up of a perturbed static black brane, we could recover non-linear information while solving trivial equations of motion. This particular example could be extended to recover not only the entropy density but other relevant quantities such as the evolving energy density. Such a computation as applied to an Kerr-Schwarzschild solution would be useful for computing corrections to gravitation waves as observed by LIGO. The transseries expansion has shown success in finding solutions to a broad array of problems in classical gravity. In future works it will be interesting to apply these same techniques to expansions about other limiting cases of parameter space for this non-linear theory.

Appendix A

Appendix to Chapter 2

A.1 Introduction to asymptotic series and the Borel transform

In this thesis we will be interested in asymptotic series of the form,

$$\Phi_{\mathbf{0}} = \sum_{k=0}^{\infty} F_k^{(\mathbf{0})} g^{k+1} \,, \tag{A.1}$$

where where $g \ll 1$ is some small parameter and $F_k \sim k!$. One might expect to find Eq. (A.1) when computing a perturbative series expansion for some function with non-perturbative contributions. From the behaviour of the coefficients, we do not expect the series to converge.

One can typically define a convergent series through the map $\mathcal{B}$ defined as $g^\alpha \mapsto \frac{\xi^{\alpha-1}}{\Gamma(\alpha)}$ which modifies each term in the series (A.1). The result of applying this map to an asymptotic series is called a Borel transform $\mathcal{B}[\Phi_{\mathbf{0}}]$, where

$$\mathcal{B}[\Phi_{\mathbf{0}}](\xi) = \sum_{k=0}^{\infty} \frac{1}{k} F_k^{(\mathbf{0})} \xi^k \,. \tag{A.2}$$

When $\mathcal{B}[\Phi_{\mathbf{0}}]$ has a finite radius of convergence it can be analytically continued to some function $\mathcal{B}_+[\Phi_{\mathbf{0}}]$. One can see term by term that the inverse map of $\mathcal{B}$ will be a Laplace transform. However when applying this inverse map to an analytically continued Borel transform we don't expect to recover exactly the same function. We will call this new function the Borel sum,

$$\mathcal{I}_\theta[\mathcal{B}[\Phi_{\mathbf{0}}]] = \int_0^{e^{i\theta}\infty} d\xi e^{-\xi/g} \mathcal{B}_+[\Phi_{\mathbf{0}}](\xi) \,, \tag{A.3}$$

which is defined up to some parameter θ which determines the contour of integration. When applied to a finite polynomial the contour of integration here (assuming convergence) will not change the result. For more complicated functions the result will be highly dependent on this choice and correspond to different possible resummations of the original series.

A.1.1 Relating the Borel transforms of different sectors

In Section 2.3 we aimed to extract the coefficients of the leading non-perturbative sector from the Borel transform of the perturbative (hydrodynamic) sector. Now we will justify some of the relations between the Borel transforms of different sectors used in that section.[1] To do this we consider two asymptotic series,

$$\Phi_{\mathbf{0}} = \sum_{k=0}^{\infty} F_k^{(\mathbf{0})} g^{k+1}\,, \quad \Phi_{\mathbf{1}} = g^{\beta} \sum_{k=0}^{\infty} F_k^{(\mathbf{1})} g^{k+1}\,, \tag{A.4}$$

with asymptotic small parameter g, characteristic exponent β and exponential weight A such that the full solution generating these series is represented by

$$F(g) = \Phi_{\mathbf{0}}(g) + e^{-A/g}\Phi_{\mathbf{1}}(g) + \dots\,, \tag{A.5}$$

where the ellipses indicate other instanton solutions which will not be important for this discussion. We can note that setting $F_0^{(\mathbf{0})} = 0$, $F_{k+1}^{(\mathbf{0})} = \epsilon_k^{(\mathbf{0})}$, $g = u^{-1}$, $A = A_1$ and $\beta + 1 = \beta_{\boldsymbol{e}_1}$ will reduce Eq. (A.5) to the leading contribution to the transseries for the energy density used in Section 2.3.

For a resurgent transseries the coefficients of different sectors are related via the large order relations,

$$F_k^{(\mathbf{0})} = -\frac{S_{\mathbf{0}\to\mathbf{1}}}{2\pi i}\frac{\Gamma(k-\beta)}{A^{k-\beta}}\left(F_0^{(\mathbf{1})} + \frac{A}{k-\beta-1}F_1^{(\mathbf{1})} + \frac{A^2}{(k-\beta-1)\,(k-\beta-2)}F_2^{(\mathbf{1})} + \dots\right) + (\text{other sectors})\,, \tag{A.6}$$

where $S_{\mathbf{0}\to\mathbf{1}}$ is known as the Borel residue, a proportionality constant between the sectors of the large order relation, which is given intrinsically by the non-linear theory

[1] We thank Inês Aniceto for useful insights helpful for this section.

data. In principle $F_k^{(\mathbf{0})}$ receives contributions from all other sectors, but these will not affect the discussion below.

As stated before, the Borel transform $\mathcal{B}$ is a map that modifies each term in the series (A.4) via $g^\alpha \mapsto \frac{\xi^{\alpha-1}}{\Gamma(\alpha)}$. In our attempt to relate the asymptotic series of different sectors, it will be useful to define

$$\mathcal{B}\left[g^\gamma \Phi_{\mathbf{0}}\right](\xi) \equiv \sum_{k=0}^{\infty} F_k^{(\mathbf{0})} \frac{\xi^{k+\gamma}}{\Gamma(k+\gamma+1)}\,, \tag{A.7}$$

$$= -\frac{S_{\mathbf{0}\to\mathbf{1}}}{2\pi i} \sum_{j=0}^{\infty} \left(\sum_{k=0}^{\infty} \frac{\Gamma(k-\beta-j)}{A^{k-\beta-j}} \frac{\xi^{k+\gamma}}{\Gamma(k+\gamma+1)} \right) F_j^{(\mathbf{1})}\,, \tag{A.8}$$

$$= -\frac{S_{\mathbf{0}\to\mathbf{1}}}{2\pi i} \sum_{j=0}^{\infty} \chi_j(\xi, A, \gamma, \beta)\, F_j^{(\mathbf{1})}\,, \tag{A.9}$$

where we have defined $\chi_j(\xi, A, \gamma, \beta)$ by performing the sum over k in Eq. (A.8). As it turns out this sum can be performed analytically, the closed form solution being given by

$$\chi_j(\xi, A, \gamma, \beta) = \xi^\gamma A^{\beta+j} \frac{\Gamma(-j-\beta)}{\Gamma(\gamma+1)}\, {}_2F_1\left(1, -j-\beta; \gamma+1; \frac{\xi}{A}\right)\,. \tag{A.10}$$

In the limit of $\gamma = 0$ we find that Eq. (A.7) reduces to the usual Borel transform on $\Phi_{\mathbf{0}}$ and we find $\chi_j(\xi, A, 0, \beta) = \Gamma(-j-\beta)(A-\xi)^{\beta+j}$, which when applied to Eq. (A.9) gives us

$$\mathcal{B}\left[\Phi_{\mathbf{0}}\right](\xi) = -\frac{S_{\mathbf{0}\to\mathbf{1}}}{2\pi i}\, (A-\xi)^\beta \left(\sum_{j=0}^{\infty} \Gamma(-\beta-j) F_j^{(\mathbf{1})}\, (A-\xi)^j \right) + \text{reg.}\,, \tag{A.11}$$

where the term "reg." indicates terms that are regular at $\xi = A$. Note that the other sectors omitted from Eq. (A.6) will only contribute to this regular term. The form of Eq. (A.11) verifies that for asymptotic series of the form (A.4) related by Eq. (A.6), the Borel plane of $\mathcal{B}\left[\Phi_{\mathbf{0}}\right](\xi)$ will contain a branch cut singularity of the type $(A-\xi)^\beta$.

By tuning γ we can attempt to cancel out the exponent of this branch cut in the Borel transform. In fact by choosing $\gamma = -\beta$ we will find

$$\mathcal{B}\left[g^{-\beta}\, \Phi_{\mathbf{0}}\right](\xi) = \frac{S_{\mathbf{0}\to\mathbf{1}}}{2\pi i}\, \log(A-\xi) \left(\sum_{j=0}^{\infty} \frac{F_j^{(\mathbf{1})}}{\Gamma(j+1)} (\xi - A)^j \right) + \text{reg.}\,, \tag{A.12}$$

$$= S_{\mathbf{0}\to\mathbf{1}} \left(\mathcal{B}\left[g^{-\beta}\, \Phi_{\mathbf{1}}\right](\xi - A) \right) \frac{\log(A-\xi)}{2\pi i} + \text{reg.}\,, \tag{A.13}$$

where in the last line we have identified the sum as the Borel transform of $\mathcal{B}\left[g^{-\beta}\,\Phi_{\mathbf{1}}\right](\xi - A)$, which we note to be regular at $\xi = A$ with a radius of convergence set by the next closest instanton action.

While Eq. (A.13) is an improvement on the branch cut singularity found in Eq. (A.11), we would like to reduce the singularities in the Borel plane to a series of simple poles. It will be useful then to choose $\gamma = -\beta - 1/2$ resulting in a Borel transform of the form

$$\mathcal{B}\left[g^{-\beta-1/2}\,\Phi_{\mathbf{0}}\right](\xi) = \frac{S_{\mathbf{0}\to\mathbf{1}}}{2\sqrt{\xi - A}}\left(\sum_{j=0}^{\infty}\frac{F_j^{(\mathbf{1})}}{\Gamma(j+1/2)}\,(\xi - A)^j\right) + \text{reg}\,. \tag{A.14}$$

Finally we can perform the change of variables, $\xi = A - (\zeta - A)^2$, to transform Eq. (A.14) into a Laurent series

$$\mathcal{B}\left[g^{-\beta-1/2}\,\Phi_{\mathbf{0}}\right](\zeta) = \frac{\mathsf{S}_{\mathbf{0}\to\mathbf{1}}}{2i\,(\zeta - A)}\left(\sum_{j=0}^{\infty}\frac{(-1)^j F_j^{(\mathbf{1})}}{\Gamma(j+1/2)}\,(\zeta - A)^{2j}\right) + \text{reg}\,. \tag{A.15}$$

Using standard methods one can then recover the coefficients $F_j^{(\mathbf{1})}$ from the residues of Eq. (A.15).

Appendix B

Appendix to Chapter 3

B.1 Expressions for the Third-order Expansion of the Different Metric Functions

In this appendix we tabulate the third-order in the large-D expansion for the different metric functions, found in Subsection 3.2.1.

$$
\begin{aligned}
A_3 \;=\; & -\frac{\bar{a}_3^{\rm NH}(\tau)}{R} \\
& + \frac{4\Lambda\tau \mathrm{Li}_3\left(\frac{1}{R(\Lambda\tau+1)}\right)}{R(\Lambda\tau+1)^4} + \frac{2\Lambda\tau \mathrm{Li}_2\left(\frac{1}{R(\Lambda\tau+1)}\right)\left(2\left(1-\frac{1}{R(\Lambda\tau+1)}\right) - \frac{\log\left(\frac{1}{R(\Lambda\tau+1)}\right)}{R(\Lambda\tau+1)}\right)}{(\Lambda\tau+1)^3} \\
& - \frac{(\Lambda^2\tau^2 - 4\Lambda\tau + 1)\log^3(R)}{6R(\Lambda\tau+1)^4} - \frac{\log^2(R)\left((\Lambda^2\tau^2-1)\log(\Lambda\tau+1) + \Lambda\tau(\Lambda\tau-5)\right)}{2R(\Lambda\tau+1)^4} \\
& - \frac{\log(R)\left(-2\Lambda\tau(\Lambda\tau+2) + (\Lambda\tau+1)^2\log^2(\Lambda\tau+1) - 2(5\Lambda\tau+2)\log(\Lambda\tau+1)\right)}{2R(\Lambda\tau+1)^4} \\
& + \frac{4\Lambda\tau\left(1-\frac{1}{R(\Lambda\tau+1)}\right)\log\left(\frac{1}{R(\Lambda\tau+1)}\right)\log\left(1-\frac{1}{R(\Lambda\tau+1)}\right)}{(\Lambda\tau+1)^3}\,, \qquad \text{(B.1)}
\end{aligned}
$$

with $\bar{a}_3^{\rm NH}(\tau)$ given in Eq. (3.43) and the metric function B_3 is

$$\begin{aligned} B_3 \;=\; & -\frac{2(\Lambda\tau-1)^2\mathrm{Li}_3\left(\frac{1}{\Lambda\tau R+R}\right)}{(\Lambda\tau+1)^3}+\frac{4(\Lambda\tau-1)\mathrm{Li}_3(1-R(\Lambda\tau+1))}{(\Lambda\tau+1)^3} \\ & -\frac{2\Lambda\tau\mathrm{Li}_2\left(\frac{1}{\Lambda\tau R+R}\right)(\Lambda\tau+(\Lambda\tau-1)\log(R)-2)}{(\Lambda\tau+1)^3}+\frac{2(\Lambda\tau-1)\log^3(R(\Lambda\tau+1))}{3(\Lambda\tau+1)^3} \\ & \frac{2\left(\pi^2(\Lambda\tau-1)+\frac{3\Lambda\tau((\Lambda\tau+1)\log(\Lambda\tau+1)-\log(R)+2)}{1-(1+\Lambda\tau)R}\right)\log(R(\Lambda\tau+1))}{3(\Lambda\tau+1)^3} \\ -\frac{\log\left(\frac{1}{R(\Lambda\tau+1)}\right)(2\Lambda\tau(\Lambda\tau-2)+(\Lambda\tau-1)^2(-\log(\Lambda\tau+1))+(\Lambda^2\tau^2-1)\log(R))\log\left(1-\frac{1}{\Lambda R\tau+R}\right)}{(\Lambda\tau+1)^3}&. \end{aligned} \tag{B.2}$$

As stated in Subsection 3.2.1

$$S_3 = 0\,. \tag{B.3}$$

However, to be able to compute A_3 and B_3 it is necessary to determine S_4, which is given by

$$S_4 = \frac{2\Lambda\tau\left(2\mathrm{Li}_3\left(\frac{1}{R(\Lambda\tau+1)}\right)-\mathrm{Li}_2\left(\frac{1}{R(\Lambda\tau+1)}\right)\log\left(\frac{1}{R(\Lambda\tau+1)}\right)\right)}{(\Lambda\tau+1)^3}\,. \tag{B.4}$$

B.2 Comparison of perturbative large-D solutions at late times

To aid in the analysis of Subsection 3.2.1 in this section we aim to compare the solutions in the near horizon region obtained through the perturbative large-D expansion, with an alternate expansion for Bjorken flow at large τ for Einstein's equations at fixed number of spacetime dimensions $D = n+1$. For the case of $D = 5$ this analysis reduces to the low order perturbative (in gradient) solutions for the expansion of Eqs. (2.18)–(2.20), first performed in [82]. In this section we will generalise the analysis of [82] to arbitary D for our comparison in the large-D limit.

To make contact with the notation in [82] and to facilitate the late-time analysis,

we introduce the following field redefinition

$$A = r^2 \bar{A}(\tau, r), \tag{B.5}$$

$$B = \frac{1}{n-1}\left(\log\left(\frac{r^2}{(1+r\tau)^2}\right) + \frac{n-1}{n-2}\left(2\,\bar{d}(\tau,r) - \bar{B}(\tau,r)\right)\right), \tag{B.6}$$

$$S = r^{\frac{n-2}{n-1}}(1+r\tau)^{\frac{1}{n-1}} e^{\bar{d}(\tau,r)}. \tag{B.7}$$

At late times the dual gravity spacetime should be close to that of a boosted black-brane with a time-dependent energy density predicted by ideal hydrodynamics. The corrections to this approximate solution are controlled by a dimensionless inverse gradient $u^{-1} = \tau^{-\frac{n-2}{n-1}} \sim \frac{1}{\tau T}$ (see Subsection 1.1.2). So that as $\tau \to \infty$ the horizon stays at a fixed location it is convenient to parametrise the holographic direction in terms of a new variable that tracks the position of the boosted blackbrane horizon,

$$s = \frac{\Lambda}{r}\frac{1}{(\tau\Lambda)^{-1/(n-1)}}\,. \tag{B.8}$$

As such $s = 1$ corresponds to the position of the horizon to leading order in gradients. The gradient expansion of the different metric functions is

$$\bar{A}(r,\tau) = \sum_{i=0}^{\infty} u^{-i}\bar{A}_i(s)\ , \quad \bar{B}(r,\tau) = \sum_{i=0}^{\infty} u^{-i}\bar{b}_i(s)\ , \quad \bar{d}(r,\tau) = \sum_{i=0}^{\infty} u^{-i}\bar{d}_i(s)\ . \tag{B.9}$$

Introducing these expansions into Einstein's equations and expanding in the dimensionless inverse gradient, u^{-1}, the leading order (in gradients) solution is simply the boosted black brane

$$\bar{A}_0(s) = 1 - s^n\,, \quad \bar{b}_0(s) = 0\,, \quad \bar{d}_0(s) = 0. \tag{B.10}$$

Going to next-to-leading order in gradients, the metric functions include the effect of the shear viscosity and they read

$$\bar{A}_1(s) = \frac{(2+(n-2)s)s^n}{n-1}\,, \tag{B.11}$$

$$\bar{b}_1(s) = \frac{2(n-2)}{n(n-1)}\left(\beta(s^n\,; 1+\frac{1}{n}, 0) + \log\left(1-s^n\right)\right)\,, \tag{B.12}$$

$$\bar{d}_1(s) = 0\,, \tag{B.13}$$

where $\beta(z;a,b)$ is the incomplete beta function. Note that we have chosen a gauge consistent with the near-boundary behaviours (3.22)-(3.24). We have not been able to find closed form expressions for these metric functions beyond this order.

Inserting this gradient expansion into Eqs. (B.5)-(B.7) and expressing them in $(\tau,\, R)$, we can compare the fluid-gravity expectation for the different metric functions with the near horizon result derived in the previous section. After taking the large-D limit and expanding to $\mathcal{O}\left(n^{-3}\right)$

$$\begin{aligned}
\tilde{A}_{\text{hydro}}(r,\tau) &= \left(1-\left(\frac{1}{\tau\Lambda}-\frac{1}{(\tau\Lambda)^2}\right)\frac{1}{R}\right)+\frac{1}{n}\left(\frac{1+(-1+\tau\Lambda)\log(\tau)}{(\tau\Lambda)^2 R}-\frac{\log R}{(\tau\Lambda)^2 R}\right)+ \qquad \text{(B.14)}\\
&\quad+\frac{1}{n^2}\left(\frac{2+2\tau\Lambda\log\tau\Lambda-(-1+\tau\Lambda)\log(\tau\Lambda)^2}{2(\tau\Lambda)^2 R}+\frac{(1+\log\tau\Lambda)\log R}{(\tau\Lambda)^2 R}+\frac{(\log R)^2}{2(\tau\Lambda)^2 R}\right),\\
\tilde{B}_{\text{hydro}}(r,\tau) &= \frac{1}{n^2}\left(\frac{2\left(\text{Li}_2\left(\frac{1}{R\Lambda\tau}\right)+\log\left(1-\frac{1}{\Lambda R\tau}\right)\log\left(\frac{1}{\Lambda R\tau}\right)\right)}{\Lambda\tau}\right), \qquad \text{(B.15)}\\
\tilde{S}_{\text{hydro}}(r,\tau) &= 1\,. \qquad \text{(B.16)}
\end{aligned}$$

These solutions come from a gradient analysis and as such they are only valid up to $\mathcal{O}(\tau^{-2})$. Notably they coincide with the late-time expansion of Eqs. (3.30)-(3.41) up to order $\mathcal{O}(\tau^{-2})$, indicating consistency between the two expansions. The matching of these approaches may be considered as an example of the compatibility of the gradient and the large-D expansions [149].

B.3 Quasi-normal modes of blackbranes at large-D

In Subsection 3.3.3 we constrain the non-perturbative modes of the large-D expansion evolving on an evolving horizon by matching the near horizon and near boundary solutions in an overlap region of mutual validity. In fact the condition of consistency between these regions fixes the leading behaviour of the frequency $\hat{\omega}$ at which these modes oscillate. These same excitations control the non-perturbative contributions in $1/D$ to the Bjorken flow, as discussed in Section 3.3.

For the sake of clarity in this section we will review a computation for the quasi-normal spectrum of static blackbranes in the large-D limit at zero spatial momentum, following a similar approach as the analysis of black-holes in [140]. In standard Eddington-Finkelstein form, to leading order in the perturbation, the metric is

$$ds^2_{\rm BB+fluc} = -r^2 A_{\rm BB}(r) dt^2 + 2\, dt dr + r^2 \left(1 - \epsilon\, Z(t,r)\right) dx_\parallel^2 + r^2 \left(1 + \frac{\epsilon}{n-2} Z(t,r)\right) dx_\perp^2 \tag{B.17}$$

with $A_{\rm BB} = 1-(\Lambda/r)^n$ the blackening factor of the brane in $D = n+1$ dimension and ϵ is a book-keeping parameter that indicates that the anisotropic fluctuation $Z(t,r)$ is small.[1] Linearising Einstein's equations in ϵ and after performing a Fourier transform the equation of motion for the fluctuation given in terms of the coordinate $z = \Lambda/r$ is

$$Z''(z) - \frac{((n-1) + z^n - 2i\bar{\omega}_j\, z)}{z(1-z^n)} Z'(z) - \frac{(n-1) i\bar{\omega}_j}{z(1-z^n)}\, Z(z) = 0\,, \tag{B.18}$$

which coincides with the Eq. (3.114) for the leading order transseries term in Bjorken flow.[2] This equation exhibits two distinct regions in the coordinate z: 1) the near boundary region $z \ll 1$, where the quickly changing function z^n can be neglected so that $Z(z)$ evolves in the background of vacuum AdS_D; and the near horizon region where $z \sim 1$ where the dynamics of the fluctuation is sensitive to the blackbrane horizon.

To zoom into the near horizon region, we fix $R = 1/z^n$, as was done in Section 3.2. For non-trivial solutions at large-D we also introduce the scaled variable $\hat{\omega} = \omega/n$ with $\hat{\omega} \sim \mathcal{O}(n^0)$, which can be motivated by a numerical analysis of the QNM spectrum of Eq. (B.18). In the near horizon region at $n \to \infty$, Eq. (B.18) becomes

$$\frac{(1 + 2\,(i\hat{\omega} - 1)\, R)\, Z'_{\rm NH}(R)}{R\,(1-R)} - \frac{i\hat{\omega} Z_{\rm NH}(R)}{(R-1)R} + Z''_{\rm NH}(R) = 0\,, \tag{B.19}$$

which coincides with the equation for the non-perturbative phase, Eq. (3.93). Regular

[1] Note that Eq. (B.17) bares some similarities to Eq. (3.14) of Section 3.2, where instead of τ and η the metric functions depends on time t, the volume is given by $S = r$, and B is given by a small perturbation.

[2] The Fourier transform has a plane wave factor of the form $e^{-i\bar{\omega}_j \Lambda t}$ such that $\bar{\omega}_j$ is dimensionless.

or ingoing solutions of this equation at the horizon, $R = 1$, are given by

$$Z_{\rm NH}^{QNM}(R) = {}_2F_1\left(-\frac{1}{2}\sqrt{1-4\hat{\omega}^2} - i\hat{\omega} + \frac{1}{2}, \frac{1}{2}\sqrt{1-4\hat{\omega}^2} - i\hat{\omega} + \frac{1}{2}; 1 - 2i\hat{\omega}; 1 - R\right), \tag{B.20}$$

with ${}_2F_1$ the ordinary hypergeometric function.

To obtain the spectrum of QNMs, we must impose normalizability at the boundary. In this region the fluctuation evolves in a vacuum-like background where the effects of the blackbrane are suppressed. Neglecting all z^n terms in Eq. (B.18) which vanish in the near boundary limit, we find a simpler equation

$$Z''_{\rm NB}(z) - \frac{(n-1-2i\bar{\omega}_j\, z)}{z} Z'_{\rm NB}(z) - \frac{(n-1)i\bar{\omega}_j}{z}\, Z_{\rm NB}(z) = 0\,. \tag{B.21}$$

Analytic solutions of this equation, in terms of the Bessel-J function can be found and analysed as in [140]. However we will instead follow an equivalent WKB approach which can be readily generalised for non-trivial horizons, as is the case when studying fluctuations evolving on a Bjorken-like background. Following this strategy we search for solutions of Eq. (B.18) in the near boundary region in the form

$$Z_{\rm NB}^{QNM}(z) = z^{n/2} e^{-in\hat{\omega}z} e^{n\sigma(z)}\,. \tag{B.22}$$

While one can find that $e^{n\sigma} = J_{\frac{n}{2}}(n\hat{\omega}z)$, for most of the analysis it will be more convenient to use the WKB form of the wave function. At large-D, we expand σ in inverse powers of n

$$\sigma = \sigma_0(z) + \frac{1}{n}\sigma_1(z) + \ldots\,, \tag{B.23}$$

where the ellipses denote additional orders in the large D-expansion. The equation for σ_0 is non-linear and is given by

$$\sigma_0'(z) = \pm\frac{1}{2}\sqrt{\frac{1}{z^2} - 4\hat{\omega}^2}\,. \tag{B.24}$$

Only the "+" branch leads to a normalisable solution at the boundary. Note that in this solution there is a special point $z_{\rm T} = 1/2\hat{\omega}$ around which the phase varies slowly. This means that the WKB approximation is not valid in the vicinity of this point and may be viewed as the analogue of a stationary point in quantum mechanics.

For $\hat{\omega} < 1/2$ the stationary point lies behind the horizon of the blackbrane, meaning that the WKB expansion is valid for all $z \leq 1$. However with fixed R at large n, the asymptotic behaviour of this WKB solution is inconsistent with the near horizon solution, Eq. (B.20), and therefore no QNMs can be found.

For $\hat{\omega} \gtrsim 1/2$ the WKB expression is valid in the entire near boundary region and fails only in the vicinity of the horizon $z_{\rm T} \sim 1$. This range of frequencies corresponds to the least damped QNMs of the blackbrane [140] and have been previously studied in the context of Chamblin-Reall holography [150]. Using standard arguments, the WKB expansion will hold in the region where $n(\sigma_0'(z))^2 \ll \sigma_0''(z)$ which implies that when

$$|x| \ll 1 \quad \text{with} \quad x \equiv \left(\frac{1}{z} - 2\hat{\omega}\right) n^{2/3}\,, \tag{B.25}$$

the equation for the fluctuations must be solved in a different way. Keeping x-fixed while taking the large n-limit brings the validity of the WKB region closer and closer to $z_{\rm T} = 1$. Therefore, in the *stationary point* region given by Eq. (B.25) we perform the large-D expansion with x fixed as

$$\tilde{Z}_{\rm NB} = \sum_{j=0} \psi_j(x) n^{-j/3}\,, \tag{B.26}$$

where $\tilde{Z}_{\rm NB} \equiv e^{n\sigma}$. In this expansion, the origin of the fractional powers arises from the definition of x in Eq. (B.25). Similarly, we expand the QNM frequency in inverse fractional powers of the number of spacetime dimensions

$$\omega = n\left(\frac{1}{2} + \delta\omega_1 \frac{1}{n^{2/3}} + \delta\omega_2 \frac{1}{n} + \delta\omega_3 \frac{1}{n^{4/3}} + \delta\omega_4 \frac{1}{n^{5/3}} + ...\right)\,, \tag{B.27}$$

where the absence of an $n^{-1/3}$ contribution is a consequence of matching this result with the near horizon region [140]. The validity of the near boundary approximation, Eq. (B.21), follows from the same argument as in Eq. (3.96).

Up to order $1/n$, solutions for the functions $\psi_i(x)$ can be found in terms of Airy functions. Imposing that in the $x \gg 1$ region these solutions can be matched to a normalisable mode given by the WKB solution Eq. (B.23), these functions up to an

overall normalization are

$$\psi_0(x) = \mathrm{Ai}\left(\frac{x}{\sqrt[3]{2}}\right), \tag{B.28}$$

$$\psi_1(x) = c_1\mathrm{Ai}\left(\frac{x}{\sqrt[3]{2}}\right), \tag{B.29}$$

$$\psi_2(x) = \frac{1}{20}\left(4\mathrm{Ai}\left(\frac{x}{\sqrt[3]{2}}\right)(5c_2+5\delta\omega_1+x) - 2^{2/3}x\,(20\delta\omega_1+7x)\,\mathrm{Ai}'\left(\frac{x}{\sqrt[3]{2}}\right)\right) \tag{B.30}$$

$$\psi_3(x) = \frac{1}{20}\left(4\mathrm{Ai}\left(\frac{x}{\sqrt[3]{2}}\right)(5c_1\delta\omega_1+c_1x+5c_3+5\delta\omega_2)\right. \tag{B.31}$$
$$\left. -2^{2/3}x\mathrm{Ai}'\left(\frac{x}{\sqrt[3]{2}}\right)(20c_1\delta\omega_1+7c_1x+20\delta\omega_2)\right),$$

with $\mathrm{Ai}(x)$ the Airy function of the first kind, and c_i and $\delta\omega_i$ are constants determined by matching Eqs. (B.28)-(B.31) to the near horizon solution in the intermediate region, where the coordinate $R \gg 1$ with large n. Note that at leading order, this procedure implies

$$x = -2\delta\omega_1 + \mathcal{O}\left(\frac{1}{n^{1/3}}\right). \tag{B.32}$$

Using Eqs. (B.22), (B.28), and (B.32), the leading order in $1/n$ expression for the QNM profile in the intermediate region from the linearized solution is given by

$$Z_{\mathrm{NB}}^{QNM} = e^{-i\delta\omega_2 - i\delta\omega_1 n^{1/3} - \frac{in}{2} - \frac{1}{2}} R^{-\frac{1}{2}+\frac{i}{2}}\left(\mathrm{Ai}\left(-2^{2/3}\delta\omega_1\right) + \mathcal{O}\left(n^{-1/3}\right),\right)$$

However the near horizon expression in the intermediate region coming from Eq. (B.20) in the limit $R \to \infty$ goes as

$$Z_{\mathrm{NH}}^{QNM} = \frac{R^{-\frac{1}{2}\sqrt{1-4\hat{\omega}^2}+i\hat{\omega}-\frac{1}{2}}\Gamma(1-2i\hat{\omega})\Gamma\left(-\sqrt{1-4\hat{\omega}^2}\right)}{\Gamma\left(\frac{1}{2}\left(-2i\hat{\omega}-\sqrt{1-4\hat{\omega}^2}+1\right)\right)^2} + \tag{B.33}$$
$$\frac{R^{\frac{1}{2}\sqrt{1-4\hat{\omega}^2}+i\hat{\omega}-\frac{1}{2}}\Gamma(1-2i\hat{\omega})\Gamma\left(\sqrt{1-4\hat{\omega}^2}\right)}{\Gamma\left(\frac{1}{2}\left(-2i\hat{\omega}+\sqrt{1-4\hat{\omega}^2}+1\right)\right)^2},$$

Expanding this expression in the vicinity of $\hat{\omega} = 1/2 + \delta\omega$, with $\delta\omega$ small and given by the expansion Eq. (B.27), the near horizon profile becomes

$$Z_{\mathrm{NH}}^{QNM} = R^{-\frac{1}{2}+\frac{i}{2}}\left(\frac{\Gamma(1-i)\left(\log(R) - 2H_{-\frac{1}{2}-\frac{i}{2}}\right)}{\Gamma\left(\frac{1}{2}-\frac{i}{2}\right)^2}\right. \tag{B.34}$$
$$\left. +2\delta\omega\frac{\Gamma(1-i)}{6\Gamma\left(\frac{1}{2}-\frac{i}{2}\right)^2}\left(c_{\mathrm{L}\,0} + c_{\mathrm{L}\,1}\log R + c_{\mathrm{L}\,2}\log R^2 - \frac{1}{2}\log R^3\right),\right)$$

with

$$
\begin{aligned}
c_{\mathrm{L}\,0} &= 2H_{-\frac{1}{2}-\frac{i}{2}}\left(2\left(H_{-\frac{1}{2}-\frac{i}{2}}\right)^2+\pi^2-6i\psi^{(0)}\left(\frac{1}{2}-\frac{i}{2}\right)+6i\psi^{(0)}(1-i)-3\psi^{(1)}\left(\frac{1}{2}-\frac{i}{2}\right)\right)\\
&\quad +8\zeta(3)+6i\psi^{(1)}\left(\frac{1}{2}-\frac{i}{2}\right)+\psi^{(2)}\left(\frac{1}{2}-\frac{i}{2}\right), \qquad \text{(B.35)}\\
c_{\mathrm{L}\,1} &= -6\left(H_{-\frac{1}{2}-\frac{i}{2}}\right)^2-6i\gamma_E-\pi^2-6i\psi^{(0)}(1-i)+3\psi^{(1)}\left(\frac{1}{2}-\frac{i}{2}\right), \qquad \text{(B.36)}\\
c_{\mathrm{L}\,2} &= 3H_{-\frac{1}{2}-\frac{i}{2}}+3i\,, \qquad \text{(B.37)}
\end{aligned}
$$

where H_n is the n^{th}-Harmonic number, γ_E is the Euler-Mascheroni constant, $\zeta(s)$ is the Riemann ζ-function and $\psi^{(i)}$ is the polygamma function of order i. Comparing the expected behaviour from the near horizon region (B.34) and near boundary region (B.33), we find that these expressions can only be consistent if $-2^{2/3}\delta\omega_1$ is a zero of the Airy function which may be approximated by [140]

$$\delta\omega_1 \simeq \left(\frac{3\pi}{16}(4k-1)\right)^{2/3}, \quad k=1,\,2,\,....\,, \qquad \text{(B.38)}$$

which becomes a more accurate approximation as k grows. Subsequent orders in the $n^{-1/3}$-expansion can be similarly matched to find

$$
\begin{aligned}
\delta\omega_2 &= H_{-\frac{1}{2}-\frac{i}{2}}\,, \qquad \text{(B.39)}\\
\delta\omega_3 &= \frac{3\delta\omega_1^2}{5}\,, \qquad \text{(B.40)}\\
\delta\omega_4 &= \frac{1}{6}\delta\omega_1\left(12H_{-\frac{1}{2}-\frac{i}{2}}-8\zeta(3)-6i\psi^{(1)}\left(\frac{1}{2}-\frac{i}{2}\right)-\psi^{(2)}\left(\frac{1}{2}-\frac{i}{2}\right)\right), \qquad \text{(B.41)}
\end{aligned}
$$

as well as the undetermined constants in Eq. (B.29) and Eq. (B.30)

$$
\begin{aligned}
c_1 &= \frac{3i\delta\omega_1^2}{5}\,, \qquad \text{(B.42)}\\
c_2 &= -\frac{1}{150}\delta\omega_1\left(27\delta\omega_1^3+50\pi^2-300i\gamma_E\right. \qquad \text{(B.43)}\\
&\qquad +5\left(40i\zeta(3)+42-120i\psi^{(0)}\left(\frac{1}{2}-\frac{i}{2}\right)+60i\psi^{(0)}(1-i)\right.\\
&\qquad\qquad \left.\left.-60\psi^{(1)}\left(\frac{1}{2}-\frac{i}{2}\right)+5i\psi^{(2)}\left(\frac{1}{2}-\frac{i}{2}\right)\right)\right).
\end{aligned}
$$

Beyond the stated order, the calculation becomes sensitive to both $1/n$ corrections to the near horizon wave function and to additional powers in the expansion of the QNM frequency.

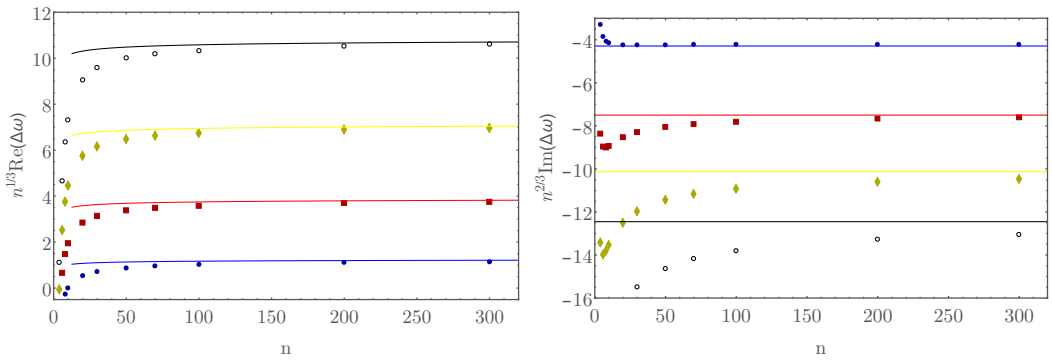

Figure B.1: Figure taken from [3]. Real (left) and imaginary (right) parts of the first four quasi normal modes of blackbranes in different numbers of dimension $D = 1 + n$ at zero spatial momentum. In both panels $\Delta\omega = \omega_{\mathrm{QNM}} - n\left(1/2 + \delta\omega_1 n^{-2/3} + \delta\omega_2 n^{-1}\right)$, with $\delta\omega_1$ the corresponding zero of the Airy function and $\delta\omega_2$ given in Eq. (B.39). The lines correspond to the real and imaginary parts of $\Delta\omega_{\mathrm{LD}} \equiv n\left(\delta\omega_3 n^{-4/3} + \delta\omega_4 n^{-5/3}\right)$ with the expression for each coefficient given in Eqs. (B.40) and (B.41) multiplied by the power of n stated in the y-axis.

The results for $\delta\omega_1$ and $\delta\omega_2$ are the same that we found in the computation of the transseries for Bjorken flow in Section 3.3. Here however we include corrections for $\delta\omega_3$ and $\delta\omega_4$ as well which would presumably emerge in the Bjorken case as well. To gain confidence in the results, in Fig. (B.1) we compare with numerical evaluations of the QNM spectrum for blackbranes for $n = 4$ to 300.

Appendix C

Appendix to Chapter 4

C.1 Divergence of the entropy current from all pairs of QNMs

In Chapter 4 we outlined a computation for the divergence of the entropy current due to all pairs of two modes, given by the transseries expansion. In that chapter we stated only the least damped contribution which we analysed for our intuition. In this appendix we state the full expression for $\partial_\mu s^\mu$ including all pairs of modes. We find,

$$\partial_\mu s^\mu = \sum_{\mathcal{H}\in\{\mathcal{X},\mathcal{Y},\mathcal{Z}\}} \sum_{i\geq j} A_{ij}\, e^{(\omega_i+\omega_j)^I t} \left[\cos\left(\Theta_{ij}^+ + \delta_{ij}^+\right) + C_{ij}\cos\left(\Theta_{ij}^- + \delta_{ij}^-\right)\right] + \mathcal{O}\left(\Omega_{\boldsymbol{e}_i+\boldsymbol{e}_j+\boldsymbol{e}_k}\right) \tag{C.1}$$

where the sum over $i \geq j$ sums each combination of QNM frequencies once[1], where $\Theta_{ij}^\pm = (k_i + k_j)x - (\omega_i + \omega_j)^R t$, and redefining $q_\pm = 1/2(q_i \pm q_j)$ and $\lambda_\pm = 1/2(\lambda_i \pm \lambda_j)$ the remaining normalization is given by

$$A_{ij} = \frac{1}{8} c_i c_j \begin{cases} \dfrac{1}{(1+q_+^2)} & (\text{AH})\,, \\ \dfrac{1}{|\lambda_+ - i|} & (\text{EH}) \end{cases} \quad \text{with} \quad c_i = \begin{cases} (\pi T)^2 \left|\lambda_i\right| \mathcal{X}_n & \text{tensor}\,, \\ \mathcal{Y}_i \frac{1}{(\pi T)} & \text{shear}\,, \\ \sqrt{\frac{1}{12}} \frac{|\lambda_i| \mathcal{Z}_i}{(\pi T)^2 \left|\lambda_i^2 - q_i^2\right|} & \text{sound}\,. \end{cases}, \tag{C.2}$$

[1] We also take this to be a sum over QNM frequencies with positive real part to prevent double counting.

the oscillation suppression C_{ij} is the same for all channels given by,

$$C_{ij} = \begin{cases} \dfrac{1+q_+^2}{1+q_-^2} & \text{(AH)}\,, \\ \sqrt{\dfrac{\left(\lambda_+^R\right)^2 + \left(\lambda_+^I - 1\right)^2}{\left(\lambda_-^R\right)^2 + \left(\lambda_+^I - 1\right)^2}} & \text{(EH)}\,, \end{cases} \tag{C.3}$$

and the phases for the apparent horizon are given by,

$$\delta^{\pm} \equiv \frac{\alpha_i^{\mathcal{H}} \pm \alpha_j^{\mathcal{H}}}{2} - \Delta^{\pm}_{\mathcal{H}_i\mathcal{H}_j}\,, \tag{C.4}$$

with

$$\text{Tensor: } \Delta^{\pm}_{\mathcal{X}_i\mathcal{X}_j} = \arctan\left(\frac{\pm\mu_{ij}^{\pm}}{\mp\nu_{ij}^{\mp}}\right)\,, \tag{C.5}$$

$$\text{Shear: } \Delta^{\pm}_{\mathcal{Y}_i\mathcal{Y}_j} = 0\,, \tag{C.6}$$

$$\text{Scalar: } \Delta^{\pm}_{\mathcal{Z}_i\mathcal{Z}_j} = \arctan\left(\frac{\mp\left[\mu_{ij}^{\pm}\kappa_{ij}^{-} + \mu_{ij}^{\mp}\xi_{ij}^{-}\right]}{\pm\left[-\nu_{ij}^{\mp}\kappa_{ij}^{+} + \nu_{ij}^{\pm}\xi_{ij}^{+}\right]}\right)\,, \tag{C.7}$$

where

$$\begin{aligned} &\nu_{ij}^{\pm} = \lambda_i^R\lambda_j^R \pm \lambda_i^I\lambda_j^I\,, \quad \mu_{ij}^{\pm} = \lambda_i^R\lambda_j^I \pm \lambda_i^R\lambda_j^I\,, \\ &\kappa_{ij}^{\pm} = \left|\lambda_i\right|^2\left|\lambda_j\right|^2 \pm q_i^2q_j^2\,, \quad \xi_{ij}^{\pm} = q_i^2\left|\lambda_j\right|^2 \pm q_j^2\left|\lambda_i\right|^2\,. \end{aligned} \tag{C.8}$$

A simple relation exists for each channel that can be used to recover the event horizon phases from the apparent horizon,

$$\delta_{ij}^{\pm\,\mathrm{EH}} - \delta_{ij}^{\pm\,\mathrm{AH}} = \arctan\left(\frac{\lambda_{\pm}^R}{\lambda_+^I - 1}\right)\,. \tag{C.9}$$

References

[1] J. Casalderrey-Solana, N. I. Gushterov, and B. Meiring, *Resurgence and Hydrodynamic Attractors in Gauss-Bonnet Holography*, JHEP **04** (2018) 042, arXiv:1712.02772.

[2] I. Aniceto, B. Meiring, J. Jankowski, and M. Spaliński, *The large proper-time expansion of Yang-Mills plasma as a resurgent transseries*, JHEP **02** (2019) 073, arXiv:1810.07130.

[3] J. Casalderrey-Solana, C. P. Herzog, and B. Meiring, *Holographic Bjorken Flow at Large-D*, JHEP **01** (2019) 181, arXiv:1810.02314.

[4] A. Jansen and B. Meiring, *Entropy production from quasinormal modes*, Phys. Rev. D **101** (2020) 126012, arXiv:2001.07220.

[5] I. Aniceto, G. Basar, and R. Schiappa, *A Primer on Resurgent Transseries and Their Asymptotics*, Phys. Rept. **809** (2019) 1, arXiv:1802.10441.

[6] J. M. Maldacena, *The Large N limit of superconformal field theories and supergravity*, Int. J. Theor. Phys. **38** (1999) 1113, arXiv:hep-th/9711200, [Adv. Theor. Math. Phys.2,231(1998)].

[7] E. Witten, *Anti-de Sitter space, thermal phase transition, and confinement in gauge theories*, Adv. Theor. Math. Phys. **2** (1998) 505, arXiv:hep-th/9803131.

[8] O. Aharony *et al.*, *Large N field theories, string theory and gravity*, Phys. Rept. **323** (2000) 183, arXiv:hep-th/9905111.

[9] K. Skenderis, *Lecture notes on holographic renormalization*, Class. Quant. Grav. **19** (2002) 5849, arXiv:hep-th/0209067.

[10] J. Casalderrey-Solana *et al.*, *Gauge/String Duality, Hot QCD and Heavy Ion Collisions*, arXiv:1101.0618arXiv:1101.0618.

[11] STAR, K. H. Ackermann *et al.*, *Elliptic flow in Au + Au collisions at* $\sqrt{s_{NN}}$*= 130 GeV*, Phys. Rev. Lett. **86** (2001) 402, arXiv:nucl-ex/0009011.

[12] PHENIX, S. S. Adler *et al.*, *Elliptic flow of identified hadrons in Au+Au collisions at* $\sqrt{s_{NN}}$ *= 200-GeV*, Phys. Rev. Lett. **91** (2003) 182301, arXiv:nucl-ex/0305013.

[13] PHOBOS, B. B. Back *et al.*, *Centrality and pseudorapidity dependence of elliptic flow for charged hadrons in Au+Au collisions at* $\sqrt{s_{NN}}$ *= 200-GeV*, Phys. Rev. **C72** (2005) 051901, arXiv:nucl-ex/0407012.

[14] ATLAS, G. Aad *et al.*, *Measurement of the azimuthal anisotropy for charged particle production in* $\sqrt{s_{NN}}$ = 2.76 *TeV lead-lead collisions with the ATLAS detector*, Phys. Rev. **C86** (2012) 014907, arXiv:1203.3087.

[15] CMS, S. Chatrchyan *et al.*, *Measurement of the elliptic anisotropy of charged particles produced in PbPb collisions at* $\sqrt{s}_{NN}$*=2.76 TeV*, Phys. Rev. **C87** (2013) 014902, arXiv:1204.1409.

[16] ALICE, K. Aamodt *et al.*, *Elliptic flow of charged particles in Pb-Pb collisions at 2.76 TeV*, Phys. Rev. Lett. **105** (2010) 252302, arXiv:1011.3914.

[17] A. Monnai, *Landau and Eckart frames for relativistic fluids in nuclear collisions*, Phys. Rev. C **100** (2019) 014901, arXiv:1904.11940.

[18] P. Kovtun, *Lectures on hydrodynamic fluctuations in relativistic theories*, J. Phys. A **45** (2012) 473001, arXiv:1205.5040.

[19] J. Ghiglieri, G. D. Moore, and D. Teaney, *QCD Shear Viscosity at (almost) NLO*, JHEP **03** (2018) 179, arXiv:1802.09535.

[20] G. Jackson and A. Peshier, *Re-running the QCD shear viscosity*, J. Phys. G **45** (2018) 095001, arXiv:1711.02119.

[21] P. B. Arnold, G. D. Moore, and L. G. Yaffe, *Transport coefficients in high temperature gauge theories. 2. Beyond leading log*, JHEP **05** (2003) 051, arXiv:hep-ph/0302165.

[22] P. Kovtun, D. T. Son, and A. O. Starinets, *Viscosity in strongly interacting quantum field theories from black hole physics*, Phys. Rev. Lett. **94** (2005) 111601, arXiv:hep-th/0405231.

[23] S. Bhattacharyya *et al.*, *Conformal Nonlinear Fluid Dynamics from Gravity in Arbitrary Dimensions*, JHEP **12** (2008) 116, arXiv:0809.4272.

[24] J. D. Bjorken, *Highly Relativistic Nucleus-Nucleus Collisions: The Central Rapidity Region*, Phys. Rev. **D27** (1983) 140.

[25] S. Jeon and U. Heinz, *Introduction to Hydrodynamics*, Int. J. Mod. Phys. **E24** (2015) 1530010, arXiv:1503.03931.

[26] R. A. Janik and R. B. Peschanski, *Asymptotic perfect fluid dynamics as a consequence of Ads/CFT*, Phys. Rev. **D73** (2006) 045013, arXiv:hep-th/0512162.

[27] R. Baier *et al.*, *Relativistic viscous hydrodynamics, conformal invariance, and holography*, JHEP **04** (2008) 100, arXiv:0712.2451.

[28] M. P. Heller, R. A. Janik, and P. Witaszczyk, *Hydrodynamic Gradient Expansion in Gauge Theory Plasmas*, Phys. Rev. Lett. **110** (2013) 211602, arXiv:1302.0697.

[29] M. P. Heller, A. Kurkela, and M. Spalinski, *Hydrodynamization and transient modes of expanding plasma in kinetic theory*, arXiv:1609.04803.

[30] M. P. Heller and V. Svensson, *How does relativistic kinetic theory remember about initial conditions?*, arXiv:1802.08225.

[31] W. Florkowski, M. P. Heller, and M. Spalinski, *New theories of relativistic hydrodynamics in the LHC era*, Rept. Prog. Phys. **81** (2018) 046001, arXiv:1707.02282.

[32] M. P. Heller and M. Spalinski, *Hydrodynamics Beyond the Gradient Expansion: Resurgence and Resummation*, Phys. Rev. Lett. **115** (2015) 072501, arXiv:1503.07514.

[33] R. P. Geroch, *On hyperbolic 'theories' of relativistic dissipative fluids*, arXiv:gr-qc/0103112.

[34] M. P. Heller, R. A. Janik, M. Spaliński, and P. Witaszczyk, *Coupling hydrodynamics to nonequilibrium degrees of freedom in strongly interacting quark-gluon plasma*, Phys. Rev. Lett. **113** (2014) 261601, arXiv:1409.5087.

[35] J. Casalderrey-Solana *et al.*, *Gauge/String Duality, Hot QCD and Heavy Ion Collisions*, Cambridge University Press, 2014.

[36] S. Borsanyi *et al.*, *The QCD equation of state with dynamical quarks*, JHEP **11** (2010) 077, arXiv:1007.2580.

[37] S. A. Hartnoll, A. Lucas, and S. Sachdev, *Holographic quantum matter*, arXiv:1612.07324.

[38] J. H. Schwarz and P. C. West, *Symmetries and transformations of chiral n = 2, d = 10 supergravity*, Physics Letters B **126** (1983) 301 .

[39] J. H. Schwarz, *Covariant field equations of chiral n = 2 d = 10 supergravity*, Nuclear Physics B **226** (1983) 269 .

[40] E. Witten, *Bound states of strings and p-branes*, Nucl. Phys. B **460** (1996) 335, arXiv:hep-th/9510135.

[41] G. W. Gibbons and K. ichi Maeda, *Black holes and membranes in higher-dimensional theories with dilaton fields*, Nuclear Physics B **298** (1988) 741 .

[42] G. T. Horowitz and A. Strominger, *Black strings and p-branes*, Nuclear Physics B **360** (1991) 197 .

[43] N. I. Gushterov, *Holographic approaches to strongly-interacting systems*, PhD thesis, Oxford U., Theor. Phys., 2018.

[44] P. Breitenlohner and D. Z. Freedman, *Stability in gauged extended supergravity*, Annals of Physics **144** (1982) 249 .

[45] P. Breitenlohner and D. Z. Freedman, *Positive energy in anti-de sitter backgrounds and gauged extended supergravity*, Physics Letters B **115** (1982) 197 .

[46] J. de Boer, E. P. Verlinde, and H. L. Verlinde, *On the holographic renormalization group*, JHEP **08** (2000) 003, `arXiv:hep-th/9912012`.

[47] J. de Boer, *The Holographic renormalization group*, Fortsch. Phys. **49** (2001) 339, `arXiv:hep-th/0101026`.

[48] S. de Haro, S. N. Solodukhin, and K. Skenderis, *Holographic reconstruction of space-time and renormalization in the AdS / CFT correspondence*, Commun. Math. Phys. **217** (2001) 595, `arXiv:hep-th/0002230`.

[49] V. Balasubramanian and P. Kraus, *A Stress tensor for Anti-de Sitter gravity*, Commun. Math. Phys. **208** (1999) 413, `arXiv:hep-th/9902121`.

[50] G. W. Gibbons and S. W. Hawking, *Action integrals and partition functions in quantum gravity*, Phys. Rev. D **15** (1977) 2752.

[51] S. S. Gubser, I. R. Klebanov, and A. W. Peet, *Entropy and temperature of black 3-branes*, Phys. Rev. D **54** (1996) 3915, `arXiv:hep-th/9602135`.

[52] N. Engelhardt and A. C. Wall, *Decoding the Apparent Horizon: Coarse-Grained Holographic Entropy*, Phys. Rev. Lett. **121** (2018) 211301, arXiv:1706.02038.

[53] Y. Tian, X.-N. Wu, and H.-B. Zhang, *Holographic Entropy Production*, JHEP **10** (2014) 170, arXiv:1407.8273.

[54] S. Bhattacharyya *et al.*, *Local Fluid Dynamical Entropy from Gravity*, JHEP **06** (2008) 055, arXiv:0803.2526.

[55] I. Booth, M. P. Heller, and M. Spalinski, *Black Brane Entropy and Hydrodynamics*, Phys. Rev. **D83** (2011) 061901, arXiv:1010.6301.

[56] I. Booth, M. P. Heller, G. Plewa, and M. Spalinski, *On the apparent horizon in fluid-gravity duality*, Phys. Rev. **D83** (2011) 106005, arXiv:1102.2885.

[57] V. E. Hubeny, S. Minwalla, and M. Rangamani, *The fluid/gravity correspondence*, in *Black holes in higher dimensions*, 348–383, 2012, arXiv:1107.5780. [,817(2011)].

[58] P. Huovinen *et al.*, *Radial and elliptic flow at RHIC: Further predictions*, Phys. Lett. **B503** (2001) 58, arXiv:hep-ph/0101136.

[59] D. Teaney, J. Lauret, and E. V. Shuryak, *A Hydrodynamic description of heavy ion collisions at the SPS and RHIC*, arXiv:nucl-th/0110037.

[60] T. Hirano *et al.*, *Hadronic dissipative effects on elliptic flow in ultrarelativistic heavy-ion collisions*, Phys. Lett. **B636** (2006) 299, arXiv:nucl-th/0511046.

[61] B. Schenke, S. Jeon, and C. Gale, *Elliptic and triangular flow in event-by-event (3+1)D viscous hydrodynamics*, Phys. Rev. Lett. **106** (2011) 042301, arXiv:1009.3244.

[62] T. Hirano, P. Huovinen, and Y. Nara, *Elliptic flow in Pb+Pb collisions at* $\sqrt{s_{NN}} = 2.76$ *TeV: hybrid model assessment of the first data*, Phys. Rev. **C84** (2011) 011901, arXiv:1012.3955.

[63] C. Shen *et al.*, *The iEBE-VISHNU code package for relativistic heavy-ion collisions*, Comput. Phys. Commun. **199** (2016) 61, arXiv:1409.8164.

[64] P. F. Kolb and U. W. Heinz, *Hydrodynamic description of ultrarelativistic heavy ion collisions*, arXiv:nucl-th/0305084.

[65] M. P. Heller, R. A. Janik, and P. Witaszczyk, *The characteristics of thermalization of boost-invariant plasma from holography*, Phys. Rev. Lett. **108** (2012) 201602, arXiv:1103.3452.

[66] P. M. Chesler and L. G. Yaffe, *Boost invariant flow, black hole formation, and far-from-equilibrium dynamics in $N = 4$ supersymmetric Yang-Mills theory*, Phys. Rev. **D82** (2010) 026006, arXiv:0906.4426.

[67] P. M. Chesler and L. G. Yaffe, *Holography and colliding gravitational shock waves in asymptotically AdS_5 spacetime*, Phys. Rev. Lett. **106** (2011) 021601, arXiv:1011.3562.

[68] P. M. Chesler and L. G. Yaffe, *Holography and off-center collisions of localized shock waves*, JHEP **10** (2015) 070, arXiv:1501.04644.

[69] M. Attems *et al.*, *Holographic Collisions in Non-conformal Theories*, JHEP **01** (2017) 026, arXiv:1604.06439.

[70] A. Kurkela and Y. Zhu, *Isotropization and hydrodynamization in weakly coupled heavy-ion collisions*, Phys. Rev. Lett. **115** (2015) 182301, arXiv:1506.06647.

[71] P. Romatschke, *Far From Equilibrium Fluid Dynamics*, arXiv:1704.08699.

[72] W. Israel and J. M. Stewart, *Transient relativistic thermodynamics and kinetic theory*, Annals Phys. **118** (1979) 341.

[73] G. S. Denicol and J. Noronha, *Analytical attractor and the divergence of the slow-roll expansion in relativistic hydrodynamics*, arXiv:1711.01657.

[74] M. Spaliński, *On the hydrodynamic attractor of Yang-Mills plasma*, arXiv:1708.01921.

[75] J.-P. Blaizot and L. Yan, *Fluid dynamics of out of equilibrium boost invariant plasmas*, Phys. Lett. B **780** (2018) 283, arXiv:1712.03856.

[76] M. Strickland, J. Noronha, and G. Denicol, *The anisotropic non-equilibrium hydrodynamic attractor*, arXiv:1709.06644.

[77] P. Romatschke, *Relativistic Hydrodynamic Attractors with Broken Symmetries: Non-Conformal and Non-Homogeneous*, arXiv:1710.03234.

[78] A. Behtash, C. N. Cruz-Camacho, and M. Martinez, *Far-from-equilibrium attractors and nonlinear dynamical systems approach to the Gubser flow*, Phys. Rev. **D97** (2018) 044041, arXiv:1711.01745.

[79] A. Behtash, S. Kamata, M. Martinez, and C. N. Cruz-Camacho, *Non-perturbative rheological behavior of a far-from-equilibrium expanding plasma*, arXiv:1805.07881.

[80] G. S. Denicol and J. Noronha, *Hydrodynamic attractor and the fate of perturbative expansions in Gubser flow*, arXiv:1804.04771.

[81] S. Grozdanov, N. Kaplis, and A. O. Starinets, *From strong to weak coupling in holographic models of thermalization*, JHEP **07** (2016) 151, arXiv:1605.02173.

[82] S. Kinoshita, S. Mukohyama, S. Nakamura, and K.-y. Oda, *A Holographic Dual of Bjorken Flow*, Prog. Theor. Phys. **121** (2009) 121, arXiv:0807.3797.

[83] R. A. Janik and R. B. Peschanski, *Gauge/gravity duality and thermalization of a boost-invariant perfect fluid*, Phys. Rev. **D74** (2006) 046007, arXiv:hep-th/0606149.

[84] P. Benincasa, A. Buchel, M. P. Heller, and R. A. Janik, *On the supergravity description of boost invariant conformal plasma at strong coupling*, Phys. Rev. **D77** (2008) 046006, arXiv:0712.2025.

[85] G. Beuf, M. P. Heller, R. A. Janik, and R. Peschanski, *Boost-invariant early time dynamics from AdS/CFT*, JHEP **10** (2009) 043, arXiv:0906.4423.

[86] M. P. Heller, R. A. Janik, and P. Witaszczyk, *A numerical relativity approach to the initial value problem in asymptotically Anti-de Sitter spacetime for plasma thermalization - an ADM formulation*, Phys. Rev. **D85** (2012) 126002, arXiv:1203.0755.

[87] P. M. Chesler and L. G. Yaffe, *Numerical solution of gravitational dynamics in asymptotically anti-de Sitter spacetimes*, JHEP **07** (2014) 086, arXiv:1309.1439.

[88] R. A. Janik, G. Plewa, H. Soltanpanahi, and M. Spalinski, *Linearized nonequilibrium dynamics in nonconformal plasma*, Phys. Rev. D **91** (2015) 126013, arXiv:1503.07149.

[89] P. K. Kovtun and A. O. Starinets, *Quasinormal modes and holography*, Phys. Rev. **D72** (2005) 086009, arXiv:hep-th/0506184.

[90] P. Grandclement, *Introduction to spectral methods*, EAS Publ. Ser. **21** (2006) 153, arXiv:gr-qc/0609020.

[91] I. Aniceto and M. Spaliński, *Resurgence in Extended Hydrodynamics*, Phys. Rev. **D93** (2016) 085008, arXiv:1511.06358.

[92] G. Basar and G. V. Dunne, *Hydrodynamics, resurgence, and transasymptotics*, Phys. Rev. **D92** (2015) 125011, arXiv:1509.05046.

[93] S. S. Gubser, I. R. Klebanov, and A. A. Tseytlin, *Coupling constant dependence in the thermodynamics of N=4 supersymmetric Yang-Mills theory*, Nucl. Phys. **B534** (1998) 202, arXiv:hep-th/9805156.

[94] J. Pawelczyk and S. Theisen, *$AdS_5 \times S^5$ black hole metric at $O(\alpha'^3)$*, JHEP **09** (1998) 010, arXiv:hep-th/9808126.

[95] S. Grozdanov and A. O. Starinets, *Second-order transport, quasinormal modes and zero-viscosity limit in the Gauss-Bonnet holographic fluid*, JHEP **03** (2017) 166, arXiv:1611.07053.

[96] S. Grozdanov and W. van der Schee, *Coupling Constant Corrections in a Holographic Model of Heavy Ion Collisions*, Phys. Rev. Lett. **119** (2017) 011601, arXiv:1610.08976.

[97] T. Andrade, J. Casalderrey-Solana, and A. Ficnar, *Holographic Isotropisation in Gauss-Bonnet Gravity*, JHEP **02** (2017) 016, arXiv:1610.08987.

[98] B. S. DiNunno, S. Grozdanov, J. F. Pedraza, and S. Young, *Holographic constraints on Bjorken hydrodynamics at finite coupling*, JHEP **10** (2017) 110, arXiv:1707.08812.

[99] A. Buchel, R. C. Myers, and A. Sinha, *Beyond $\eta/s = 1/4\pi$*, JHEP **03** (2009) 084, arXiv:0812.2521.

[100] D. M. Hofman and J. Maldacena, *Conformal collider physics: Energy and charge correlations*, JHEP **05** (2008) 012, arXiv:0803.1467.

[101] D. M. Hofman, *Higher Derivative Gravity, Causality and Positivity of Energy in a UV complete QFT*, Nucl. Phys. **B823** (2009) 174, arXiv:0907.1625.

[102] A. Buchel and R. C. Myers, *Causality of Holographic Hydrodynamics*, JHEP **08** (2009) 016, arXiv:0906.2922.

[103] X. O. Camanho, J. D. Edelstein, J. Maldacena, and A. Zhiboedov, *Causality Constraints on Corrections to the Graviton Three-Point Coupling*, JHEP **02** (2016) 020, arXiv:1407.5597.

[104] G. Papallo and H. S. Reall, *Graviton time delay and a speed limit for small black holes in Einstein-Gauss-Bonnet theory*, JHEP **11** (2015) 109, arXiv:1508.05303.

[105] T. Andrade, E. Caceres, and C. Keeler, *Boundary causality versus hyperbolicity for spherical black holes in Gauss?Bonnet gravity*, Class. Quant. Grav. **34** (2017) 135003, arXiv:1610.06078.

[106] R. A. Konoplya and A. Zhidenko, *Quasinormal modes of Gauss-Bonnet-AdS black holes: towards holographic description of finite coupling*, JHEP **09** (2017) 139, arXiv:1705.07732.

[107] M. Brigante *et al.*, *Viscosity Bound Violation in Higher Derivative Gravity*, Phys. Rev. **D77** (2008) 126006, arXiv:0712.0805.

[108] Y. Brihaye and E. Radu, *Black objects in the Einstein-Gauss-Bonnet theory with negative cosmological constant and the boundary counterterm method*, JHEP **09** (2008) 006, arXiv:0806.1396.

[109] D. Astefanesei, N. Banerjee, and S. Dutta, *(Un)attractor black holes in higher derivative AdS gravity*, JHEP **11** (2008) 070, arXiv:0806.1334.

[110] D. Dorigoni, *An Introduction to Resurgence, Trans-Series and Alien Calculus*, Annals Phys. **409** (2019) 167914, arXiv:1411.3585.

[111] S. Bhattacharyya, V. E. Hubeny, S. Minwalla, and M. Rangamani, *Nonlinear Fluid Dynamics from Gravity*, JHEP **02** (2008) 045, arXiv:0712.2456.

[112] R. Emparan, R. Suzuki, and K. Tanabe, *The large D limit of General Relativity*, JHEP **06** (2013) 009, arXiv:1302.6382.

[113] R. Emparan, D. Grumiller, and K. Tanabe, *Large-D gravity and low-D strings*, Phys. Rev. Lett. **110** (2013) 251102, arXiv:1303.1995.

[114] R. Emparan and K. Tanabe, *Holographic superconductivity in the large D expansion*, JHEP **01** (2014) 145, arXiv:1312.1108.

[115] A. M. García-García and A. Romero-Bermúdez, *Conductivity and entanglement entropy of high dimensional holographic superconductors*, JHEP **09** (2015) 033, arXiv:1502.03616.

[116] R. Emparan, R. Suzuki, and K. Tanabe, *Quasinormal modes of (Anti-)de Sitter black holes in the 1/D expansion*, JHEP **04** (2015) 085, arXiv:1502.02820.

[117] T. Andrade, S. A. Gentle, and B. Withers, *Drude in D major*, JHEP **06** (2016) 134, arXiv:1512.06263.

[118] C. P. Herzog, M. Spillane, and A. Yarom, *The holographic dual of a Riemann problem in a large number of dimensions*, JHEP **08** (2016) 120, arXiv:1605.01404.

[119] M. Rozali, E. Sabag, and A. Yarom, *Holographic Turbulence in a Large Number of Dimensions*, JHEP **04** (2018) 065, arXiv:1707.08973.

[120] R. Emparan *et al.*, *Hydro-elastic Complementarity in Black Branes at large D*, JHEP **06** (2016) 117, arXiv:1602.05752.

[121] N. Iizuka, A. Ishibashi, and K. Maeda, *Cosmic Censorship at Large D: Stability analysis in polarized AdS black branes (holes)*, JHEP **03** (2018) 177, arXiv:1801.07268.

[122] K. Tanabe, *Black rings at large D*, JHEP **02** (2016) 151, arXiv:1510.02200.

[123] S. Bhattacharyya, M. Mandlik, S. Minwalla, and S. Thakur, *A Charged Membrane Paradigm at Large D*, JHEP **04** (2016) 128, arXiv:1511.03432.

[124] K. Tanabe, *Charged rotating black holes at large D*, arXiv:1605.08854.

[125] M. Rozali and A. Vincart-Emard, *On Brane Instabilities in the Large D Limit*, JHEP **08** (2016) 166, arXiv:1607.01747.

[126] Y. Dandekar *et al.*, *The large D black hole Membrane Paradigm at first subleading order*, JHEP **12** (2016) 113, arXiv:1607.06475.

[127] Y. Dandekar, S. Mazumdar, S. Minwalla, and A. Saha, *Unstable 'black branes' from scaled membranes at large D*, JHEP **12** (2016) 140, arXiv:1609.02912.

[128] S. Bhattacharyya *et al.*, *Currents and Radiation from the large D Black Hole Membrane*, JHEP **05** (2017) 098, arXiv:1611.09310.

[129] B. Chen, P.-C. Li, and Z.-z. Wang, *Charged Black Rings at large D*, JHEP **04** (2017) 167, arXiv:1702.00886.

[130] B. Chen and P.-C. Li, *Static Gauss-Bonnet Black Holes at Large D*, JHEP **05** (2017) 025, arXiv:1703.06381.

[131] S. Bhattacharyya *et al.*, *The large D black hole dynamics in AdS/dS backgrounds*, arXiv:1704.06076.

[132] U. Miyamoto, *Non-linear perturbation of black branes at large D*, JHEP **06** (2017) 033, arXiv:1705.00486.

[133] B. Chen, P.-C. Li, and C.-Y. Zhang, *Einstein-Gauss-Bonnet Black Strings at Large D*, JHEP **10** (2017) 123, arXiv:1707.09766.

[134] C. P. Herzog and Y. Kim, *The Large Dimension Limit of a Small Black Hole Instability in Anti-de Sitter Space*, JHEP **02** (2018) 167, arXiv:1711.04865.

[135] Y. Dandekar *et al.*, *An Action for and Hydrodynamics from the improved Large D membrane*, arXiv:1712.09400.

[136] R. Emparan *et al.*, *Phases and Stability of Non-Uniform Black Strings*, JHEP **05** (2018) 104, arXiv:1802.08191.

[137] T. Andrade, C. Pantelidou, and B. Withers, *Large D holography with metric deformations*, arXiv:1806.00306.

[138] T. Andrade, R. Emparan, and D. Licht, *Rotating black holes and black bars at large D*, JHEP **09** (2018) 107, arXiv:1807.01131.

[139] R. Emparan and K. Tanabe, *Universal quasinormal modes of large D black holes*, Phys. Rev. **D89** (2014) 064028, arXiv:1401.1957.

[140] R. Emparan, R. Suzuki, and K. Tanabe, *Decoupling and non-decoupling dynamics of large D black holes*, JHEP **07** (2014) 113, arXiv:1406.1258.

[141] S. Grozdanov and N. Kaplis, *Constructing higher-order hydrodynamics: The third order*, Phys. Rev. **D93** (2016) 066012, arXiv:1507.02461.

[142] A. Jansen and J. M. Magan, *Black hole collapse and democratic models*, Phys. Rev. **D94** (2016) 104007, arXiv:1604.03772.

[143] LIGO Scientific, Virgo, B. P. Abbott *et al.*, *GW151226: Observation of Gravitational Waves from a 22-Solar-Mass Binary Black Hole Coalescence*, Phys. Rev. Lett. **116** (2016) 241103, arXiv:1606.04855.

[144] S. W. Hawking, *Particle creation by black holes*, Comm. Math. Phys. **43** (1975) 199.

[145] G. 't Hooft, *Dimensional reduction in quantum gravity*, 1993.

[146] L. Susskind, *The World as a hologram*, J. Math. Phys. **36** (1995) 6377, arXiv:hep-th/9409089.

[147] M. P. Heller, D. Mateos, W. van der Schee, and M. Triana, *Holographic isotropization linearized*, JHEP **09** (2013) 026, arXiv:1304.5172.

[148] M. P. Heller, D. Mateos, W. van der Schee, and D. Trancanelli, *Strong Coupling Isotropization of Non-Abelian Plasmas Simplified*, Phys. Rev. Lett. **108** (2012) 191601, arXiv:1202.0981.

[149] S. Bhattacharyya, P. Biswas, and M. Patra, *A leading-order comparison between fluid-gravity and membrane-gravity dualities*, arXiv:1807.05058.

[150] P. Betzios, U. Gursoy, M. Jarvinen, and G. Policastro, *Fluctuations in non-conformal holographic plasma at criticality*, arXiv:1807.01718.